SOUTHERN PLAINS
TRANSPORTATION CENTER

Evaluating Post-Wildfire Flood Impacts on Transportation Infrastructure for Mitigation Planning

Vanessa Valentin, Ph.D.
John Stormont, Ph.D.

SPTC15.1-50-F

Southern Plains Transportation Center
201 Stephenson Parkway, Suite 4200
The University of Oklahoma
Norman, Oklahoma 73019

TECHNICAL REPORT DOCUMENTATION PAGE

1. REPORT NO.	2. GOVERNMENT ACCESSION NO.	3. RECIPIENTS CATALOG NO.
SPTC15.1-50-F		

4. TITLE AND SUBTITLE	5. REPORT DATE
Evaluating post-wildfire flood impacts on transportation infrastructure for mitigation planning	November 30, 2019
	6. PERFORMING ORGANIZATION CODE
7. AUTHOR(S) Vanessa Valentin John Stormont	8. PERFORMING ORGANIZATION REPORT
9. PERFORMING ORGANIZATION NAME AND ADDRESS Department of Civil, Construction and Environmental Engineering University of New Mexico 1 University of New Mexico, MSC01 1070 Albuquerque, NM 87131	10. WORK UNIT NO.
	11. CONTRACT OR GRANT NO. DTRT13-G-UTC36
12. SPONSORING AGENCY NAME AND ADDRESS Southern Plains Transportation Center 201 Stephenson Pkwy, Suite 4200 The University of Oklahoma Norman, OK 73019	13. TYPE OF REPORT AND PERIOD COVERED Final January 2017 – November 2019
	14. SPONSORING AGENCY CODE

15. SUPPLEMENTARY NOTES

16. ABSTRACT

Wildfires have seen a sharp increase in severity and frequency due to changes in climate, especially in the Southwestern U.S., where prevailing conditions of arid climate such as heat waves and droughts can have a dramatic effect on the risk of fire. This study investigated the impacts of post-wildfire floods on transportation infrastructure. Drainages and bridges were specifically targeted as they are especially vulnerable to fire-related damage, whether directly from fire heat or from subsequent flash flooding that results from fire-induced changes to the watershed. The specific objectives of this study were to: (1) identify post-wildfire flash flood impacts as well as risk mitigation and rehabilitation alternatives for transportation infrastructure, (2) evaluate the sensitivity of a hydrology model to site-specific input data and identify transportation infrastructure components at risk of inundation, and (3) develop a decision-support approach for prioritizing and selecting mitigation and rehabilitation options. In response to these objectives, we developed a modeling framework which integrates pre- and post-wildfire rainfall-runoff modeling and floodplain mapping under different climate and burn severity scenarios. Results from a case study analyzed using the model showed that preventing partial or complete blockage of the culverts will preclude roadway inundation under different climate and burn severity scenarios. Thus, the resulting modeling framework can be used as a screening tool for identifying potential problem areas and deciding where to focus further analyses on failure mechanisms, damage assessment, risk mitigation alternatives, and resource allocation. Finally, the proposed decision-making approach explores a wildfire vulnerability assessment process for transportation infrastructure and provides suggestions, resources, and examples for prioritizing infrastructure components and selecting mitigation and rehabilitation measures while considering asset criticality and other characteristics.

17. KEY WORDS	18. DISTRIBUTION STATEMENT
Wildfire, flooding, inundation, mitigation, rehabilitation	No restrictions. This publication is available at www.sptc.org and from the NTIS.

19. SECURITY CLASSIF. (OF THIS REPORT)	20. SECURITY CLASSIF. (OF THIS PAGE)	21. NO. OF PAGES	22. PRICE
Unclassified	Unclassified	90	

SI* (MODERN METRIC) CONVERSION FACTORS

APPROXIMATE CONVERSIONS TO SI UNITS

SYMBOL	WHEN YOU KNOW	MULTIPLY BY	TO FIND	SYMBOL
		LENGTH		
in	inches	25.4	millimeters	mm
ft	feet	0.305	meters	m
yd	yards	0.914	meters	m
mi	miles	1.61	kilometers	km
		AREA		
in^2	square inches	645.2	square millimeters	mm^2
ft^2	square feet	0.093	square meters	m^2
yd^2	square yard	0.836	square meters	m^2
ac	acres	0.405	hectares	ha
mi^2	square miles	2.59	square kilometers	km^2
		VOLUME		
fl oz	fluid ounces	29.57	milliliters	mL
gal	gallons	3.785	liters	L
ft^3	cubic feet	0.028	cubic meters	m^3
yd^3	cubic yards	0.765	cubic meters	m^3
	NOTE: volumes greater than 1000 L shall be shown in m^3			
		MASS		
oz	ounces	28.35	grams	g
lb	pounds	0.454	kilograms	kg
T	short tons (2000 lb)	0.907	megagrams (or "metric ton")	Mg (or "t")
		TEMPERATURE (exact degrees)		
°F	Fahrenheit	5 (F-32)/9 or (F-32)/1.8	Celsius	°C
		ILLUMINATION		
fc	foot-candles	10.76	lux	lx
fl	foot-Lamberts	3.426	candela/m^2	cd/m^2
		FORCE and PRESSURE or STRESS		
lbf	poundforce	4.45	newtons	N
lbf/in^2	poundforce per square inch	6.89	kilopascals	kPa

APPROXIMATE CONVERSIONS FROM SI UNITS

SYMBOL	WHEN YOU KNOW	MULTIPLY BY	TO FIND	SYMBOL
		LENGTH		
mm	millimeters	0.039	inches	in
m	meters	3.28	feet	ft
m	meters	1.09	yards	yd
km	kilometers	0.621	miles	mi
		AREA		
mm^2	square millimeters	0.0016	square inches	in^2
m^2	square meters	10.764	square feet	ft^2
m^2	square meters	1.195	square yards	yd^2
ha	hectares	2.47	acres	ac
km^2	square kilometers	0.386	square miles	mi^2
		VOLUME		
mL	milliliters	0.034	fluid ounces	fl oz
L	liters	0.264	gallons	gal
m^3	cubic meters	35.314	cubic feet	ft^3
m^3	cubic meters	1.307	cubic yards	yd^3
		MASS		
g	grams	0.035	ounces	oz
kg	kilograms	2.202	pounds	lb
Mg (or "t")	megagrams (or "metric ton")	1.103	short tons (2000 lb)	T
		TEMPERATURE (exact degrees)		
°C	Celsius	1.8C+32	Fahrenheit	°F
		ILLUMINATION		
lx	lux	0.0929	foot-candles	fc
cd/m^2	candela/m^2	0.2919	foot-Lamberts	fl
		FORCE and PRESSURE or STRESS		
N	newtons	0.225	poundforce	lbf
kPa	kilopascals	0.145	poundforce per square inch	lbf/in^2

*SI is the symbol for the International System of Units. Appropriate rounding should be made to comply with Section 4 of ASTM E380.
(Revised March 2003)

CONTENTS

List of Figures vi
List of Tables vii
Executive Summary viii
1. Introduction 1
1.1 Background 1
1.1.1 Impacts of wildfire on transportation infrastructure 1
1.2. Wildfire management 2
1.3 Point of departure and project Objectives 2
2. Post-wildfire flash flood impacts and risk mitigation and rehabilitation alternatives for bridges and drainages 4
2.1 General hazards associated with wildfires 4
2.1.1 Introduction 4
2.1.2 Post-Wildfire Flash Flood 4
2.1.3 Debris Flows 4
2.1.4 Erosion 4
2.1.5 Landslides 5
2.2 Post-wildfire flood impacts on bridges and drainages 5
2.2.1 Erosion Of Transportation-Purposed Embankments 5
2.2.2 Weakening of Embankments from Increased Saturation 6
2.2.3 Debris Flows 6
2.2.4 Scour 6
2.2.5 Landslides 7
2.3 Mitigation and rehabilitation of general hazards from wildfires 7
2.3.1 Wildfire Mitigation 7
2.3.2 Slope Erosion Rehabilitation 7
2.3.3 Landslide Mitigation 8
2.4 Flood-related hazard mitigation for bridges and drainage 8
2.4.1 Reducing Transportation-Purposed Embankment Erosion 8
2.4.2 Debris Flow Mitigation 8
2.4.3 Scour Protection 10
2.5 Summary 11

3. Hydrologic modeling to estimate transportation infrastructure components at risk . 12
3.1 Introduction 12
3.2 Rainfall-Runoff Model 13
3.3 Floodplain Model 13
3.4 Modeling approach to assess the impact of post-wildfire floods on transportation infrastructure 14
3.5 Case Study 15
3.5.1 Site 15
3.5.2 Modeled Scenarios 19
3.5.3 Data Collection 22
3.6 Results 23
3.6.1 Rainfall-Runoff Modeling 23
3.6.2 Steady Flow Floodplain Modeling 24
3.6.3. Results from Unsteady Flow Analysis 40
3.7 Conclusions 41
4. Vulnerability Assessment and decision-making approach for wildfire mitigation and rehabilitation strategies 42
4.1 Introduction 42
4.2 Vulnerability assessment 42
4.2.1 Data Collection of Transportation Assets 42
4.2.2 Climate and Disturbance Inputs: Wildfire 43
42.3 Identifying Vulnerabilities and Asset Sensitivity to Climate and Disturbances 43
4.2.4 Asset Criticality 44
4.2.5 Applicability of Mitigation and Rehabilitation Strategies 45
4.2.6 Evaluation of Strategies 46
4.3 Summary 47
References 48
Appendix 57

LIST OF FIGURES

Figure 1. Major Steps Involved in Modeling Framework Using ArcGIS, HEC-GeoRAS, and HEC-RAS 14
Figure 2. Location of the Study Site 17
Figure 3. Location of Culverts and Reaches in Los Alamos Canyon Watershed 18
Figure 4. Culverts Located in the Study Area (Looking Downstream) 19
Figure 5. Scenarios Considered for Analysis Under Baseline and Climate Change Conditions 20
Figure 6. Burn Severity Map for Las Conchas Fire 21
Figure 7. Floodplain Model 23
Figure 8. Flood Depth at Culvert Inlet for Culvert C1 as a Function of Percentage of Culvert Blocked 25
Figure 9. Flood Depth at Culvert Inlet for Culvert C1 as a Function of Burn Severity 26
Figure 10. Flood Depth at Culvert Inlet for Culvert C2 as a Function of Percentage of Culvert Blocked 27
Figure 11. Flood Depth at Culvert Inlet for Culvert C1 as a Function of Burn Severity 28
Figure 12. Floodplain Modeling Conditions for Which the Roadway Embankment Above Culvert 1 Was Inundated Are Indicated by Shading 31
Figure 13. Floodplain Modeling Conditions for Which the Roadway Embankment Above Culvert 2 Was Inundated Are Indicated by Shading 32
Figure 14. Floodplain Modeling Conditions for Which the Roadway Embankment Above Culvert 3 Was Inundated Are Indicated by Shading 33
Figure 15. Floodplains at Culvert C2, 25% Blockage, Baseline Climate 34
Figure 16. Floodplains at Culvert C1, 50% Blockage, Baseline Climate 35
Figure 17. Floodplains at Culvert C3, 50% Blockage, Baseline Climate 36
Figure 18. Flood Depth (Culvert C1, 200-year High Burn Severity) for No Blockage and 25% Blockage 37
Figure 19. Flood Depth (Culvert C1, 200-year High Burn Severity) for 50% and 75% Blockage 38
Figure 20. Example of Disruption due to Inundation in the Case Study and Example Alternative Routes (Source: Google Maps) 44
Figure 21. Conditions for Determining Applicability of Mitigation Measures 46

LIST OF TABLES

Table 1. Countermeasures to Reduce the Impacts of Debris Flow 9
Table 2. Examples of Countermeasures to Reduce the Impacts of Debris Flow Related to Wildfire (61) 10
Table 3. Countermeasures to Protect Piers From Local Scour 10
Table 4. Culverts located in Los Alamos Canyon Watershed 16
Table 5. Data and Their Sources 22
Table 6. Runoff and Total Sediment Yield 24
Table 7. Summary of Scenarios Resulting in Inundation for C1, C2 and C3 30
Table 8. Velocities at Different Sections Near the Culverts: No Blockage 39
Table 9. Velocities at Different Sections Near the Culverts: 25% Blockage 39
Table 10. Velocities at Different Sections Near the Culverts: 50% Blockage 40
Table 11. Velocities at Different Sections Near the Culverts: 75% Blockage 40
Table 12. Results of the Unsteady Flow Analysis 40
Table 13. Description of Conditions as Referenced in Table 12 41
Table 14. Examples of items from the NBI useful for asset criticality analysis (From NBI) 43

EXECUTIVE SUMMARY

Transportation infrastructure is being affected by unprecedented extreme weather/climate events such as wildfires. Bridges and drainages are especially vulnerable to fire-related damage, whether directly from fire heat or from subsequent flash flooding that results from fire-induced changes to the watershed and soil properties. Some of these changes include: reduced vegetation cover, soil erosion and sedimentation, slope failure, and the development of water repellency. Extensive research has investigated the vulnerability of transportation infrastructure to disaster events such as hurricanes and earthquakes, but only limited research has considered the vulnerability of transportation infrastructure to wildfires.

This study aimed to help reduce wildfire impacts on transportation infrastructure. The specific objectives of this study were to: (1) identify post-wildfire flash flood impacts, as well as risk mitigation and rehabilitation alternatives for transportation infrastructure, (2) evaluate the sensitivity of a hydrology model to site-specific input data and identify transportation infrastructure components at risk of inundation, and (3) develop a decision support approach for prioritizing and selecting mitigation and rehabilitation options.

To achieve these objectives, we developed a modeling framework which integrates pre- and post-wildfire rainfall-runoff modeling and floodplain mapping under different climate and burn severity scenarios. The framework is demonstrated using the case study of the Las Conchas wildfire in the state of New Mexico. Model predictions of roadway inundation due to overtopping at road–stream culvert crossings are used to quantify the impact of the post-wildfire flooding because inundation can have a range of deleterious consequences—from roadway closure during the flooding event to long-term deterioration of the roadway foundation. Results from the case study indicate that preventing partial or complete blockage of the culverts will preclude roadway inundation under different climate and burn severity scenarios and suggest prioritizing mitigation efforts on keeping culverts clear of debris. This modeling framework can be used by decision-makers as a screening tool for identifying potential problem areas and deciding where to focus further analyses on failure mechanisms, damage assessment, risk mitigation alternatives, and resource allocation.

The modeling framework was expanded to a decision-making approach by exploring wildfire vulnerability assessment for transportation infrastructure and providing suggestions, resources, and examples for prioritizing infrastructure components and selecting mitigation and rehabilitation measures. In this approach, we considered asset criticality, and pre- and post-wildfire watershed conditions, among others.

This study contributed to the move towards preventive methods to quantify, manage, and decrease the vulnerability of transportation infrastructure—specifically bridges and drainages—to wildfires. The results can be immediately used through the implementation of the proposed decision-making approach, which can be utilized to manage and reduce the risks associated with wildfires.

1. INTRODUCTION

Wildfire is a natural and essential process in ecosystems (*1–3*). While wildfires have many important benefits, they can also produce disastrous effects in the wildland urban interface (*4*). In the United States, wildfires are the most prominent land management issues (*5*) and they are reported to be increasing in size, frequency, and severity (*6*, *7*). The increase in number and duration of wildfires can be attributed in part to climate-related factors including: unusually warm springs, longer dry seasons, drier vegetation, decrease in winter precipitation, and early spring snowmelt (*3*). These conditions are now commonplace, as a consequence of climate changes in much of the United States and the world; thus, climate change can be considered a major factor contributing to wildfires (*8–10*). On average, 100,000 wildfires burn about 4 to 5 million acres of land annually in the United States (*11*). It is anticipated that there will be an increase in burned area, fire occurrence, and fire intensity, in addition to fire severity, and that there will be longer fire seasons as a consequence of future climate change (*1*, *12–14*).

Therefore, there will be an intensification of the effect of wildfires on transportation infrastructure, which has already experienced notable damage. For example, the California Department of Transportation incurred approximately $15 million in damage to existing infrastructure as a result of the 2003 wildfires in San Diego (*15*). In cases such as these, proper planning for potential risk mitigation alternatives could help decrease the recovery time and disruptions to communities. However, due to the uncertainty of these events and limited budgets, it is a challenge for state departments of transportation (DOTs) to anticipate the impacts and subsequently choose and prioritize among mitigation options.

Even though extensive research has studied the vulnerability of transportation infrastructure to disaster events such as hurricanes and earthquakes, there has been limited investigation on the vulnerability of transportation infrastructure to wildfires. Bridges and drainages are especially vulnerable to wildfire-related damage, whether directly from fire heat or from subsequent flash flooding that results from fire-induced changes to the watershed and soil properties. Some of the expected post-fire induced changes include: reduced vegetation cover, soil erosion and sedimentation, slope failure, and the development of water repellency (*16*). Additional damages to transportation infrastructure might include channel degradation and drainage blockage, among others. It is thus of utmost importance to study the effect of wildfires on transportation infrastructure. The knowledge acquired in these studies would allow for the development and implementation of effective wildfire mitigation strategies and rehabilitation alternatives for infrastructure management agencies in wildfire prone areas.

1.1 BACKGROUND

1.1.1 Impacts of wildfire on transportation infrastructure

The National Research Council (NRC) states that wildfires have the following impacts on transportation infrastructure; they: (1) cause road closures due to fire threat or reduced visibility, (2) threaten transportation infrastructure directly, and (3) increase

susceptibility to mudslides. Also, watershed characteristics are directly changed by wildfires and the degree of change is correlated with the severity of the fire. Wildfire-induced changes to the watershed can result in flash floods that will affect bridges and drainages. Moderate to intense fires result in drastic changes in rainfall-runoff processes and can increase flood flows by several orders of magnitude. Hence, downstream infrastructure such as bridges and drainages that were designed to withstand a given stream discharge become inadequate to function under new conditions. Increased flood flows are often accompanied by extreme sedimentation and debris flows. The ability of the watershed to recover from such events depends on the severity of the fire, watershed characteristics (e.g., soils types and slopes), and local climate. However, previous and ongoing efforts to map flood risks and inundation patterns do not account for risks associated with drastic changes in watershed conditions—such as the occurrence of a wildfire within the basin. Classic flood risk assessments assume static background conditions or use simple modifiers to account for predicted changes such as urbanization. Wildfires, on the other hand, represent an unpredictable, sudden, and potentially severe change in basin characteristics and processes. Therefore, additional research is needed to develop techniques for incorporating this risk mechanism into assessment, mitigation, and rehabilitation methods.

1.2. WILDFIRE MANAGEMENT

Wildland and fire management is subject to sources of uncertainty and complexity including, but not limited to: metrics to guide prioritization across fires and resources at risk, lack of understanding about fire behavior response to treatments, and inaccurate and missing data (*17*). One of the major challenges in wildfire management is to determine how a fire will spread or propagate through the wildland. Thus, the main objective of a fire propagation model is to predict the spread of fire through a fuel bed. Factors that affect fire propagation can be categorized into three groups: (1) forest fuels; (2) topography; and (3) meteorological conditions (*18*).

However, wildfire management and decision-making are much more complex problems of a different nature than those of the purely physical aspects of the issue, given that wildland is typically owned by different entities with different objectives and legal/resource constraints. Water quantity and quality, sediment yield, avoided cost, avoided risk, infrastructure protection, affected community and interstate and international water compacts are some of the targeted decision factors from different agencies when determining how to distribute the limited funds for wildfire risk mitigation and planning.

1.3 POINT OF DEPARTURE AND PROJECT OBJECTIVES

Many state DOTs have bridge flood monitoring programs and inundation mapping for structures that are susceptible to bridge scour, but these tools do not include the potential of wildfires in nearby watersheds. This study integrated hydrology models and wildfire vulnerability assessment to evaluate the impact of wildfire on transportation infrastructure and potential mitigation strategies.

This study aimed to help reduce wildfire impacts on transportation infrastructure. The specific objectives of this study were to: (1) identify post-wildfire flash flood impacts, as well as risk mitigation and rehabilitation alternatives for transportation infrastructure, (2) evaluate the sensitivity of a hydrology model to site-specific input data and identify transportation infrastructure components at risk of inundation, and (3) develop a decision support approach for prioritizing and selecting mitigation and rehabilitation options.

The resulting modeling framework can be used by decision-makers as a screening tool for identifying potential problem areas and deciding where to focus further analyses on failure mechanisms, damage assessment, risk mitigation alternatives, and resource allocation. The modeling framework was expanded to include a decision-making approach by exploring wildfire vulnerability assessment for transportation infrastructure and providing suggestions, resources, and examples for prioritizing infrastructure components and selecting mitigation and rehabilitation measures. In this approach, we considered asset criticality and pre- and post-wildfire watershed conditions, among others.

2. POST-WILDFIRE FLASH FLOOD IMPACTS AND RISK MITIGATION AND REHABILITATION ALTERNATIVES FOR BRIDGES AND DRAINAGES

2.1 GENERAL HAZARDS ASSOCIATED WITH WILDFIRES

2.1.1 Introduction

Threats to life and property in wildland urban interfaces increase with the increasing number and severity of wildfires (*19*). Fire can have a direct effect by causing loss of life and property (e.g., burned structures). In addition, wildfire-related hazards can cause significant impacts on infrastructure in or near the forested land. Infrastructure refers to any development done by humans, including transportation systems. This study is concerned with transportation infrastructure—specifically bridges and drainages. In this section, general hazards associated with wildfires will first be discussed, followed by hazards specifically related to bridges and drainages, and finally mitigation measures for these hazards.

2.1.2 Post-Wildfire Flash Flood

Post-wildfire flooding is the result of the change in hydrologic parameters of the forest watershed (*5*). Hydrologic parameters such as infiltration, runoff, and peak discharge in streams change as a consequence of wildfire (*7*), due to the destruction of vegetation and alteration of soil physical properties (*20*). The hydrologic parameters modified during wildfire can take years to recover (*21*, *22*). Destruction of vegetation exposes the forest floor, which increases the erodibility of soil in the hill slope and ultimately leads to an increase in surface erosion and runoff (*5*). Due to the extreme temperature induced during wildfire, soil exhibits water repellency (*23*). After a wildfire, water repellency can be found as a layer on the soil surface or a few centimeters below the soil surface. The hypothesis for water repellency during wildfire is that organic materials are heated to such a temperature that they coat and are chemically bonded to soil particles to form a water repellent layer (*24*). Water repellency caused by wildfire reduces the rate of infiltration (*23*–*25*). Reduction in infiltration substantially increases the surface runoff, which in turn produces peak flows in rivers (*23*). Studies have shown that watersheds in the southwest are extremely vulnerable to post-wildfire floods due to the interactions of fire regimes, soils, geology, slope, and climate (*20*).

2.1.3 Debris Flows

Debris flows are one of the devastating effects of wildfires (*26*). Debris flows are exacerbated by an increase in runoff from burned areas and by an increase in erosion of soils (*27*). Debris flows generally occur as a result of the first influential rainfall just after a wildfire (*28*). Runoff from burned areas can consist of boulders, ash, mud, and vegetation, which while moving downstream can damage bridges and drainages (*29*). The intensity of storms that can initiate debris flow ranges between 1mm/h and 32mm/h with recurrence interval of two years or less (*30*).

2.1.4 Erosion

Soil erosion increases after a wildfire due to a loss of vegetation from the forest floor and exposure of bare soil to overland flow and raindrop impact (*31*). Also, soil non-

wettability may increase after a wildfire, which intensifies the surface runoff and erosion from burned watersheds (*32*). Some of the factors determining the rate of sediment production are fire severity, vegetation cover, erosion by rainfall, the hydrophobic character of soil, and soil texture (*33*).

2.1.5 Landslides

Landslides are the downslope movement of soil, rock, and organic material under the effects of gravity (*34*). Steep slopes are a principal cause of landslides (*34*, *35*). An increase in the level of water in rivers during intense rainfall can cause undercutting and erosion of the slope, which makes the slope unstable and vulnerable to landslide (*34*). Wildfire and deforestation expose the slope surface due to loss of vegetation (*34*, *36*), which can lead to weathering and changes in soil chemistry (e.g., water repellency), which ultimately can exacerbate the landslide (*34*, *37*).

2.2 POST-WILDFIRE FLOOD IMPACTS ON BRIDGES AND DRAINAGES

2.2.1 Erosion Of Transportation-Purposed Embankments

Embankments with roadways are often used to cross low elevations. Culverts are often used in the embankments to allow water to pass beneath them. If the capacity of the culvert is inadequate (e.g., due to a post-wildfire flood), water will impinge on the side of the embankment. Roadway embankments are generally not designed to be barriers against water (in contrast to levees) and can suffer deleterious consequences as a result.

Flood waters that overtop a roadway embankment can cause serious problems, including significant erosion of the embankment. As water moves over the embankment, erosion can be initiated on the downstream slope or at the downstream toe, depending on the flow conditions and geometry (*38*). Continued flow results in progressive erosion of the downstream slope of the embankment. Eventually the erosion can reach the top slope and result in a complete breach and failure of the embankment. Overtopping erosion can also erode granular shoulders and pavements, as well as the gravel surface of unpaved roadways (*39*).

Internal seepage erosion occurs when water moves through or beneath the embankment. Depending on the materials that comprise the embankment and its foundation, the flow may be sufficient to displace particles within the embankment. This internal erosion often begins on the downstream side and develops backwards against the direction of flow. This type of erosion is often referred to as “piping.” Internal erosion that begins inside the embankment is possible, especially if flow is concentrated along a crack or discontinuity within the embankment. Internal erosion can result in voids developing within the pavement foundation (*39*). If there is sufficient internal erosion, a complete breach of the embankment can occur. Bonelli (*40*) indicated the internal erosion can be initiated at the contact between soil and culverts in part because relatively poor compaction immediately adjacent to the culvert can result in preferential flow in this region.

2.2.2 Weakening of Embankments from Increased Saturation

When an embankment with a drainage structure is wetted due to flooding, the strength and stiffness of the materials that comprise the embankment decrease significantly (*39*, *41*). Falling weight deflectometer measurements indicated that the modulus values were 1.3 to 3.6 times lower in flooded sections compared to non-flooded sections (*39*). The lowered strength and modulus of the pavement system may result in pavement damage such as severe rutting and cracking. Even after the flood waters recede, some layers within the embankment may remain at or near saturation, and the strength and modulus of these layers will remain significantly reduced compared to their design values.

2.2.3 Debris Flows

Debris flows can have a severe impact on bridges, including a decrease in water conveyance capacity, an increase in contraction and local scour, an increase in hydraulic loading, and flooding effects in the upstream zone (*27*). Erosion of abutments and riverbanks may occur due to contraction of the conveyance channel by accumulation of debris near the bridge structure (*27*). Debris flow during flooding can clog the inlet of the culvert (*42*). As a consequence, the conveyance capacity of the culvert decreases (*43*), leading to effects such as flooding on the upstream side, change in peak flow on the downstream side, and overflow of water at the culvert, causing failure of the road embankment and drainage structure (*43*).

Barthelmess and Rigby (*44*) have discussed a simplified approach to estimating culvert and bridge blockages. The three factors that influence the debris potential at a site are debris availability, debris mobility, and debris transportability (*45*). The extent of blockage is determined by the interaction between structure geometry and debris geometry (*44*). The simplified approach to estimating culvert blockages considers individual qualitative debris potential, mobility and transportability and the combination of the three, and quantify the debris potential at a site based upon the source. Further, the likelihood of culvert blockage can be obtained by identifying the dominant debris and blockage type together with delivery timing and debris size.

Tillery, et al. (*46*) provided a method to estimate the probability and volume of debris due to a wildfire. Their approach considers drainage basin ruggedness, percentage of drainage basin area burned at moderate and high severity, average storm intensity (the total storm rainfall divided by the storm duration, in millimeters per hour), percent clay content of the soil, liquid limit of the soil, and total storm rainfall (in millimeters), among other factors.

2.2.4 Scour

Bridge scour is a principal cause of the failure of bridge foundations (*47*). Bridge scour is caused by flowing water, which erodes soil surrounding the foundation of bridge piers (*48*). Because scour increases with water velocity, significant scour often occurs during periods of high flows (*49*). General scour, contraction scour, and local scour are the major scour types at bridge sites (*50*). General scour is classified as long term or short term. Short-term general scour occurs due to single or closely spaced floods, whereas long-term general scour is generally due to long term events. Scour due to shifting of thalwegs and scour at bends are some examples of short-term general scour, and progressive degradation and bank erosion are results of long term scour. Contraction

scour occurs when a river channel is narrowed at the bridge section, which results in increased flow acceleration. Lastly, local scour is the result of flow obstruction by the bridge structure itself, and it can damage the bridge pier or abutments (*50*). Local scour occurs when a complex vortex system is generated around the bridge pier or abutment. When flow hits the pier, downflow occurs at its upstream face. The downflow initiates a scour hole in front of the pier and rolls back to generate a horseshoe vortex. In addition, due to separation of flow, wake vortices are formed. These wake vortices generate independent scour holes at the downstream of the pier (*49*, *51*).

2.2.5 Landslides

Landslides can cause devastating effects on transportation infrastructure, including bridges (*52*, *53*). There can be direct effects caused by a direct strike on the bridge, or there can be indirect effects, such as through mixing of a landslide with water bodies (*34*). For example, landslides may dam a river and cause flooding. When this artificial dam bursts it can cause destruction on downstream structures (*34*).

2.3 MITIGATION AND REHABILITATION OF GENERAL HAZARDS FROM WILDFIRES

2.3.1 Wildfire Mitigation

In the 20th century, wildfire suppression was a widely practiced mitigation strategy to minimize the adverse impacts of wildfire (*8*, *54*). Studies have found that wildfire suppression contributes to fuel accumulation in the forest (*55*), which in turn causes more severe wildfire in the future (*2*, *8*). Thus, fire suppression policy should include vegetation management for effective forest management (*54*). Fuel reduction and prescribed fire are the two widely used methods of vegetation management (*19*, *56*), but since the sources of ignition are widespread, it is almost impossible to avoid wildfire (*57*). Therefore, the main objective of vegetation management is to reduce the severity of wildfire and make it more acceptable, rather than to decrease the extent of wildfire or to make wildfire suppression easier (*57*).

2.3.2 Slope Erosion Rehabilitation

Generally applied methods to check post-wildfire erosion are seeding, mulching, and erosion barriers (*58*). After the Valley Complex Fire in Montana in 2000, Robichaud et al. (*58*) studied the effectiveness of runoff erosion mitigation strategies like contour felled logs, straw wattle, and hand-dug contour trench erosion barriers. They did the comprehensive field experiment to determine the effectiveness of mitigation methods to reduce runoff and erosion. Robichaud et al. (*58*) determined that effectiveness depends upon many factors, including rainfall intensity, soil cover, time after wildfire, and selection of sampling sites.

Robichaud et al. (*59*) studied the production and application of wood shred mulch to reduce erosion on post-wildfire hill slopes, and they also compared the effectiveness of wood shred mulch with agricultural straw. They selected sites near the Schultz Fire (2010), Cascade Complex Fire (2007), Fourmile Canyon Fire (2010), Waldo Canyon Fire (2012), Beal Mountain Abandoned Mine Site (2011), and High Park Fire (2012). They determined that wood shred mulch works well in areas with a steep slope as well as areas with heavy winds. They concluded that wood shred mulch was more effective

than agricultural straw to reduce the erosion rate. Further, dry mulches were more effective to reduce post-fire runoff than hydromulches (*5*). Robichaud et al. (*5*) also concluded that the use of dry mulch such as agricultural straw, wood strands, and wood shreds is more common and effective than erosion barrier treatments like contour felled logs and straw wattles in reducing the erosion rate from post-wildfire lands.

2.3.3 Landslide Mitigation

Landslide mitigation can be done by stabilizing the slopes in landslide vulnerable zones. Some of the measures suggested by Highland and Bobrowsky (*34*) are construction of structures including rock curtains, retaining walls, and anchoring of unstable slopes. Mitigation measures suggested by Dai et al. (*52*) include provision for drainage on slopes and modification of highly unstable slopes. They also suggested to avoid or minimize the development through landslide-susceptible zone in order to reduce the risk of landslide effects.

2.4 FLOOD-RELATED HAZARD MITIGATION FOR BRIDGES AND DRAINAGE

2.4.1 Reducing Transportation-Purposed Embankment Erosion

Overtopping erosion can be mitigated by increasing the erosion resistance of embankment slopes. This can be accomplished by vegetation, especially grasses (*41*). Of course, the effectiveness of relying on vegetation to improve erosional stability depends on the climate and soil conditions. Armoring the slope with riprap, gabions, and precast articulated concrete block blankets are other options for reducing erosion susceptibility.

To reduce internal erosion, drainage features would need to be designed into the embankment. In particular, a toe drain on the downstream side would be helpful in reducing the initiation of piping erosion.

2.4.2 Debris Flow Mitigation

Tyler (*60*) studied the impact of debris flows on engineering structures such as bridges. He has discussed possible mitigation measures to minimize the damage to structures. One technique discussed is the Treibholzfange debris-detention device, used to reduce the impact of debris on structures. To capture the debris, the device has a circular post that is driven into the river bed. Depending upon the geometry of the post, different sizes of debris can be accumulated and handled. Another is the use of debris booms. Debris booms can deflect surface debris only. Another widely used technique in bridge construction is the use of debris fins. Debris fins are constructed in the upstream vicinity of a bridge and they guide the debris to flow in one direction. River training structures are another method to reduce debris impacts. These structures change the flow direction of the river to try to accumulate the debris on the riverbank before it reaches the bridge structure. Sweepers and deflectors are placed near the bridge on the upstream side; their main job is to prevent the accumulation of debris near the bridge.

Bradley et al. (*27*) listed countermeasures to protect bridges from the impacts of debris flow. They divided the countermeasures into two categories: structural and non-structural measures. The countermeasures described by Bradley et al. (*27*) are listed in **Table 1**. Table 2 shows examples of countermeasures for post-wildfire debris flow *(61)*.

Table 1. Countermeasures to Reduce the Impacts of Debris Flow

Type	Countermeasure	Method of Application	Purpose of application
Structural	Debris fins	Construction of wall on the upstream side of river	To make floating trees parallel to the flow so that they can pass easily
Structural	In-channel debris basin	Constructed across the specified channel	To form a basin and accumulate detritus and floating debris before it reaches the bridge
Structural	River training structure	Constructed across the river cross section	To redistribute flow and sediment transport
Structural	Crib structure	Construction of wall between open-pile bents	To prevent accumulation of debris in bents
Structural	Flood relief sections	Construction of structures near the bridge	To divert the excess flow and debris away from the bridge
Structural	Debris deflectors	Constructed upstream of a bridge-generally in V shape in plan with notch in upstream	To deflect and make debris pass easily through the bridge opening
Structural	Debris sweeper	Polyethylene device placed upstream of the bridge; it can rotate on its vertical axis and rise and fall as per the flow level	To spread debris away from the pier
Structural	Booms	Floating logs or timbers by supporting them laterally	To collect floating drift
Structural	Design feature	Providing adequate freeboard, aligning the pier in the direction of flow, providing proper spacing of piers and providing proper access to different parts of bridge for maintenance	To reduce the effect of debris on the bridge
Non-Structural	Emergency Maintenance	Removing debris, construction of riprap and cleaning of debris from channel	To immediately protect the bridge from debris
Non-Structural	Annual Maintenance	Debris removal and repair of damaged structure	To keep the bridge in working condition
Non-Structural	Management of upstream watershed		To reduce the debris volume reaching the bridge

Table 2. Examples of Countermeasures to Reduce the Impacts of Debris Flow Related to Wildfire (61)

Countermeasure	Method of Application	Purpose of application
Surface treatment	a) Seeding of burned landscape b) Mulching	To reduce erosion of burned landscape
Debris rack		To contain debris

2.4.3 Scour Protection

Zarrati et al. (*51*) have defined countermeasures to prevent local scour at bridges. They divided the mitigation measures into two categories: armoring devices and flow-altering devices. The mitigation measures are listed in Table 3.

Table 3. Countermeasures to Protect Piers From Local Scour (51)

Armoring Devices	Flow-Altering Devices
Cable-tied blocks, tetrapods, dolos, placed riprap rocks, flexible mattresses, grout mat and bags, anchors	Sacrificial piles upstream of the pier, Iowa vanes, flow deflectors attached to pier (e.g., collars and slots)

Zarrati et al. (*51*) discussed the effectiveness of flow deflectors, that is, collars attached to piers, in reducing the effect of local scour on bridge piers. They concluded that collars are most effective on the two piers which are aligned in the direction of. Collars were not effective for the two piers in the transverse direction of flow.

Grimaldi et al. (*62*) studied the effectiveness of bed sills to protect bridge piers from scouring. They stated that reduction of scour holes should be the primary objective of countermeasures for scouring. From experimental results, they found that if a bed sill is placed in front of a pier, downstream, the scour depth can be reduced by 26% and the scour area and volume can be reduced by more than 80%.

Chiew (*63*) described some of the methods to protect bridges from scour, including traditional methods such as boulders and riprap in the bridge vicinity. Chiew emphasized that riprap requires the use of an underlying filter to prevent leaching of sediment particles through the voids of the riprap stone. Using slots in the pier, near the water surface or at the bed, was found effective to reduce scour. Slots allow flow through the pier with minimum obstruction, which in turn decreases the erosion potential of the flow (*63*). Using a collar around the bridge pier was also found to be an effective way to reduce the erosion caused by downflow (*63*). The effectiveness of sacrificial

piles, installed upstream of a bridge pier, to reduce the scour around the bridge pier was studied by Wang et al.(*64*). They performed an experimental study and numerical simulation for the investigation. They found that sacrificial piles change the flow field and reduce the erosive force of the flow before it reaches the bridge pier and can reduce scour up to 50%.

2.5 SUMMARY

Numerous hazards from post-fire flooding have been identified for transportation infrastructure; in particular, bridges and drainages. A key issue is whether the bridge or drainage has the capacity to handle the increased runoff from a post-fire flood. If there is insufficient capacity with the anticipated flow, it will be necessary to take measures to reduce the runoff. These measures might include managing the forested land through controlled burns and debris removal to minimize the size and intensity of inevitable wildfires. Additional measures may include armoring and protecting select bridges and drainages from scour and erosion.

If the bridges and drainages have sufficient capacity for the anticipated post-fire flood event, then damage to the transportation infrastructure should not occur, unless the capacity of the bridge or drainage is reduced from partial or complete blockage from debris or sediment. In these cases, preventing debris from blocking bridge openings and culverts is a principal mitigation strategy.

3. HYDROLOGIC MODELING TO ESTIMATE TRANSPORTATION INFRASTRUCTURE COMPONENTS AT RISK

3.1 INTRODUCTION

Post-wildfire runoff and flooding can adversely affect bridges and locations where roadways cross drainage structures such as culverts (*7*). Flooding can cause damage and failure of bridges due to hydraulic loading on the piers, hydraulic loading on the bridge deck, scour of bridge foundations, erosion of the abutments, and impact from debris such as logs hitting the bridge (*65*, *66*). Additionally, erosion associated with flooding has been linked to the failure of many highway culverts (*67*).

Post-wildfire damage to transportation infrastructure is mainly driven by increased runoff, erosion, and debris flow from fire-related changes in vegetative cover and soil properties. The ability of the post-fire hydrology model to effectively describe and account for these changes is critical in estimating (predicting) the damage from a fire event as well as informing risk mitigation and rehabilitation decisions. The hydrology model describes the complicated interaction between water, land surface, and underlying soil under time-varying climate conditions. Many individual processes are combined in the hydrology model (e.g., rainfall interception, infiltration, soil detachment, etc.); each process requires input data. For example, modeling infiltration requires post-fire saturated and unsaturated soil properties as a function of the depth in the near surface. Site-specific data are most often not well known, especially for soil properties, and approximate values based on very limited data and/or judgment are used.

Transportation infrastructure, particularly bridges and other locations where roads or rail lines cross drainage structures, are vulnerable to direct and indirect hazards produced by wildfires. Overtopping of roadway embankments can occur for a wide range of transportation systems, especially at road–stream culvert crossings. Overtopping is therefore a common concern to many transportation agencies and jurisdictions (*68*). Roadway inundation from overtopping often requires road closure, a direct impact that results in costs associated with lost time and increased travel miles to avoid the closure. Overtopping can deteriorate the transportation system through erosional processes on the surface (*69*) as well as internally to the roadway embankment (*40*). Roadway inundation results in a softening of the roadway foundation (*68*), contributing to pavement-system deterioration such as rutting and cracking.

In this section, we propose a framework which integrates pre- and post-wildfire rainfall-runoff modeling and floodplain analysis under different climate and burn severity scenarios to quantify the impacts of post-wildfire flood on transportation infrastructure. The framework is demonstrated using the case study of the Las Conchas wildfire in the state of New Mexico. Model predictions of roadway inundation due to overtopping of roadway embankments at road–stream culvert crossings are used to quantify the impact of the flooding under different climate and burn severity scenarios. The framework to quantify the impacts of post-wildfire roadway inundation on transportation

infrastructure integrates rainfall-runoff modeling, floodplain modeling, GIS modeling, and hazard assessment for the evaluation of post-wildfire hazard.

3.2 RAINFALL-RUNOFF MODEL

Rainfall-runoff modeling is conducted using the kinematic runoff and erosion model, KINEROS, in the Automated Geospatial Watershed Assessment (AGWA) tool. AGWA uses layers of information and data in a GIS framework to parameterize, execute, and spatially visualize results for the KINEROS watershed runoff models. AGWA is a free GIS extension and can be used with ArcGIS 10.x. The version used in this project is AGWA 3.x with ArcGIS 10.4.

The KINEROS model can reasonably describe the runoff process on the burned southwestern watersheds, where infiltration rates are low and rainfall is infrequent but intense (*70*). Canfield et al. (*70*) used the KINEROS model at the Starmer Canyon watershed, Los Alamos, New Mexico, to predict the runoff after the Cerro Grande fire. Their results showed that this model can give a good estimate of the change in peak runoff due to wildfire. Shakesby et al. (*71*) have mentioned that KINEROS2/AGWA has the capability to represent the actual wildfire effects. Sidman et al. (*72*) studied the effectiveness of KINEROS2/AGWA to represent the post-wildfire peak flow. They concluded that peak discharge in the model greatly depends upon the rainfall representation at study sites. They stated that with high-quality rainfall data the model can provide results within 20% of observed measurements, even in the absence of calibration steps. Also, rainfall representation in the model has less effect in predicting the area of high risk of the post-wildfire flood (*72*).

The input parameters important for modeling the effects of wildfire on a watershed are land cover and soil characteristics. Utilizing built-in functions in AGWA, input parameters including land cover, percent impervious, interception, and Manning's N, are obtained from the spatial land cover data layer within ArcMap for pre- and post-wildfire conditions. AGWA also extracts the soil characteristics from the spatial soil data layer within ArcMap. The land cover modification tool is used to estimate the post-wildfire land cover from the pre-fire land cover. The land cover modification tool basically converts the pixel value of land cover based upon the burn severity, which results in a change to soil properties to reflect the post-fire conditions.

3.3 FLOODPLAIN MODEL

Floodplain modeling is performed by using two tools developed by the U.S. Army Corps of Engineers (USACE)—HEC-GeoRAS and the Hydrologic Engineering Center's River Analysis System (HEC-RAS). HEC-GeoRAS is an extension for ArcGIS. It provides an interface to digitize the river in the graphical user interface so that the data can be exported to HEC-RAS for analysis. HEC-GeoRAS is also used for processing water surface profile data from the HEC-RAS simulation for GIS analysis for floodplain mapping. HEC-RAS performs the one-dimensional steady flow calculation for floodplain mapping. It uses geometric data from HEC-GeoRAS, flow data from the rainfall-runoff model (AGWA) to do the steady flow calculation. The major steps involved in the floodplain modeling framework are shown in Figure 1.

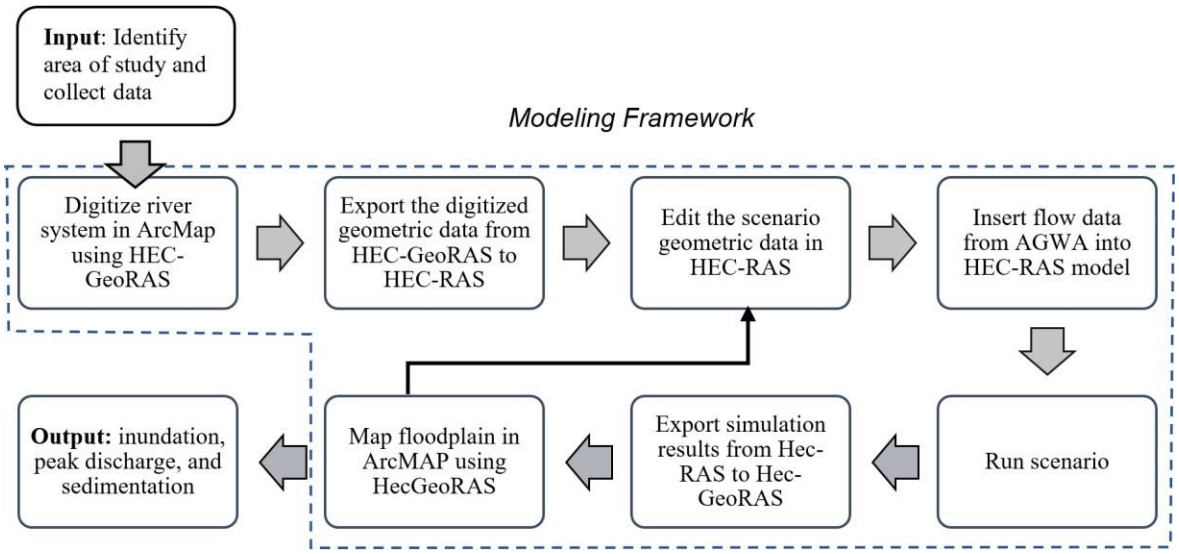

Figure 1. Major Steps Involved in Modeling Framework Using ArcGIS, HEC-GeoRAS, and HEC-RAS

HEC-GeoRAS is used along with ArcMap to digitize the river system. HEC-GeoRAS helps in defining the geometry of the river so that it can be exported to HEC-RAS for analysis. The geometrical features that are created in HEC-RAS are the river centerline, banks, flow paths, bridges, and a cross section along the river.

HEC-GeoRAS is then used to process results of HEC-RAS floodplain mapping. HEC-RAS is used to do one-dimensional steady flow and unsteady flow analysis. For steady flow simulations, the peak discharge from the runoff model is used. The river system digitized in HEC-GeoRAS is imported to HEC-RAS and modified if necessary. The bridge locations are defined before the analysis. Then the steady flow data, which is the peak discharge from the KINEROS model, is provided as the input to the software. After geometric data and steady flow data are finalized, the model is run. For better visualization, the output is exported to HEC-GeoRAS for floodplain mapping.

For unsteady flow simulations, the entire discharge vs. time data from the runoff model is used. We used unsteady flow simulations to provide a time history of flood depth along cross sections of the model.

3.4 MODELING APPROACH TO ASSESS THE IMPACT OF POST-WILDFIRE FLOODS ON TRANSPORTATION INFRASTRUCTURE

The modeling framework is used to analyze the impact of post-wildfire floods on transportation infrastructure. Specifically, the modeling is used to predict roadway

inundation due to overtopping of roadway embankments that have culverts passing through them. Roadway inundation is taken as the principal indication of impact because, as stated above:

- Roadway inundation often requires road closure, a direct impact that results in costs associated with lost time and increased travel miles to avoid the closure. In some cases, road closures may impact access to critical facilities, including health care.
- Roadway inundation can deteriorate the transportation system through erosional processes on the surface (shoulder, roadway, embankment slopes) as well as internally to the roadway embankment (piping).
- Roadway inundation results in a softening of the roadway foundation, contributing to pavement system deterioration such as rutting and cracking.
- Roadway inundation is possible for a wide range of transportation systems (locations, capacity), and is thus a common concern to many transportation agencies and jurisdictions.

Roadway inundation is used to quantify the impact of the flooding because inundation can have a range of deleterious consequences, from roadway closure during the flooding event to long-term deterioration of the roadway foundation. In this study, inundation is used as an indicator of impact to the transportation system. It is possible to estimate the damage from specific failure modes (e.g., erosion, foundation softening) associated with overtopping and inundation; however, these types of detailed analyses are beyond the scope of this work. The framework can be used by decision-makers as a screening tool for identifying potential problem areas and deciding where to focus further analyses on failure mechanisms, damage assessment, risk mitigation alternatives and resource allocation.

The modeling framework is applied to a series of different scenarios associated with post-wildfire flooding to assess the factors that control possible roadway inundation. Factors include:

- Climate—Potential future climate change scenarios will likely include higher intensity storms, which lead to more runoff.
- Burn severity—Runoff increases with burn severity due to more vegetation loss and increased impact on soil properties.
- Blockage of drainage culverts—Debris may block or partially block culverts and bridges. These effects are exacerbated post fire due to the large amount of available downed material and the increased runoff that can mobilized this debris.

3.5 CASE STUDY

3.5.1 Site

The site selected for the case study was the Los Alamos Canyon watershed. On June 2011, a tree fell onto a power line and ignited the fire referred to as the Las Conchas Fire. The wildfire became the largest wildfire in New Mexico at that time; it burned

approximately 47.8 km^2, (about 156,000 acres), equivalent to 28% of the Los Alamos Canyon watershed. The fire severity distribution was: High Severity Burn = 6.61 km^2, Medium Severity Burn = 14.25 km^2, and Low Severity Burn = 21.92 km^2. The study area along with the wildfire, streams, roads, and drainages (culverts) are shown in Figure 2. The watershed consists of three major canyons, namely Los Alamos Canyon, Pueblo Canyon, and Guaje Canyon. At the confluence of these canyons and on the canyons path itself there are drainage structures, i.e., culverts. From the National Bridge Inventory (NBI), 5 culverts were identified in the Los Alamos Canyon watershed. The culverts are described in Table 4 and the location of the culverts and reaches are depicted in Figure 3. Photographs of four drainage structures in this watershed are shown in Figure 4

Figure 4. Three culverts were selected for analysis based on data availability (C1, C2, and C3).

Table 4. Culverts located in Los Alamos Canyon Watershed

ID	Description	Diameter / other characteristics
C1	Concrete pipe culvert with two identical barrels	Diameter = 10 feet
C2	Box Culvert with three identical barrels	Each Barrel: Span =7.5 feet, Rise = 6 feet, Flared wing wall
C3	Concrete pipe culvert with two identical barrels	Diameter = 10 feet
C4	Box Culvert	Could not locate in field visit.
C5	Box Culvert with four identical barrels	Each Barrel: Span =8 feet, Rise =12 feet, Flared wing wall

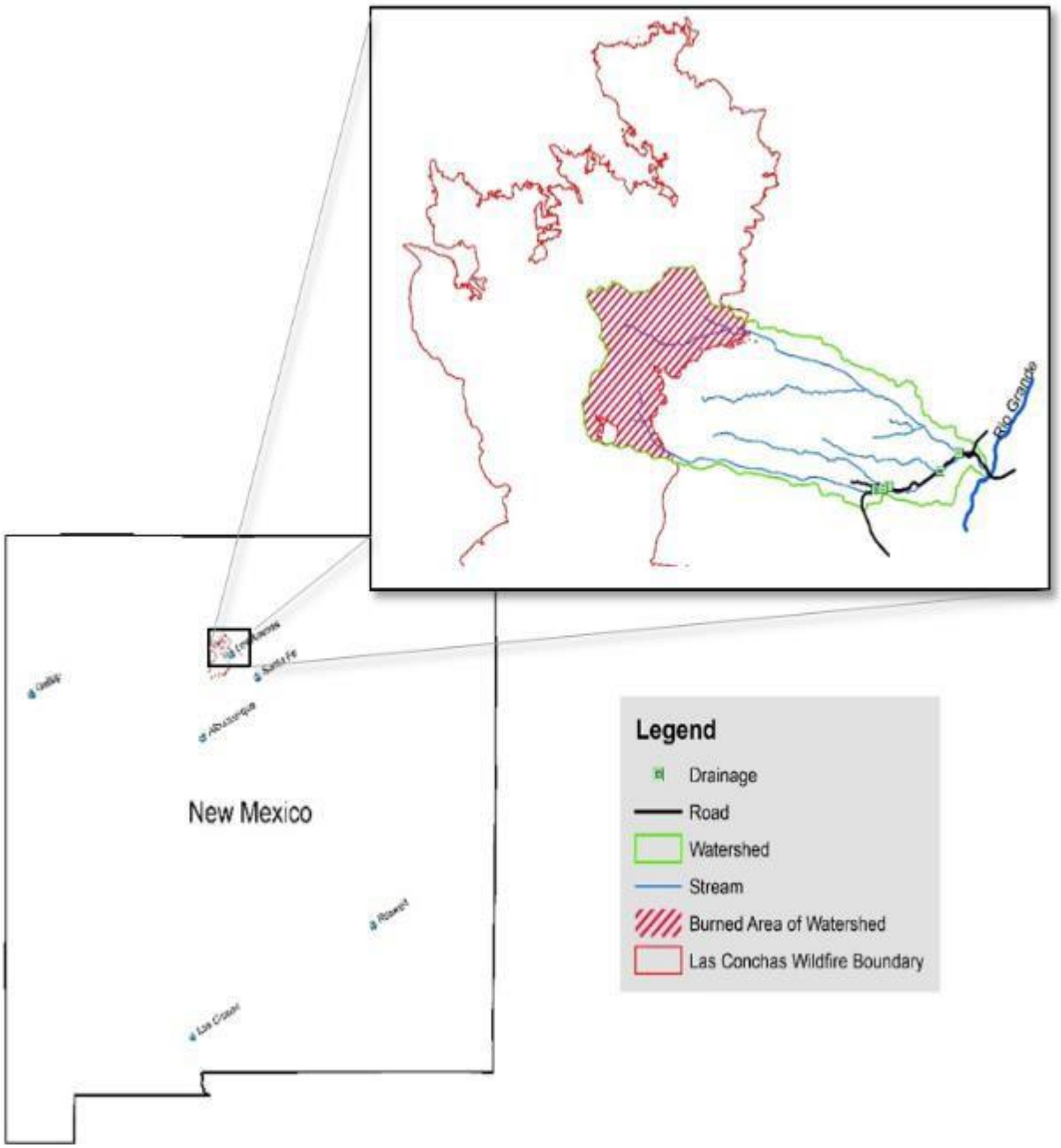

Figure 2. Location of the Study Site

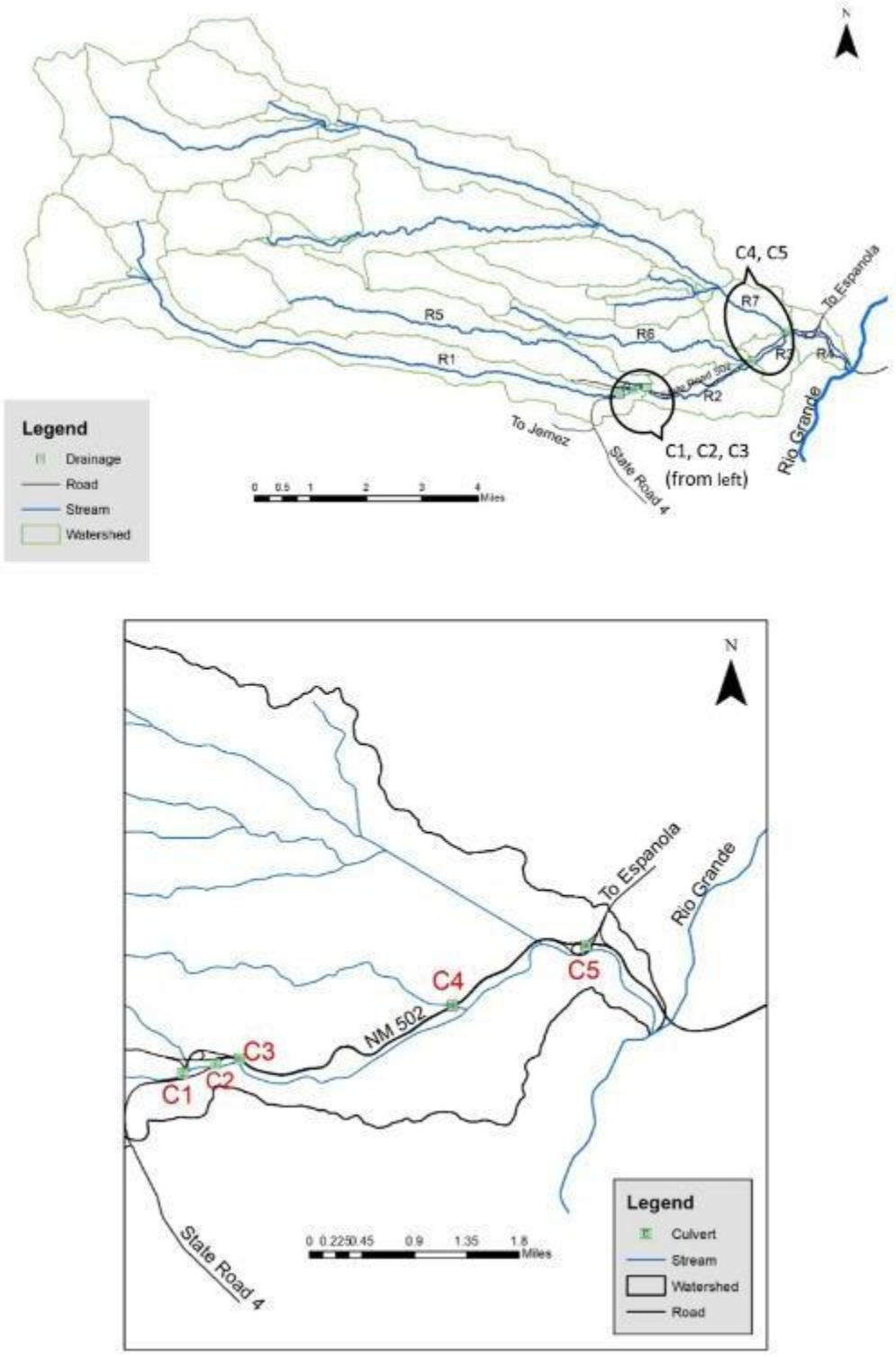

Figure 3. Location of Culverts and Reaches in Los Alamos Canyon Watershed

Figure 4. Culverts Located in the Study Area (Looking Downstream)

3.5.2 Modeled Scenarios

A number of different scenarios were modeled as illustrated in Figure 5. These scenarios included:

- Climate—Two climate scenarios were considered as input to the modeling. The baseline climate is represented by the 100-year 6-hour rainfall for the study site. The baseline input is derived from the literature (*73, 74*)). The second climate scenario was represented by a 200-year 6-hour duration rainfall in place of the 100-year 6-hour rainfall, to consider the effect of possible future climate change (*75–80*). Stated differently, the recurrence interval of rainfall has been reduced from 200 years to 100 years to model the potential future climate.
- Burn severity—Three different burn severity scenarios were modeled. The first is the burn severity data for the Las Conchas Fire, published by the United States Department of Agriculture (USDA) Forest Service (Figure 6). The map reveals that the burn severity was highly variable across the modeled site. To provide alternative burn severities, assumed uniform medium and high burn severities throughout the watershed were also evaluated.
- Culvert obstruction/blockage—Four cases of culvert obstruction were considered to model debris blockage at the entrance and within the culverts. Models were evaluated with 0, 25, 50, and 75% of the area of the culvert assumed to be blocked, which reduced the capacity of the culverts.

In addition, a pre-fire model was evaluated to establish a baseline condition.

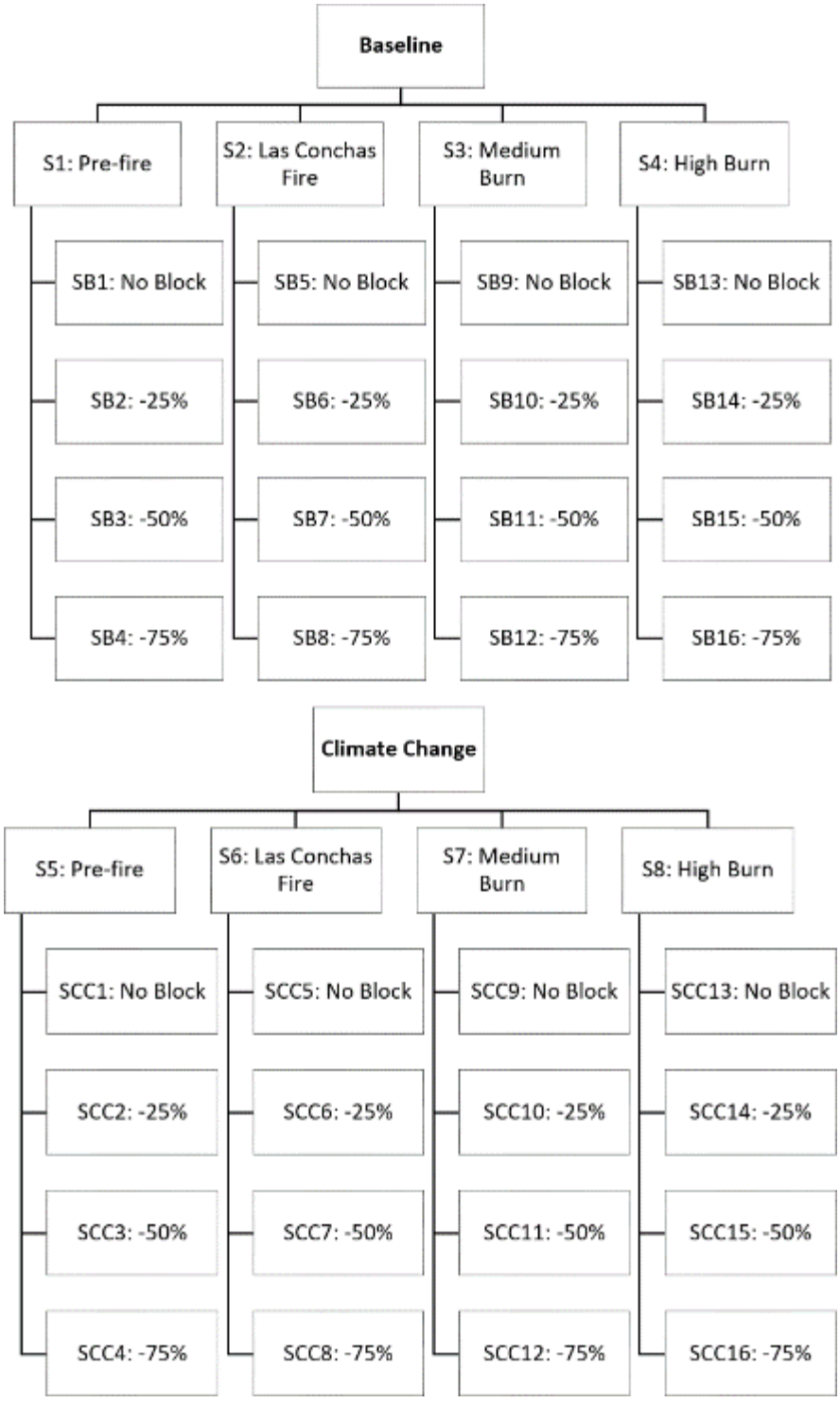

Figure 5. Scenarios Considered for Analysis Under Baseline and Climate Change Conditions

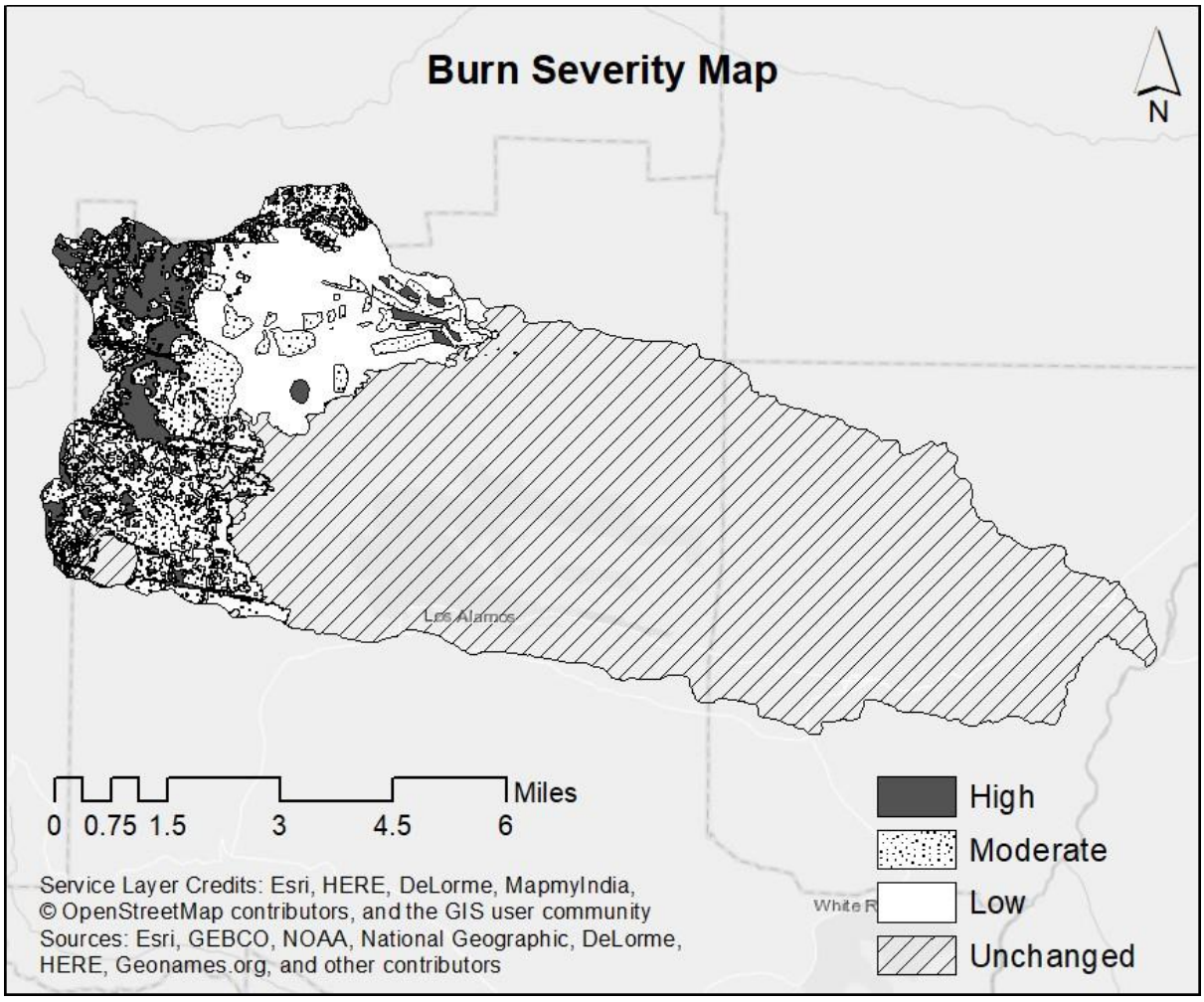

Figure 6. Burn Severity Map for Las Conchas Fire

3.5.3 Data Collection

Data were collected for the rainfall-runoff analysis and floodplain mapping. The major data collected, along with their source, are listed below in Table 5.

Table 5. Data and Their Sources

Data	Source	Description
Land Cover (30m Resolution)	Homer et al. (2015) (*81*)	Latest version of land cover product developed by Multi-Resolution Land Characteristics Consortium. This represents the land cover before the wildfire.
State Soil Geographic (STATSGO2) Dataset (1:250,000)	Web Soil Survey (2017) (*82*)	Dataset containing the properties of New Mexico soil. This contains information on soil properties such as hydraulic conductivity, composition of soil, and hydrologic group of soil.
10m DEM	EarthExplorer (2017)(*83*)	Digital elevation model of the New Mexico area. It is used to obtain the elevation of the earth surface and it is used in rainfall-runoff modelling.
1 feet DEM	Los Alamos National Laboratory (2017) (*84*)	High resolution digital elevation model which is used in the floodplain modelling.
Wildfire Boundary	NMRGIS (2017) (*85*)	Map shows the boundary of the wildfires in New Mexico, occurring from 1911 through 2014. The Las Conchas wildfire boundary was identified through this dataset.
Las Conchas Wildfire Severity Map	Remote Sensing Applications Center, USDA Forest Service (2017) (*86*)	The wildfire severity map is published by Burned Area Emergency Response Imagery Support program of the USDA Forest Service Geospatial Technology and Applications Center and the U.S. Geological Survey Center for Earth Resources Observation and Science .
National Bridge Inventory	National Bridge Inventory (NBI) Bridges (2017) (*87*)	Contains information about the nation's bridges.

3.6 RESULTS

3.6.1 Rainfall-Runoff Modeling

Figure 7 shows the floodplain model generated for the case study. Table 6 shows the output from the rainfall-runoff model for 100-year return period rainfall (baseline) and 200-year return period rainfall (representing a potential future climate). For each return period, four different scenarios with respect to burn severity were evaluated for seven reaches in the canyon. Refer to Figure 3 for the location of the reaches and culverts within the watershed, and Figure 5 for a description of the labeling of the scenarios with respect to burn severity. The total runoff and sediment yield were calculated at the end of each reach as shown in Table 6.

These results reveal that significantly different discharges develop in the different reaches under all scenarios. Reach 1, which is directly involved with the culverts under analysis, produces the highest percentage change (up to +207%) in runoff discharge rate when compared to the pre-fire scenarios. Reach 4 and Reach 7 produce the greatest runoff discharge rates, whereas Reach 6 results in a nearly zero runoff discharge rate and sediment yield. The amount of discharge is directly related to the climatic conditions and burn severity in the expected manner—runoff discharge increases with increasing burn severity and runoff increases with climate change conditions.

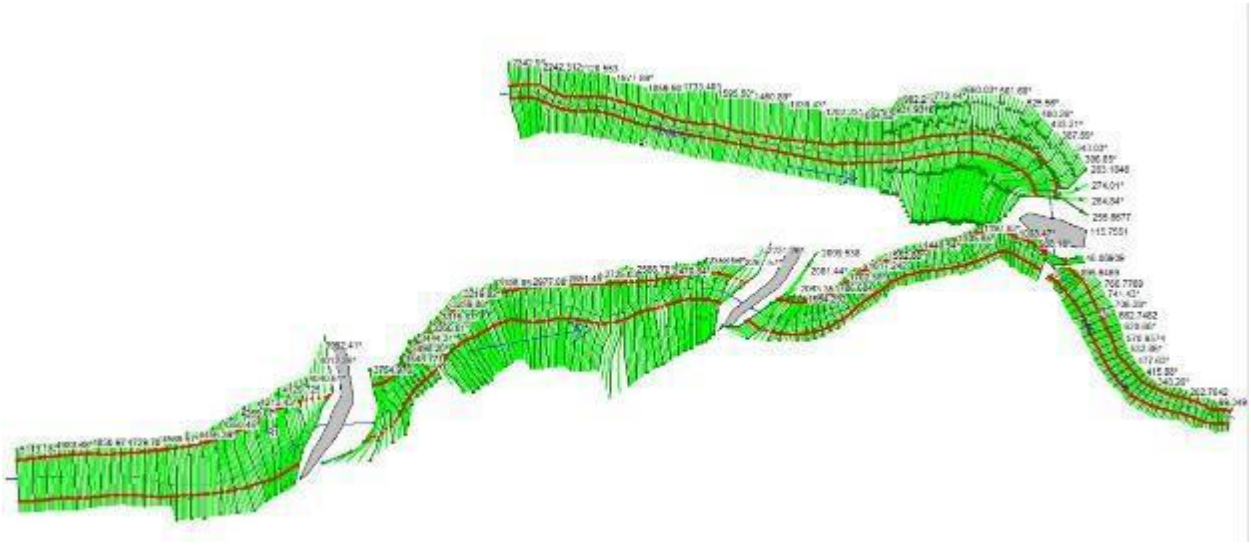

Figure 7. Floodplain Model

Table 6. Runoff and Total Sediment Yield

	Baseline 100 Year Return Period(6-hour precipitation=2.85mm)								Climate Change 200 Year Return Period(6-hour precipitation=3.17mm)							
	S1	**S1**	**S2**	**S2**	**S3**	**S3**	**S4**	**S4**	**S5**	**S5**	**S6**	**S6**	**S7**	**S7**	**S8**	**S8**
	Dis-charge (cfs)	**Sedi-ment Yield (lbs/ ac)**	**Discharge (cfs)**	**Sedi-ment Yield (lbs/ ac)**	**Discharge (cfs)**	**Sedi-ment Yield (lbs/ ac)**	**Discharge (cfs)**	**Sedi-ment Yield (lbs/ ac)**	**Discharge (cfs)**	**Sedi-ment Yield (lbs/ ac)**	**Discharge (cfs)**	**Sedi-ment Yield (lbs/ ac)**	**Discharge (cfs)**	**Sedi-ment Yield (lbs/ ac)**	**Discharge (cfs)**	**Sedi-ment Yield (lbs/ ac)**
R1	392	6015	882	22148	979	29804	1204	43403	771	15590	1366	38255	1569	50931	1860	72882
R2	902	8626	1459	17510	1596	21797	1811	28916	1635	18818	2253	31300	2538	38742	2810	50074
R3	884	4009	1441	8484	1579	10740	1793	14546	1615	9581	2233	16508	2518	20683	2791	26603
R4	3273	-	5605	-	6094	-	6731	-	5393	-	8127	-	8748	-	9428	-
R5	600	7981	618	8403	662	9198	667	9323	920	16564	952	17245	1027	19099	1031	19242
R6	1	7	1	7	1	7	1	7	7	67	7	67	7	67	7	67
R7	2389	15126	4164	33568	4515	41931	4937	55726	3778	29861	5894	56169	6230	68455	6638	87662

3.6.2 Steady Flow Floodplain Modeling

Floodplain modeling was conducted using the results from the rainfall-runoff analysis. For each rainfall-runoff scenario, four separate models were run with different amounts of culvert blockage. This results in 32 different scenarios were considered as described in Figure 5. The analyses were run for Culverts 1, 2 and 3.

3.6.2.1 Flood Depth at Culvert Inlets

One output from the steady floodplain modeling we evaluated was the flood depth at the inlet to culverts within the watershed. By considering the flood depth at select culvert inlets, the impact of parameters (climate, burn severity, culvert blockage) can be directly compared. In Figure 8, the flood depth at the inlet to Culvert 1 (C1—see Figure 3) is given as a function of the percent of culvert blockage for the baseline climate and the climate change conditions. In Figure 9, the same results are given, but are presented as flood depth as a function of burn severity for the two climate conditions. These figures clearly show the percent blockage has a very large impact on results from both climate scenarios. It appears that with increasing blockage, a maximum flood depth of about 17 feet is approached for all burn severities and climatic conditions.

In Figure 10, the flood depth at the inlet to Culvert 2 (C2—see Figure 3) is given as a function of the percent of culvert blockage for the baseline climate and the climate change condition. In Figure 11, the same results are given, but are presented as flood depth as a function of burn severity for the two climate conditions. These figures clearly show the percent blockage has a very large impact on results from both climate scenarios. The results appear to be sensitive to whether or not there was a burn, not so much as to the degree of the burn. In Figure 11, under climate change conditions and no blockage, an apparently contradictory result is shown as the flood depth for the case of high burn severity is less than that for medium burn severity. This result is a consequence of an instability in the numerical solution for these conditions as identified in the model output.

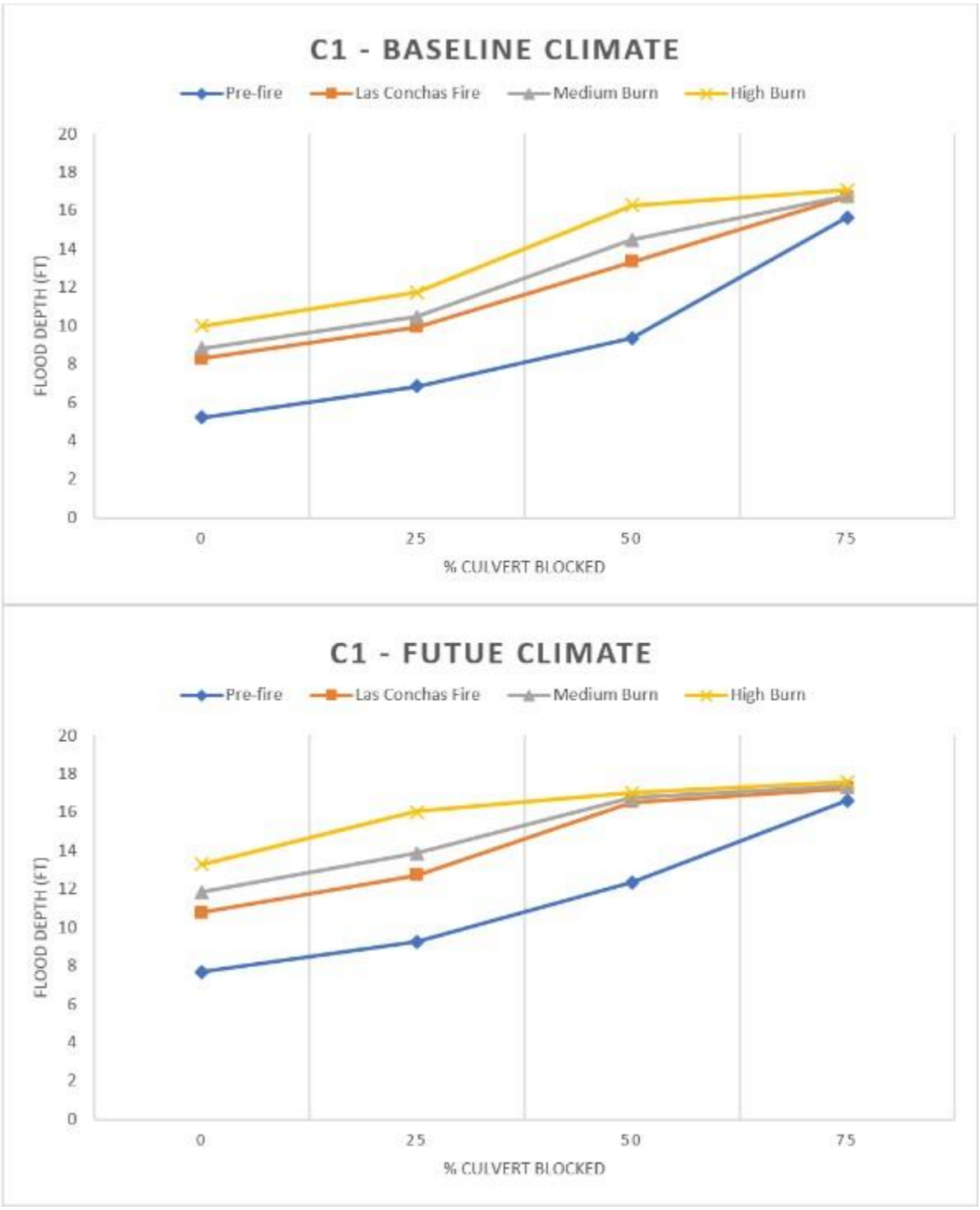

Figure 8. Flood Depth at Culvert Inlet for Culvert C1 as a Function of Percentage of Culvert Blocked

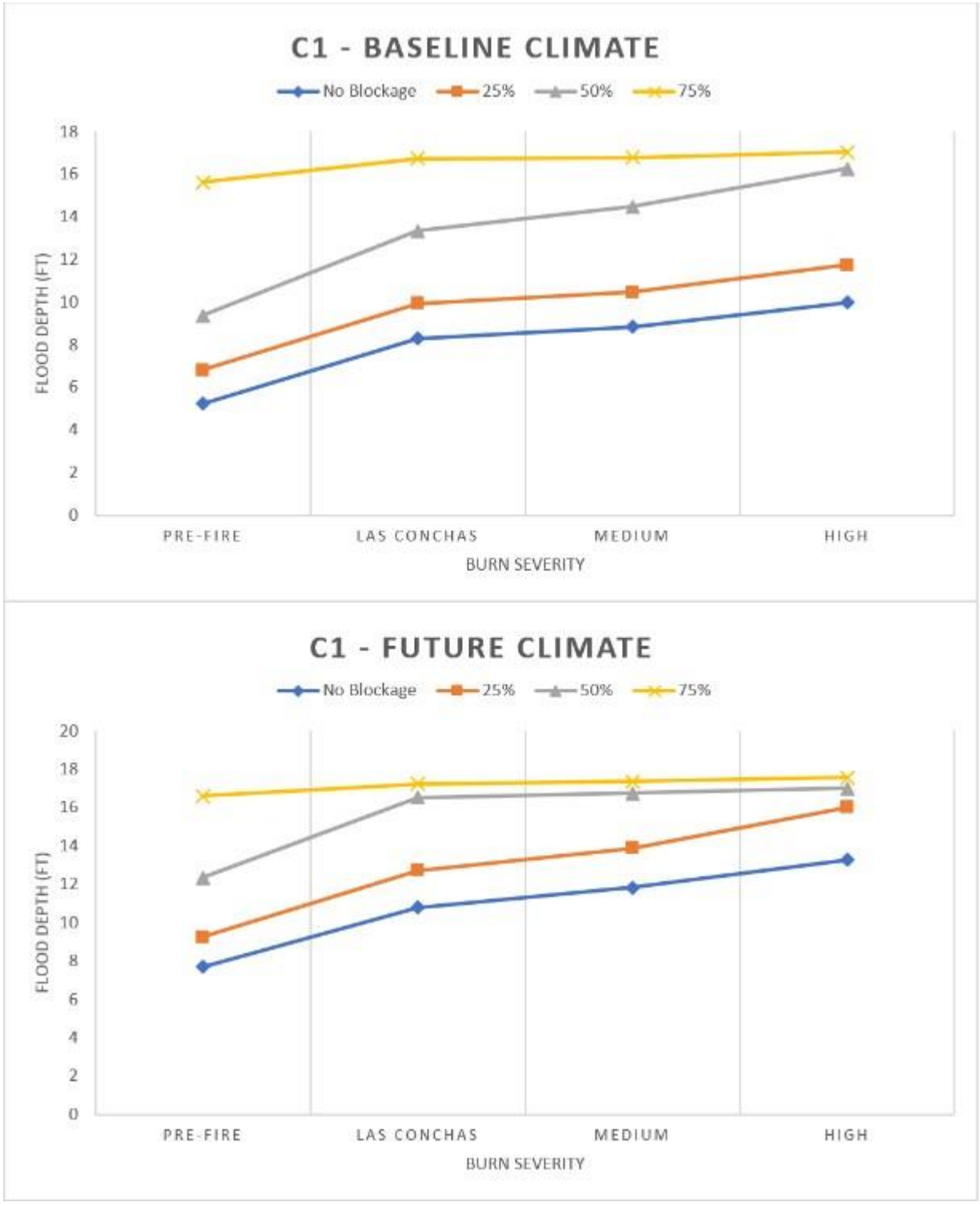

Figure 9. Flood Depth at Culvert Inlet for Culvert C1 as a Function of Burn Severity

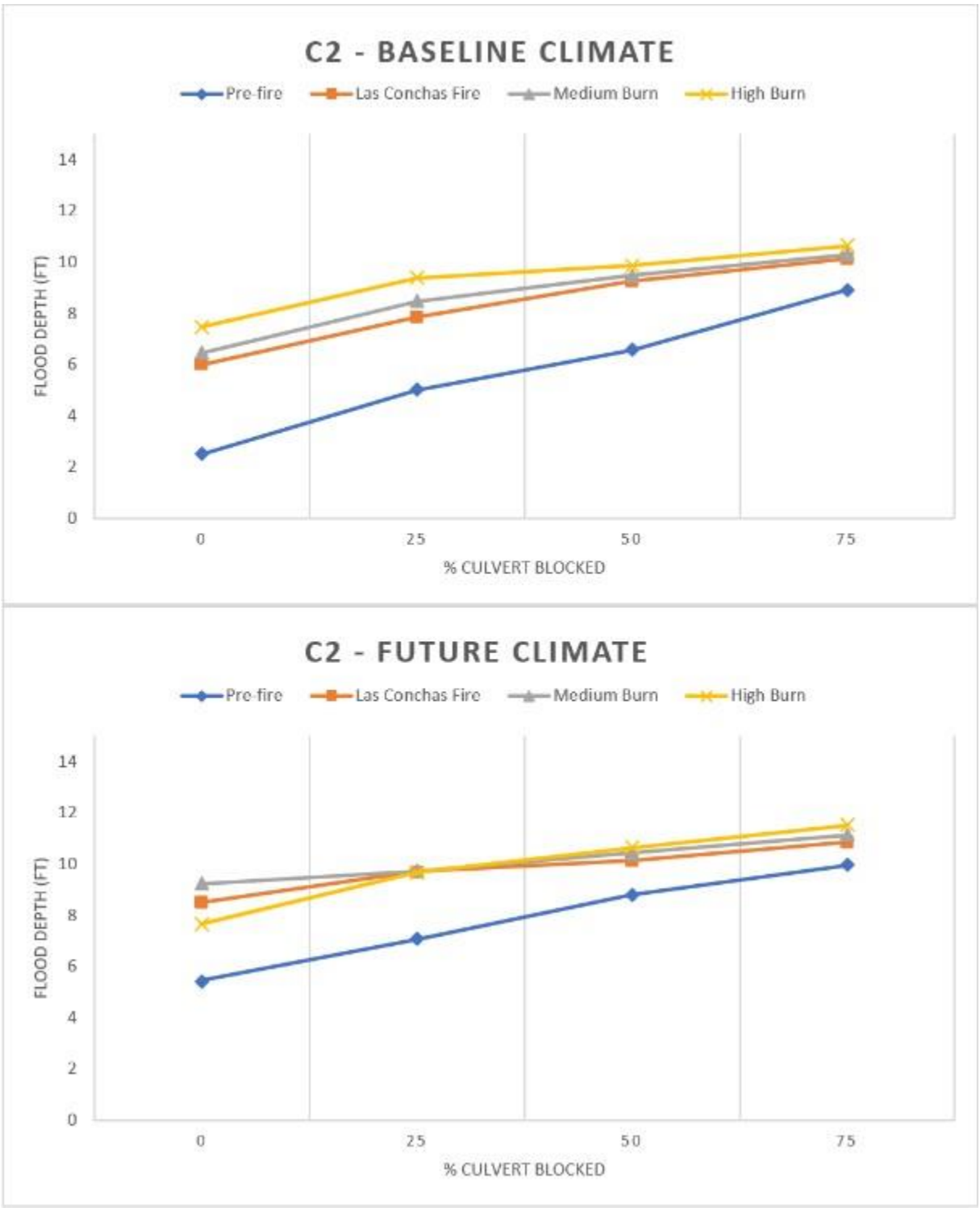

Figure 10. Flood Depth at Culvert Inlet for Culvert C2 as a Function of Percentage of Culvert Blocked

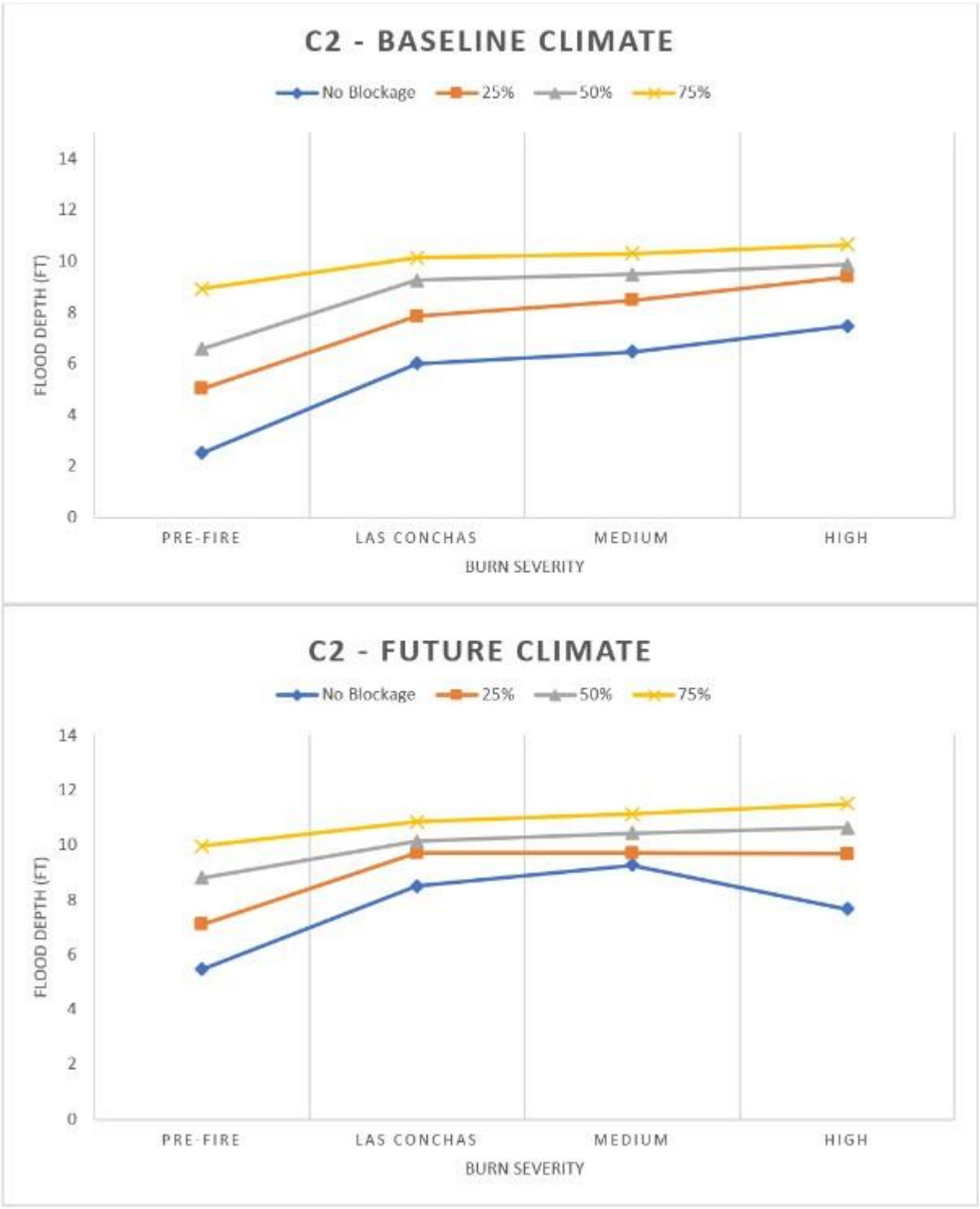

Figure 11. Flood Depth at Culvert Inlet for Culvert C1 as a Function of Burn Severity

3.6.2.2 Roadway Inundation

We considered roadway embankment inundation as a principal measure of damage to transportation infrastructure, as described in Section 3.4. Roadway embankment inundation depends on many factors, including the amount of runoff, the amount of blockage, and the topography of the site surrounding the culverts. Roadway embankment inundation occurred for Culverts C1, C2, and C3 for the conditions indicated in Figure 12, Figure 13, and Figure 14, respectively. A summary of all scenarios is provided in Table 7.

These results reveal that C2 is the location that experiences roadway embankment inundation under the greatest range of conditions. At C2, inundation occurs without any blockage under the medium and high burn severities with the climate change scenario. Other than these two cases, without some blockage, there is no roadway embankment inundation regardless of climate and burn severity. These results highlight the role that culvert blockage has in post-fire flood damage, and suggests that preventing blockage is an effective measure to limit damage. The results also reveal the significance of burn severity with respect to roadway embankment inundation. The only model that produced inundation under pre-fire conditions was that for C2 under future climate conditions with 75% blockage. In no other case did the modeling result in inundation. These results suggest the capacity of the existing infrastructure is adequate until post-fire conditions significantly increase runoff.

Inundation maps from the floodplain modeling provide a visual means to assess the extent of flooding and conditions under which roadway embankment inundation occurs. Three figures are given here to illustrate some of the results that were obtained; all inundation maps are given in the appendix. In Figure 15, results at C2 are given for 4 models. These models all utilize the baseline climate and have 25% culvert blockage. As the runoff increases due to increased burn severity, the amount of flooded area in front of the inlet increases. Eventually, in the case of severe burn conditions, there is insufficient storage adjacent to the inlet and water inundates the roadway above C2. In Figure 16, results at C1 are given for 4 models. These models all utilize the baseline climate and have 50% culvert blockage. These results show how the flooded region expands by spreading out over a larger area with increasing burn severity. With the actual burn severity, the water is immediately adjacent to the roadway but does not appear to impinge upon driving lanes. With medium burn severity, water just covers a portion of a driving lane. With high burn severity, the driving lanes are clearly flooded. In Figure 17, results are given for C3 for the same conditions as given in Figure 16 for C1 (50% blockage, baseline climate). Under these conditions at C3, there is no roadway embankment inundation. This result highlights that the impacts of post-fire flooding are site-specific. Figure 18 and Figure 19 shows the profile depiction of the depth of inundation for C1 under the S8 scenarios. Further information about inundation duration and depth is given in the section describing the unsteady floodplain modeling results.

Table 7. Summary of Scenarios Resulting in Inundation for C1, C2 and C3

Climate	Fire Conditions	Scenario	C1	C2	C3
Baseline	S1: Pre-Fire	SB1: No Block			
Baseline	S1: Pre-Fire	SB2: -25%			
Baseline	S1: Pre-Fire	SB3:-50%			
Baseline	S1: Pre-Fire	SB4:-75%			
Baseline	S2: Las Conchas Fire	SB5: No Block			
Baseline	S2: Las Conchas Fire	SB6: -25%			
Baseline	S2: Las Conchas Fire	SB7:-50%		X	
Baseline	S2: Las Conchas Fire	SB8:-75%	X	X	
Baseline	S3: Medium Burn	SB9: No Block			
Baseline	S3: Medium Burn	SB10: -25%			
Baseline	S3: Medium Burn	SB11:-50%		X	
Baseline	S3: Medium Burn	SB12:-75%	X	X	X
Baseline	S4: High Burn	SB13: No Block			
Baseline	S4: High Burn	SB14: -25%		X	
Baseline	S4: High Burn	SB15:-50%		X	
Baseline	S4: High Burn	SB16:-75%	X	X	X
Climate Change	S5: Pre-Fire	SCC1: No Block			
Climate Change	S5: Pre-Fire	SCC2: -25%			
Climate Change	S5: Pre-Fire	SCC3:-50%			
Climate Change	S5: Pre-Fire	SCC4:-75%	X	X	X
Climate Change	S6: Las Conchas Fire	SCC5: No Block			
Climate Change	S6: Las Conchas Fire	SCC6: -25%		X	
Climate Change	S6: Las Conchas Fire	SCC7:-50%	X	X	
Climate Change	S6: Las Conchas Fire	SCC8:-75%	X	X	X
Climate Change	S7: Medium Burn	SCC9: No Block		X	
Climate Change	S7: Medium Burn	SCC10: -25%		X	
Climate Change	S7: Medium Burn	SCC11:-50%	X	X	
Climate Change	S7: Medium Burn	SCC12:-75%	X	X	X
Climate Change	S8: High Burn	SCC13: No Block		X	
Climate Change	S8: High Burn	SCC14: -25%		X	
Climate Change	S8: High Burn	SCC15:-50%	X	X	
Climate Change	S8: High Burn	SCC16:-75%	X	X	X

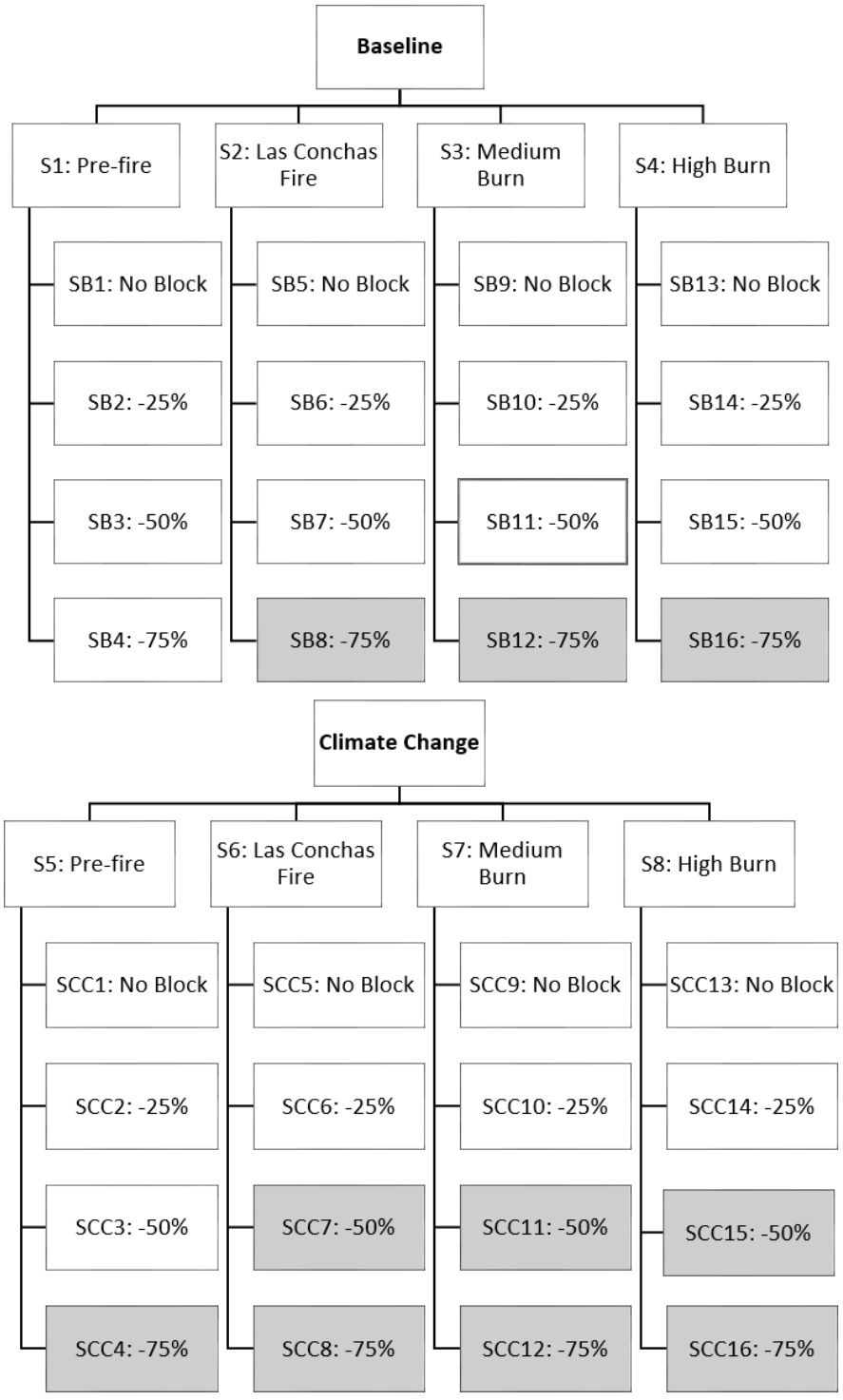

Figure 12. Floodplain Modeling Conditions for Which the Roadway Embankment Above Culvert 1 Was Inundated Are Indicated by Shading

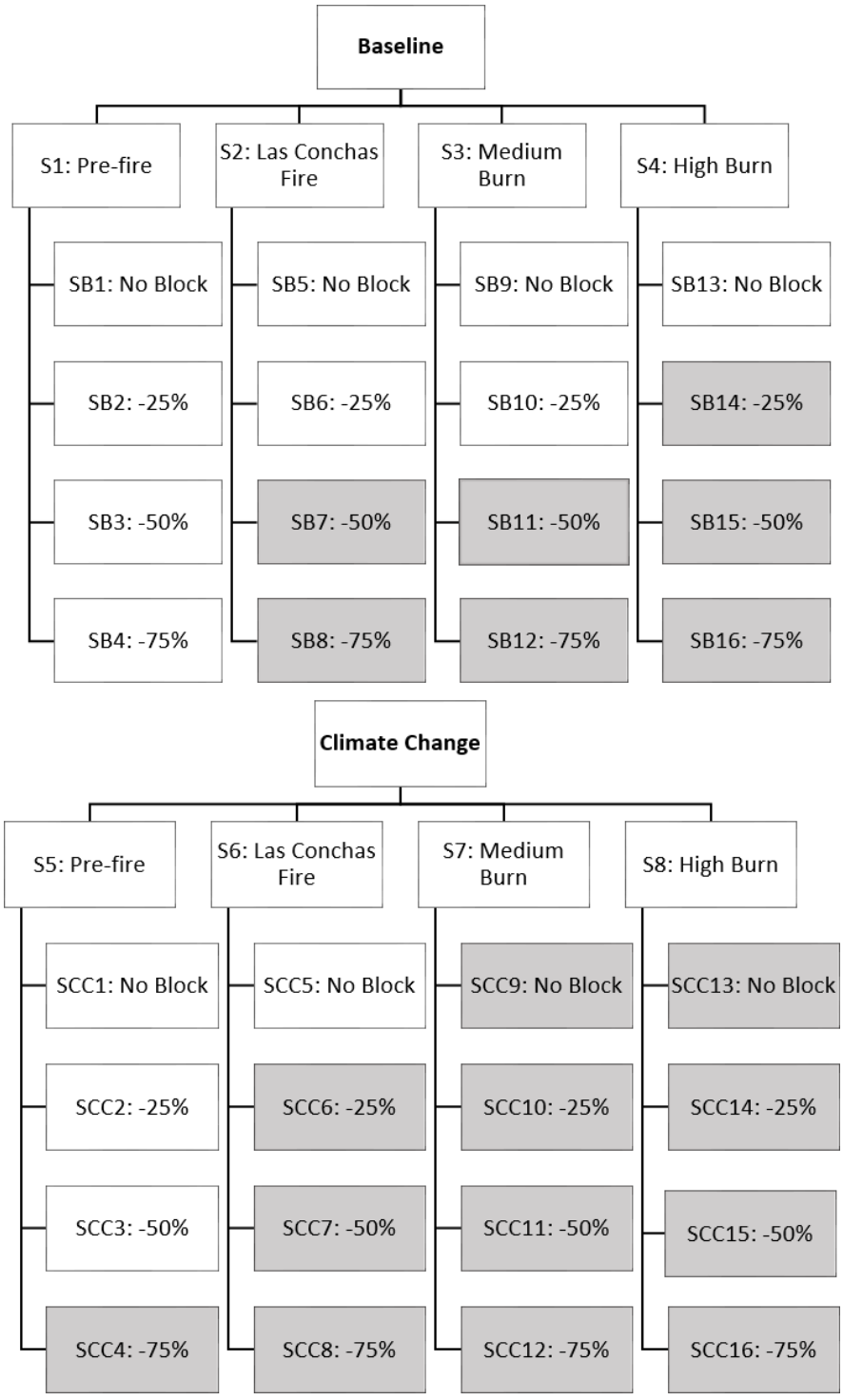

Figure 13. Floodplain Modeling Conditions for Which the Roadway Embankment Above Culvert 2 Was Inundated Are Indicated by Shading

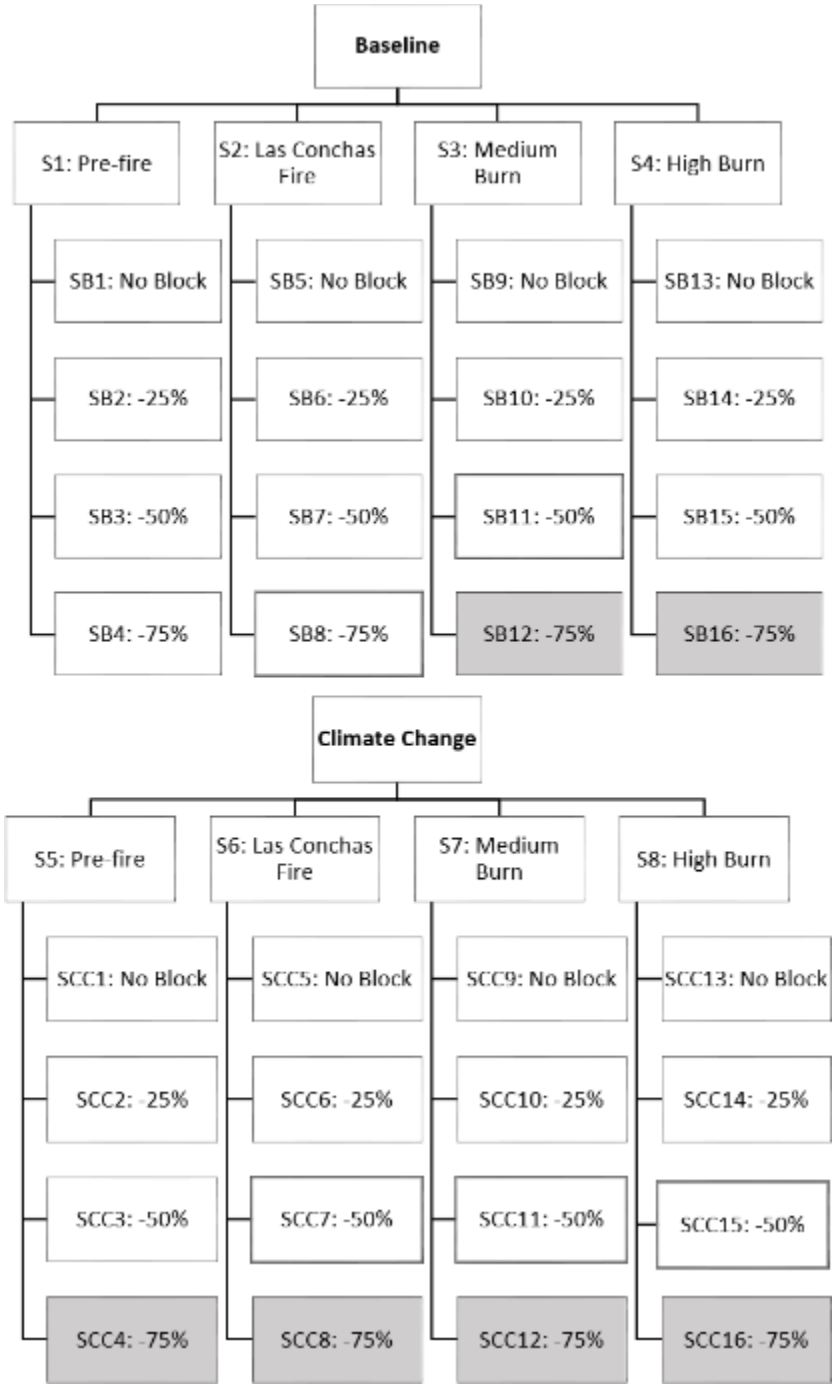

Figure 14. Floodplain Modeling Conditions for Which the Roadway Embankment Above Culvert 3 Was Inundated Are Indicated by Shading

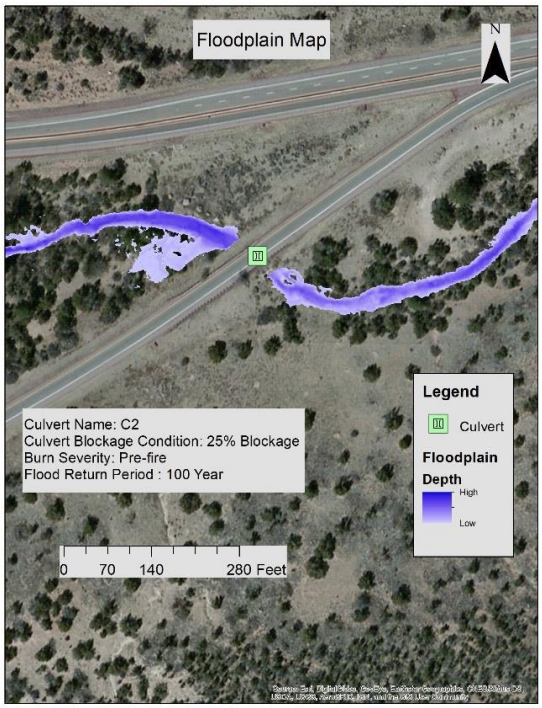

(a) PRE-FIRE

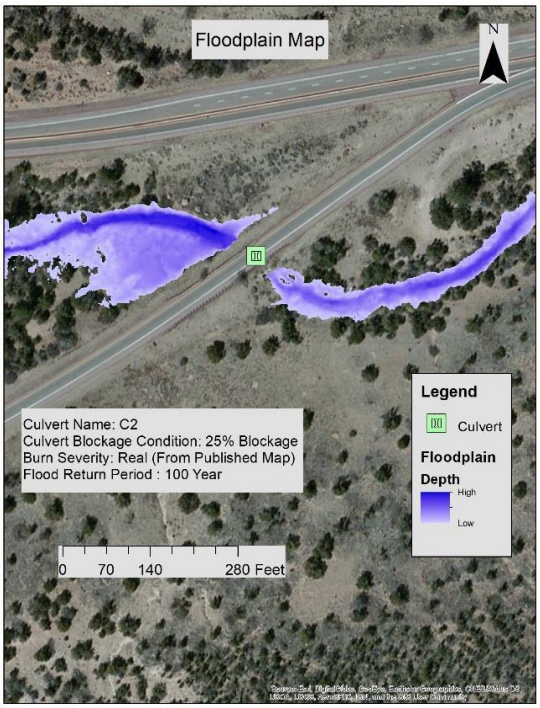

(b) LAS CONCHAS FIRE

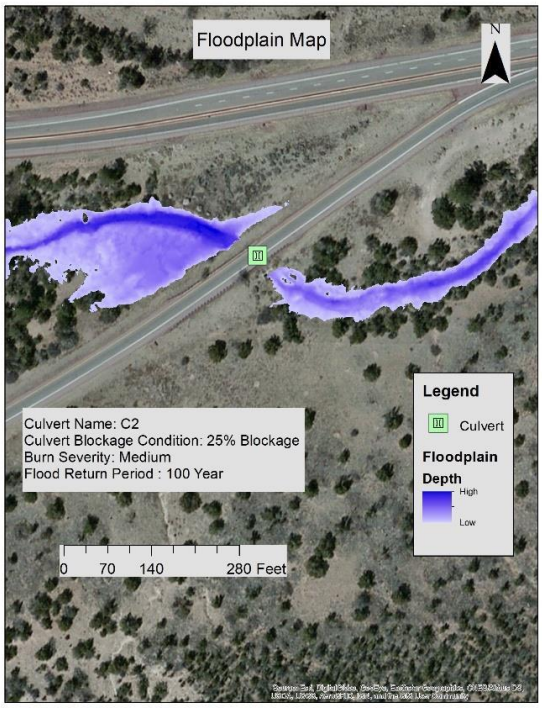

(c) MEDIUM SEVERITY

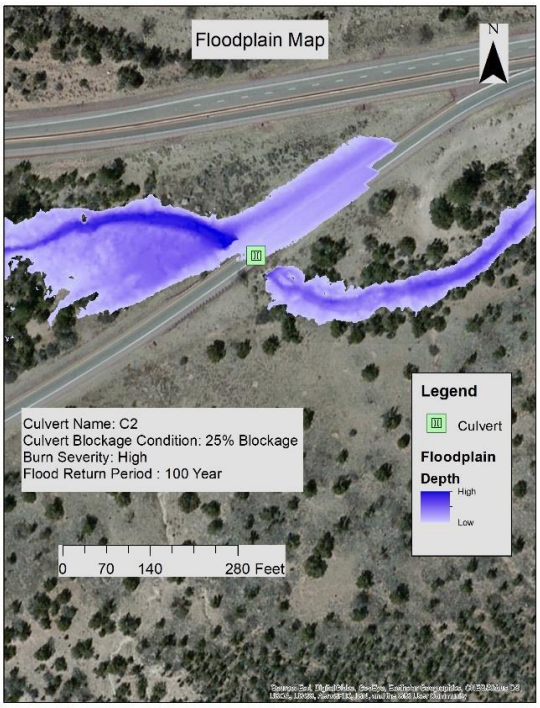

(d) HIGH SEVERITY

Figure 15. Floodplains at Culvert C2, 25% Blockage, Baseline Climate

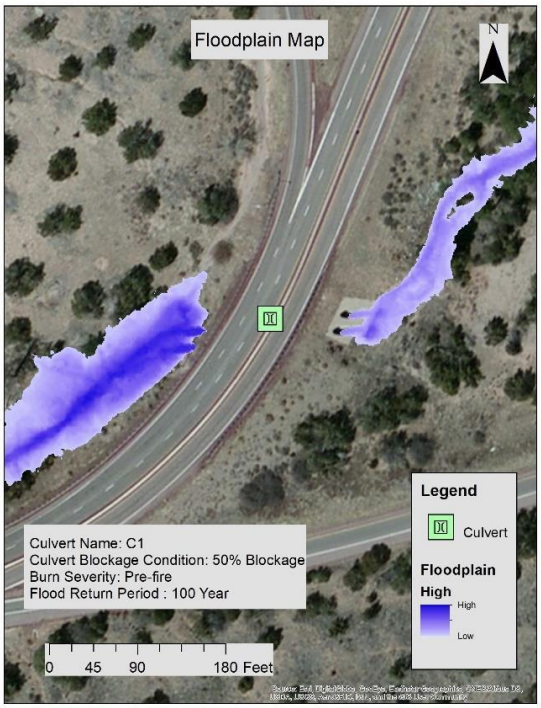

(a) PRE-FIRE

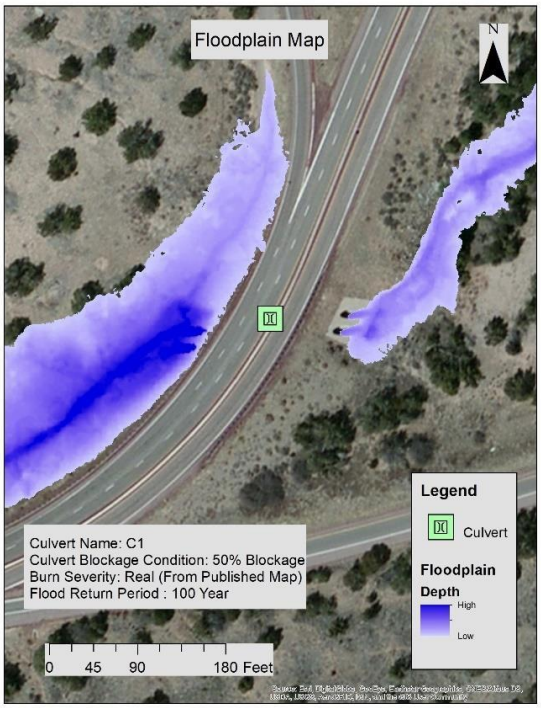

(b) LAS CONCHAS FIRE

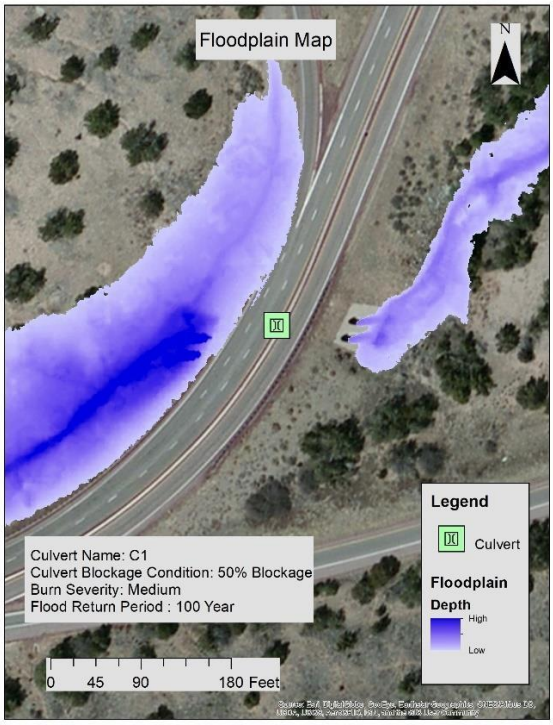

(C) MEDIUM SEVERITY

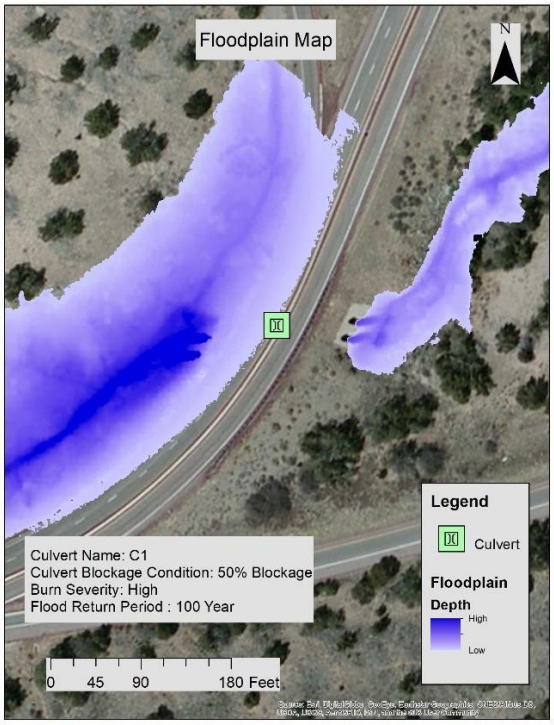

(a) HIGH SEVERITY

Figure 16. Floodplains at Culvert C1, 50% Blockage, Baseline Climate

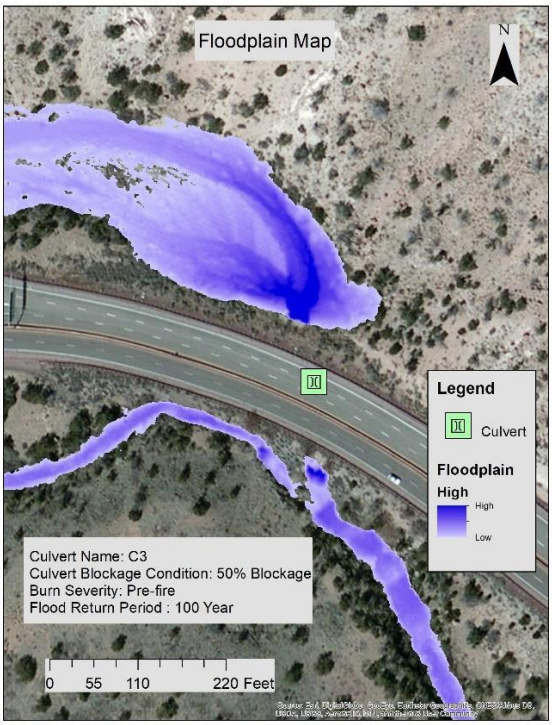

(a) PRE-FIRE

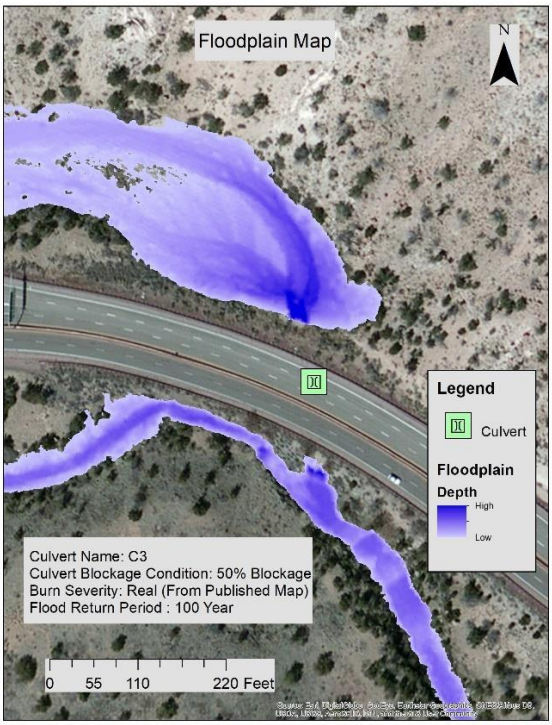

(b) LAS CONCHAS FIRE

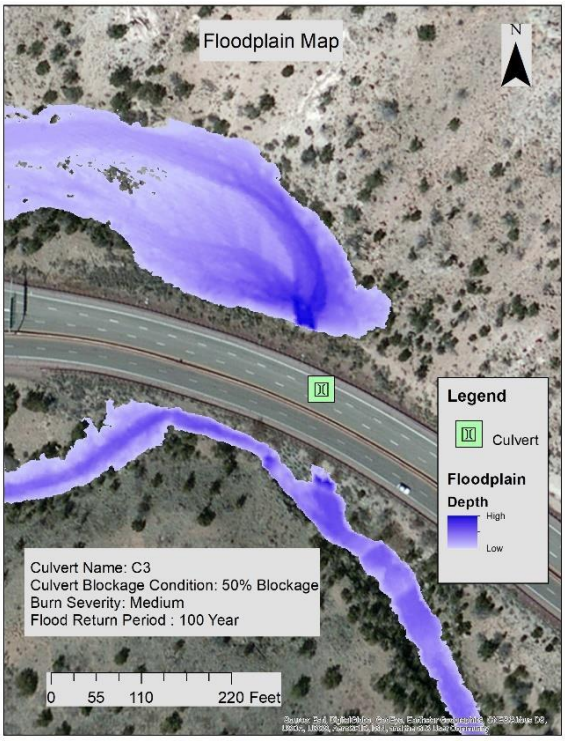

(c) MEDIUM SEVERITY

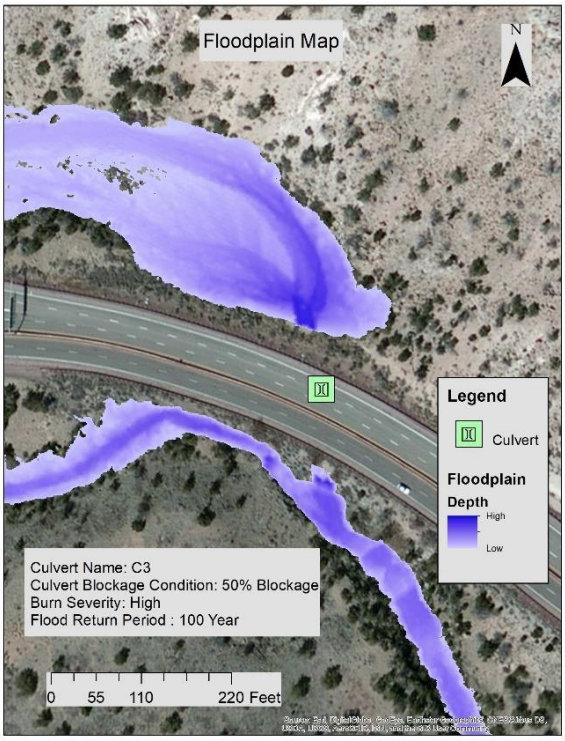

(d) HIGH SEVERITY

Figure 17. Floodplains at Culvert C3, 50% Blockage, Baseline Climate

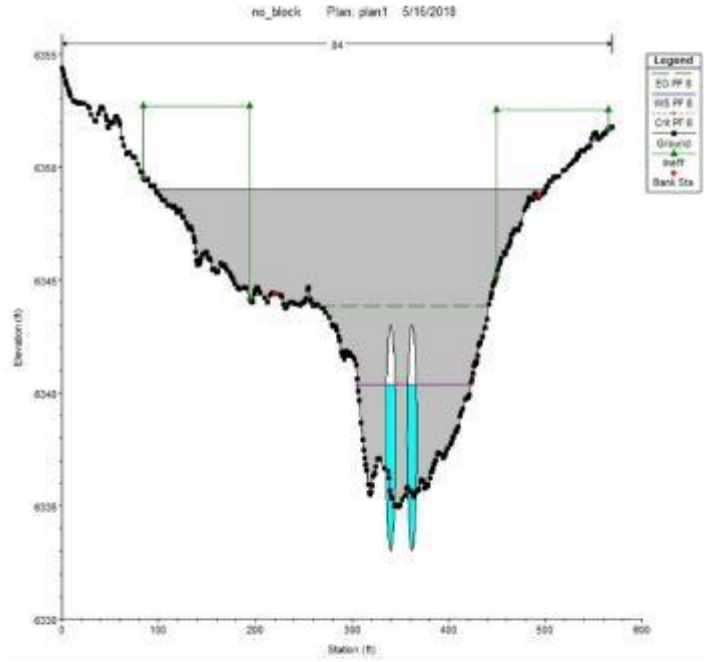

(A) NO BLOCKAGE

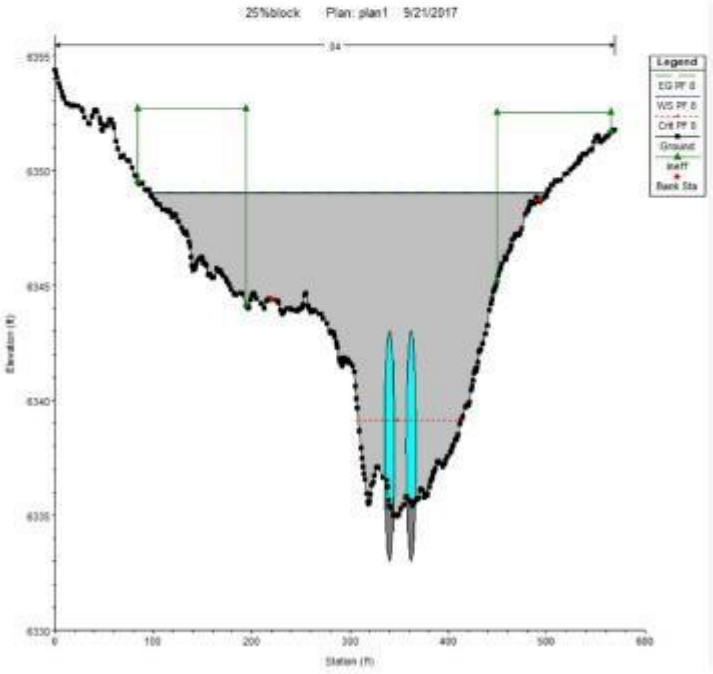

(B) 25% BLOCKAGE

Figure 18. Flood Depth (Culvert C1, 200-year High Burn Severity) for No Blockage and 25% Blockage

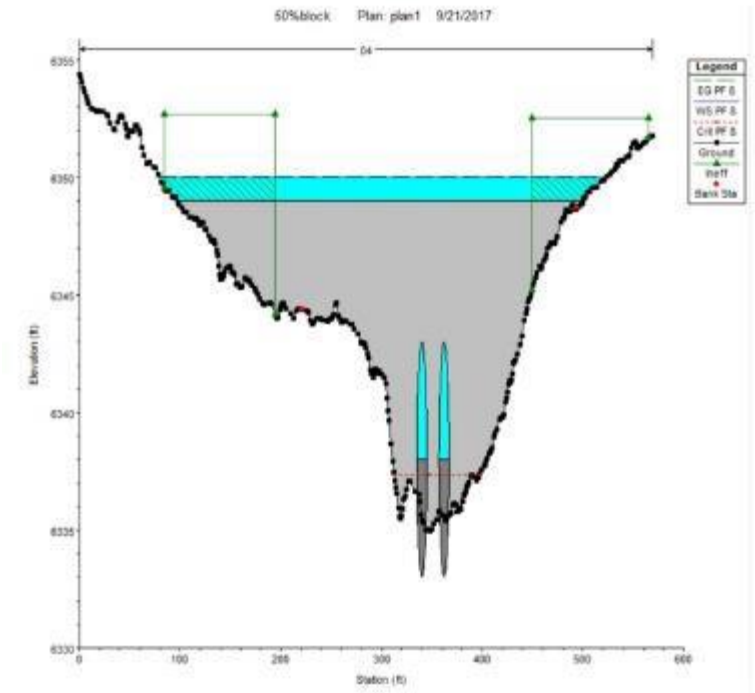

(A) 50% BLOCKAGE

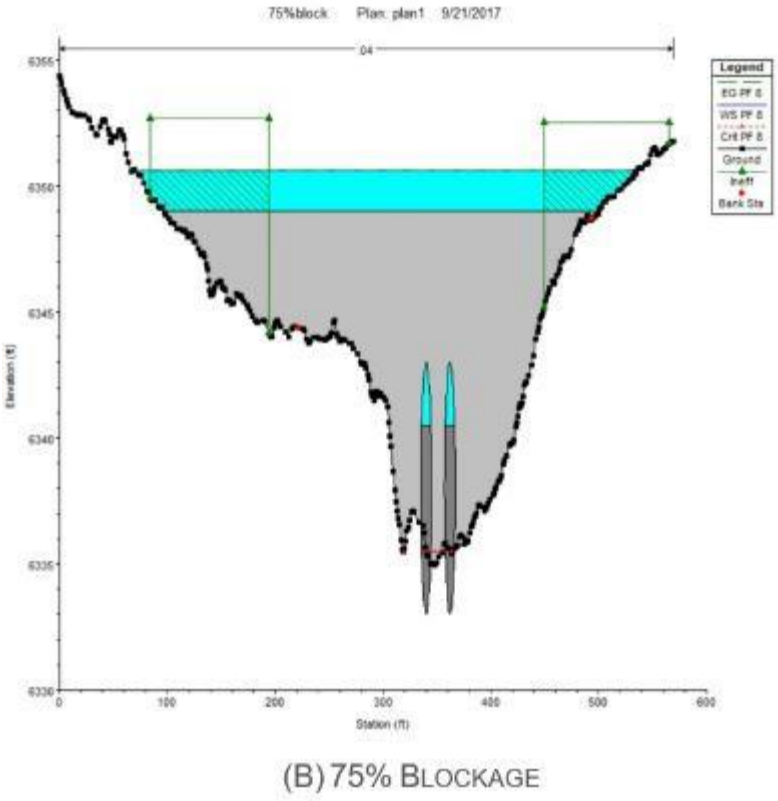

(B) 75% BLOCKAGE

Figure 19. Flood Depth (Culvert C1, 200-year High Burn Severity) for 50% and 75% Blockage

3.6.2.3 Other Metrics of Impact of Post-Fire Flooding

In addition to predictions of roadway inundation, the modeling approach described here provides information that can be used in assessing of post-fire flooding on transportation infrastructure. For example, calculated velocities can be used to calculate scour adjacent to bridge foundations (*88–90*), scour at culvert inlets and outlets (*67*), and erosion of roadway surfaces (*91*) from overtopping. Changing flood levels can be used to adjust the pore pressure that can lead to slope instability (*92*).

3.6.2.4 Scour Potential

Scour is a potential destructive force that can compromise and damage culverts and bridges (refer to Section 2). We calculated velocities near Culverts 1, 2, and 3 (C1, C2, and C3 (see Figure 3) and compiled these results in Table 8, Table 9, Table 10 and Table 11. Velocities at the inlet and outlet as well as at three downstream sections are given for each culvert. The inlet velocities increase with blockage as the flood depth is increased from the blockage, which in turn results in a greater pressure (hydraulic head) that forces water through the culvert. The outlet velocities generally increase with blockage as well. Velocities in the downstream sections largely depend on the geometry of the channel. Higher velocities should be monitored for scour potential when close to a specified velocity threshold for scour.

Table 8. Velocities at Different Sections Near the Culverts: No Blockage

Culvert	Inlet Velocity (ft/s)	Outlet Velocity (ft/s)	Section1 (ft/s)	Section2 (ft/s)	Section3 (ft/s)	Section4 (ft/s)
C1	8.76	14.64	3.23	6.93	5.49	7.19
C2	8.24	4.72	6.03	4.8	7.07	10.46
C3	9.94	4.07	7.08	19.77	23.32	25.29

Table 9. Velocities at Different Sections Near the Culverts: 25% Blockage

Culvert	Inlet Velocity (ft/s)	Outlet Velocity (ft/s)	Section1 (ft/s)	Section2 (ft/s)	Section3 (ft/s)	Section4 (ft/s)
C1	8.58	14.06	3.23	6.93	5.49	7.19
C2	8.25	15.85	10.75	4.8	7.07	10.46
C3	9.91	5.23	7.08	19.77	23.32	25.29

Table 10. Velocities at Different Sections Near the Culverts: 50% Blockage

Culvert	Inlet Velocity (ft/s)	Outlet Velocity (ft/s)	Section1 (ft/s)	Section2 (ft/s)	Section3 (ft/s)	Section4 (ft/s)
C1	8.92	13.92	3.23	6.93	5.49	7.19
C2	8.25	15.85	43.37	13.37	7.07	10.47
C3	10.65	19.03	32.66	28.53	27.27	27.31

Table 11. Velocities at Different Sections Near the Culverts: 75% Blockage

Culvert	Inlet Velocity (ft/s)	Outlet Velocity (ft/s)	Section1 (ft/s)	Section2 (ft/s)	Section3 (ft/s)	Section4 (ft/s)
C1	12.76	16.01	3.23	6.93	5.49	7.19
C2	11.61	11.61	6.03	4.8	7.07	10.46
C3	15.69	15.69	7.08	19.77	23.32	25.29

3.6.3. Results from Unsteady Flow Analysis

The unsteady flow analysis was intended to obtain estimates of the duration of roadway inundation adjacent to C1, C2, and C3. Results are shown in Table 12. The description of the conditions listed in Table 12 are described in Table 13. These results indicate that many of the scenarios which result in overtopping the roadway embankment will result in the roadways being inundated for more than an hour. Further, the depth of inundation suggests that it would not be easy or advisable for motorists to drive through the inundated roadways. Certainly these events would be disruptive to travel beyond damage to the infrastructure. In the context of the case study, the highways affected are part of the main and shortest route between Santa Fe, NM and Los Alamos, NM. Disrupting this route would result in a travel time increase of approximately 2 hours between Santa Fe and Los Alamos (as further discussed in Section 4).

Table 12. Results of the Unsteady Flow Analysis

Culvert	Blockage	Conditions (ID)*	Time of Inundation(min)	Maximum Depth (inches)
C1	50%	6	26	4.3
C1	50%	7	36	6.4
C1	50%	8	48	8.4
C1	75%	2	43	6.2
C1	75%	3	52	7.1
C1	75%	4	63	9.1
C1	75%	5	34	1.2
C1	75%	6	65	10.6
C1	75%	7	74	12.4
C1	75%	8	80	14.3

Culvert	Blockage	Conditions (ID)*	Time of Inundation(min)	Maximum Depth (inches)
C2	no blockage	7	19	2.9
C2	25%	4	23	3.7
C2	25%	6	39	7.3
C2	25%	7	47	7.9
C2	25%	8	58	9.6
C2	50%	2	23	2.0
C2	50%	3	36	5.3
C2	50%	4	48	9.7
C2	50%	6	57	12.4
C2	50%	7	66	15.1
C2	50%	8	74	17.3
C2	75%	2	61	12.2
C2	75%	3	70	13.7
C2	75%	4	79	17.0
C2	75%	5	58	10.3
C2	75%	6	80	19.0
C2	75%	7	87	21.1
C2	75%	8	93	34.9
C3	75%	3	14	2.5
C3	75%	4	15	2.8
C3	75%	5	57	9
C3	75%	6	57	9.5
C3	75%	7	61	10.4
C3	75%	8	63	10.4

Table 13. Description of Conditions as Referenced in Table 12

Conditions (ID)*	Description	Conditions (ID)*	Description
1	Pre-fire-Baseline climate	5	Pre-fire-Climate change
2	Real Burn-Baseline climate	6	Real Burn-Climate change
3	Medium Burn-Baseline climate	7	Medium Burn-Climate change
4	High Burn-Baseline climate	8	High Burn-Climate change

3.7 CONCLUSIONS

This section proposed and demonstrated a modeling framework to identify and quantify the potential of roadway overtopping and inundation. The framework integrated pre- and post-wildfire rainfall-runoff modeling and floodplain mapping under different climate and burn severity scenarios.

For the case study, the non-steady flow analysis revealed that many of the scenarios that result in overtopping of the roadway embankment will result in the roadways being inundated for more than an hour. This will be disruptive to travel beyond damage to the infrastructure, especially in remote areas where alternate routes are not available or feasible. The overtopping and inundation results highlight that the impacts of post-fire flooding are site-specific. The framework can be used by decision-makers as a screening tool for identifying potential problem areas and deciding where to focus further analyses on failure mechanisms, damage assessment, risk mitigation alternatives, and resource allocation.

4. VULNERABILITY ASSESSMENT AND DECISION-MAKING APPROACH FOR WILDFIRE MITIGATION AND REHABILITATION STRATEGIES

4.1 INTRODUCTION

The selection of appropriate wildfire mitigation and rehabilitation strategies should consider the expected wildfire impacts on transportation infrastructure assets, as well as the characteristics of the assets, and the cost and benefits of implementing particular strategies. Typical decision-making approaches involve asset and criticality identification, hazard/threat identification, risk quantification, and determination of management alternatives (*93*, *94*). In this section, we explore wildfire vulnerability assessment for transportation infrastructure components and provide suggestions, resources, and examples for implementing the proposed decision approach. We use the modeling framework and case study from Section 3 to then show the decision-making applicability of each. Sections 4.2.1 to 4.2.3 are steps included in the modeling framework in generalized terms and Sections 4.2.4 to 4.2.6 provide examples of the further evaluation required in a decision-making context.

4.2 VULNERABILITY ASSESSMENT

We expand upon the “Climate Change and Extreme Weather Vulnerability Assessment” framework developed by the Federal Highway Administration (*94*). In this framework, vulnerability assessment includes: (1) collecting and integrating data on assets, (2) developing climate inputs, (3) identifying and rating vulnerabilities, (4) developing information on asset sensitivity to climate, and (5) assessing asset criticality. Using the case study presented and analyzed in Section 3, we focus on defining vulnerability assessment for wildfire hazards for transportation infrastructure while building upon this framework. The proposed decision-making approach is described in the following sections.

4.2.1 Data Collection of Transportation Assets

As shown in Section 3, transportation assets can be identified from satellite images. Bridges and drainages can also be identified from the National Bridge Inventory. In addition to geometric, physical, and structural information about assets, the National Bridge Inventory provides other information that could be of importance in wildfire vulnerability assessment, specifically for asset criticality analysis. Thus, the modeling framework can be expanded to make it applicable in a general context. Table 14 lists some of these additional items.

Furthermore, site visits allow for verification of the information in such databases, including the location and physical properties of assets. For wildfire vulnerability assessment, additional data collected during site visits could include channel properties such as current condition, existence of debris in the surrounding area, and type of soil in the area.

Table 14. Examples of items from the NBI useful for asset criticality analysis (From NBI)

Item number	Description
Item 12	Base Highway Network
Item 19	Bypass, detour length
Item 21	Maintenance responsibility
Item 26	Functional classification
Item 27	Year Built
Item 29	Average Daily Traffic
Item 36	Traffic Safety Features
Item 37	Historical Significance
Item 41	Structure open, posted or closed to traffic
Item 42	Type of service
Item 113	Scour critical bridges

4.2.2 Climate and Disturbance Inputs: Wildfire

The analysis presented in Section 3 used severity data from a real wildfire event. However, pre-wildfire analysis is also possible for predicting wildfire impacts through the use of wildfire propagation models. As mentioned in Section 1, the main objective of a fire propagation model is to predict the spread and severity of fire through a watershed's fuel bed (*18*). Factors that affect fire propagation can be categorized in three groups: (1) forest fuels; (2) topography; and (3) meteorological conditions (*18*). Forest fuel analysis considers the types and characteristics of plant species present in the area. Topography is also an important factor for predicting fire behavior, since fire spreads faster when propagating in an uphill direction. Finally, meteorology considers the moisture content of fuels, air temperature, relative humidity, and wind conditions. Many different theoretical approaches have been developed—including cellular automata, Markov chains, and percolation modeling(*95*)—and several software packages are available (e.g., FARSITE, FireStation, FlamMap, etc.) for predicting fire propagation patterns.

4.2.3 Identifying Vulnerabilities and Asset Sensitivity to Climate and Disturbances

In order to forecast vulnerability, the fire model can provide input into the hydrology model by estimating post-fire watershed conditions if there is no real fire data, as in Section 3. Based on fire propagation patterns, burn severity estimates, and pre-fire fuel layers, sediment and debris volumes can also be estimated. Asset sensitivity to climate can be evaluated through historical databases, stakeholder input, or simulation modeling. For example, in Section 3, we used different climate scenarios (i.e., extreme precipitation) and fire severity conditions to estimate the impacts of post-wildfire floods in terms of inundation. In this case, the recurrence interval of rainfall was reduced from 200 years to 100 years to model the potential future climate. Other parameters can be adjusted to model climate scenarios such as temperature and humidity. These adjustments can be made in the fire propagation model and/or the hydrology model.

4.2.4 Asset Criticality

One important step in the vulnerability assessment of transportation infrastructure is determining asset criticality. A critical asset is an asset that is so important to the area of study that its removal would result in significant losses (*96*). Prior literature points out challenges with establishing criticality measures, such as who defines criticality and which parameters to use when defining criticality (*94*, *96*). Multi-criteria approaches for evaluating criticality are common. Examples of criteria from the Colorado Department of Transportation for determining criticality for resilience applications include: roadway classification, AADT, freight, emergency travel time, and social vulnerability index (*93*). Evaluating asset criticality results in the ranking of assets based on their importance to the area of study. These results, coupled with asset sensitivity to climate and wildfire events, aid in the prioritization of assets for mitigation and rehabilitation strategies.

As mentioned above, an important aspect when evaluating asset criticality for wildfire events is detour length (travel time). Wildfire affects remote areas in which alternative routes are limited or nonexistent, and therefore transportation assets become more critical. For example, Figure 20 shows the effect in travel time due to the closure of NM 502 (see Figure 3), as in the case of the Las Conchas Fire, which results in an increase of almost 2 hours of travel time.

(a) Alternative route 1 (125 miles, 2.5 hours) (b) Shortest route (34 miles, 42 minutes)

Figure 20. Example of Disruption due to Inundation in the Case Study and Example Alternative Routes (Source: Google Maps)

4.2.5 Applicability of Mitigation and Rehabilitation Strategies

While wildfire suppression was a widely practiced mitigation strategy used to minimize the adverse impacts of wildfire (*8*, *54*), studies have found that wildfire suppression contributes to fuel accumulation in the forest (*55*), which in turn causes more severe wildfire in the future (*2*, *8*). Thus, fire suppression policy should include vegetation management for effective forest management (*54*). Fuel reduction and prescribed fire are the two widely used methods of vegetation management (*19*, *56*). Since the causes of ignition are widespread, it is almost impossible to avoid wildfire (*57*). Therefore, the main objective of vegetation management is to reduce the severity of wildfire and make it more manageable, rather than to decrease wildfire extent or to make wildfire suppression easier (*57*). For example, the Minnesota Department of Transportation performs prescribed burns as vegetation management, which results in erosion control, stormwater-runoff filtering, and weed-invasion resistance (*97*). However, departments of transportation are rarely involved in such practices as wildfire mitigation as an objective, despite the immense effects of wildfires on transportation infrastructure, which highlights the importance of multi-agency collaborations.

On the other hand, wildfire mitigation efforts do not usually consider the effects on transportation infrastructure specifically. For that reason, we have developed a process to choose applicable mitigation measures for bridges and drainages depending on site characteristics, as shown in Figure 21. As mentioned in Section 2, a site-specific issue is, for example, whether the bridge or drainage has the capacity to handle the expected increased runoff from a post-fire flood. If there is insufficient capacity with the anticipated flow, it will be necessary to take measures to reduce the runoff, such as managing the forested land through controlled burns and debris removal to minimize the size and intensity of inevitable wildfires. Additional measures may include armoring (i.e., cable-tied blocks, riprap rocks, etc.) and protecting select bridges and drainages from scour and erosion with flow-altering devices (i.e., flow deflectors, upstream sacrificial piles, etc.) (*89*).

However, if the bridges and drainages have sufficient capacity for the anticipated post-fire flood event, then damage to the transportation infrastructure should not occur unless the capacity of the bridge or drainage is reduced by partial or complete blockage from debris or sediment. In such cases, preventing debris from blocking the bridge openings and culverts is a principal mitigation strategy. These strategies have been studied in prior research (*27*) and include structural (debris fins, in-channel debris basin, debris deflectors, etc.) and non-structural methods (emergency maintenance, annual maintenance, management of upstream watershed). Seeding and mulching of burned landscape are common surface wildfire treatments to address these issues (*61*).

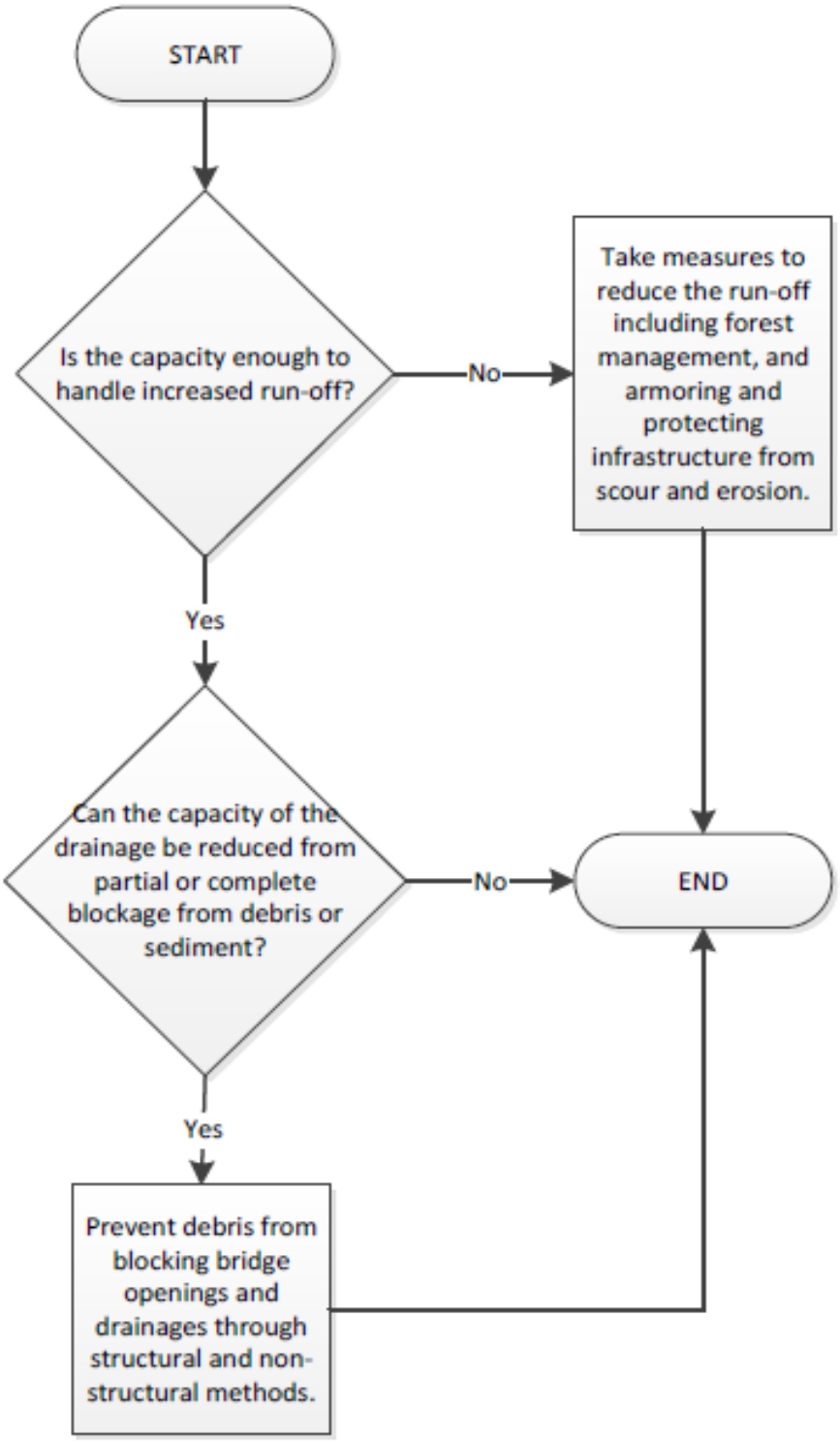

Figure 21. Conditions for Determining Applicability of Mitigation Measures: Example

4.2.6 Evaluation of Strategies

Multiple strategies might be appropriate to mitigate and respond to wildfire impacts. The literature review presented in Section 2 shows different alternatives to mitigate and respond to post-wildfire flood hazards. Once the specifics of the mitigation and rehabilitation alternatives are determined, different analytical tools (e.g., life-cycle costing, benefit/cost analysis, heuristic rules, risk analysis, and optimization), alongside asset information and business and governmental parameters, can be used to decide among applicable alternatives (*98*). For example, life-cycle cost assessment typically includes direct cost of implementation and maintenance of the alternative, as well as the estimated service life of the alternative under consideration. Cost data can be estimated from historical data or from cost estimating databases such as RSMeans. The benefits of implementing a specific mitigation or rehabilitation alternative include the avoided costs of disruptions and the costs due to decreased functionality of the transportation asset which are directly related to the asset criticality. Challenges and limitations such as capacity and lead time of implementation should also be considered in the analysis.

4.3 SUMMARY

Vulnerability assessment of transportation assets can be used as a basis for deciding among mitigation and rehabilitation strategies for wildfire events. Asset criticality is an important aspect to consider in decision approaches for these strategies, but there are challenges with establishing criticality measures, such as who defines criticality and which parameters to use when defining criticality (*94*, *96*). This section provided guidance for wildfire vulnerability assessments for transportation assets.

REFERENCES

1. Flannigan, M. D., and C. E. V. Wagner. Climate Change and Wildfire in Canada. *Canadian Journal of Forest Research*, 1991. 21(1): 66–72. https://doi.org/10.1139/x91-010.

2. Westerling, A. L., and T. W. Swetnam. Interannual to Decadal Drought and Wildfire in the Western United States. *Eos*, 2003. 84(49): 545–560.

3. Westerling, A. L., H. G. Hidalgo, D. R. Cayan, and T. W. Swetnam. Warming and Earlier Spring Increase Western U.S. Forest Wildfire Activity. *Science*, 2006. 313(5789): 940–943. https://doi.org/10.1126/science.1128834.

4. Haines, T. K., C. R. Renner, and M. A. Reams. A Review of State and Local Regulation for Wildfire Mitigation. In *The Economics of Forest Disturbances* (T. P. Holmes, J. P. Prestemon, and K. L. Abt, eds.), Springer Netherlands, pp. 273–293.

5. Robichaud, P. R., L. E. Ashmun, and B. D. Sims. *Post-Fire Treatment Effectiveness for Hillslope Stabilization*. Gen. Tech. Rep. RMRS-GTR-240. U.S. Department of Agriculture, Forest Service, Rocky Mountain Research Station, 2010.

6. Moody, J. A., R. A. Shakesby, P. R. Robichaud, S. H. Cannon, and D. A. Martin. Current Research Issues Related to Post-Wildfire Runoff and Erosion Processes. *Earth-Science Reviews*, 2013. 122: 10–37. https://doi.org/10.1016/j.earscirev.2013.03.004.

7. Neary, D. G., K. A. Koestner, and A. Youberg. Hydrologic Impacts of High Severity Wildfire: Learning from the Past and Preparing for the Future. Presented at the 24th Annual Symposium of the Arizona Hydrological Society, Flagstaff, AZ, 2010.

8. Gedalof, Z., D. L. Peterson, and N. J. Mantua. Atmospheric, Climatic, and Ecological Controls on Extreme Wildfire Years in the Northwestern United States. *Ecological Applications*, 2005. 15(1): 154–174. https://doi.org/10.1890/03-5116.

9. McKenzie, D., Z. Gedalof, D. L. Peterson, and P. Mote. Climatic Change, Wildfire, and Conservation. *Conservation Biology*, 2004. 18(4): 890–902.

10. Piñol, J., J. Terradas, and F. Lloret. Climate Warming, Wildfire Hazard, and Wildfire Occurrence in Coastal Eastern Spain. *Climatic Change*, 1998. 38(3): 345–357. https://doi.org/10.1023/A:1005316632105.

11. *Learn More About Wildfires*. National Geographic Society. https://www.nationalgeographic.com/environment/natural-disasters/wildfires/. Accessed Sep. 8, 2018.

12. Flannigan, M. D., B. D. Amiro, K. A. Logan, B. J. Stocks, and B. M. Wotton. Forest Fires and Climate Change in the 21st Century. *Mitigation and Adaptation Strategies for Global Change*, 2006. 11(4): 847–859. https://doi.org/10.1007/s11027-005-9020-7.

13. Flannigan, M. D., M. A. Krawchuk, W. J. de Groot, B. M. Wotton, and L. M. Gowman. Implications of Changing Climate for Global Wildland Fire. *International Journal of Wildland Fire*, 2009. 18(5): 483–507. https://doi.org/10.1071/WF08187.

14. Wotton, B. M., and M. D. Flannigan. Length of the Fire Season in a Changing Climate. *The Forestry Chronicle*, 1993. 69(2): 187–192. https://doi.org/10.5558/tfc69187-2.

15. Rahn, M. *Wildfire Impact Analysis*, 2009. San Diego State University. http://universe.sdsu.edu/sdsu_newscenter/images/rahn2009fireanalysis.pdf. Accessed Jul. 10, 2018.

16. Neary, D. G., K. C. Ryan, and L. F. DeBano. *Wildland Fire in Ecosystems: Effects of Fire on Soils and Water*. Gen. Tech. Rep. RMRS-GTR-42-vol. 4. U.S. Department of Agriculture, Forest Service, Rocky Mountain Research Station, 2005.

17. Thompson, M. P., and D. E. Calkin. Uncertainty and Risk in Wildland Fire Management: A Review. *Journal of Environmental Management*, 2011. 92(8): 1895–1909.

18. Viegas, D.X. Fire Behaviour and Fireline Safety. *Annal of Burns and Fire* Disasters, 1993. 6(3). http://www.medbc.com/annals/review/vol_6/num_3/text/vol6n3p179.htm. Accessed Jun. 8, 2018.

19. Davis, C. The West in Flames: The Intergovernmental Politics of Wildfire Suppression and Prevention. *Publius*, 2001. 31(3): 97–110.

20. Neary, D. G., G. J. Gottfried, and P. F. Ffolliott. Post-Wildfire Watershed Flood Responses. Presented at . 2nd International Wildland Fire Ecology and Fire Management Congress and 5th Symposium on Fire Forest Meteorology, Orlando, FL., 2003.

21. Brown, J. A. H. Hydrologic Effects of a Bushfire in a Catchment in South-Eastern New South Wales. *Journal of Hydrology*, 1972. 15(1): 77–96. https://doi.org/10.1016/0022-1694(72)90077-7.

22. Candela, A., G. Aronica, and M. Santoro. Effects of Forest Fires on Flood Frequency Curves in a Mediterranean Catchment/Effets d'incendies de Forêt Sur Les Courbes de Fréquence de Crue Dans Un Bassin Versant Méditerranéen. *Hydrological Sciences Journal*, 2005. 50(2). https://doi.org/10.1623/hysj.50.2.193.61795.

23. Doerr, S. H., R. A. Shakesby, W. H. Blake, C. J. Chafer, G. S. Humphreys, and P. J. Wallbrink. Effects of Differing Wildfire Severities on Soil Wettability and Implications for Hydrological Response. *Journal of Hydrology*, 2006. 319(1–4): 295–311. https://doi.org/10.1016/j.jhydrol.2005.06.038.

24. DeBano, L. F. The Role of Fire and Soil Heating on Water Repellency in Wildland Environments: A Review. *Journal of Hydrology*, 2000. 231–232: 195–206. https://doi.org/10.1016/S0022-1694(00)00194-3.

25. Moody, J. A., B. A. Ebel, P. Nyman, D. A. Martin, C. Stoof, and R. McKinley. Relations between Soil Hydraulic Properties and Burn Severity. *International Journal of Wildland Fire*, 2016. 25(3): 279–293. https://doi.org/10.1071/WF14062.

26. Cannon, S. H., J. E. Gartner, M. G. Rupert, J. A. Michael, A. H. Rea, and C. Parrett. Predicting the Probability and Volume of Postwildfire Debris Flows in the Intermountain Western United States. *GSA Bulletin*, 2010. 122(1–2): 127–144. https://doi.org/10.1130/B26459.1.

27. Bradley, J. B., D. L. Richards, and C. C. Bahner. *Debris Control Structures: Evaluation and Countermeasures*. FHWA-IF-04-016 HEC-9. FHWA, U.S. Department of Transportation, 2005.

28. Cannon, S. H., E. R. Bigio, and E. Mine. A Process for Fire-Related Debris Flow Initiation, Cerro Grande Fire, New Mexico. *Hydrological Processes*, 2001. 15(15): 3011–3023. https://doi.org/10.1002/hyp.388.

29. Cannon, S. H., E. M. Boldt, J. L. Laber, J. W. Kean, and D. M. Staley. Rainfall Intensity–Duration Thresholds for Postfire Debris-Flow Emergency-Response Planning. *Natural Hazards*, 2011. 59(1): 209–236. https://doi.org/10.1007/s11069-011-9747-2.

30. Cannon, S. H., J. E. Gartner, R. C. Wilson, J. C. Bowers, and J. L. Laber. Storm Rainfall Conditions for Floods and Debris Flows from Recently Burned Areas in Southwestern Colorado and Southern California. *Geomorphology*, 2008. 96(3–4): 250–269. https://doi.org/10.1016/j.geomorph.2007.03.019.

31. Spigel, K. M., and P. R. Robichaud. First-Year Post-Fire Erosion Rates in Bitterroot National Forest, Montana. *Hydrological Processes*, 2007. 21(8): 998–1005. https://doi.org/10.1002/hyp.6295.

32. Debano, L. F., and J. S. Krammes. Water Repellent Soils and Their Relation to Wildfire Temperatures. *International Association of Scientific Hydrology. Bulletin*, 1966. 11(2): 14–19. https://doi.org/10.1080/02626666609493457.

33. Benavides-Solorio, J. de D., and L. H. MacDonald. Measurement and Prediction of Post-Fire Erosion at the Hillslope Scale, Colorado Front Range. *International Journal of Wildland Fire*, 2005. 14(4): 457–474. https://doi.org/10.1071/WF05042.

34. Highland, L., and P. T. Bobrowsky. *The Landslide Handbook: A Guide to Understanding Landslides*. Circular 1325, U.S. Geological Survey, 2008.

35. Ohlmacher, G. C., and J. C. Davis. Using Multiple Logistic Regression and GIS Technology to Predict Landslide Hazard in Northeast Kansas, USA. *Engineering Geology*, 2003. 69(3–4): 331–343. https://doi.org/10.1016/S0013-7952(03)00069-3.

36. Promper, C., A. Puissant, J.-P. Malet, and T. Glade. Analysis of Land Cover Changes in the Past and the Future as Contribution to Landslide Risk Scenarios. *Applied Geography*, 2014. 53: 11–19. https://doi.org/10.1016/j.apgeog.2014.05.020.

37. Shakesby, R. A., and S. H. Doerr. Wildfire as a Hydrological and Geomorphological Agent. *Earth-Science Reviews*, 2006. 74(3–4): pp. 269–307. https://doi.org/10.1016/j.earscirev.2005.10.006.

38. Clopper, P. E., and Y-H. Chen. Minimizing Embankment Damage During Overtopping Flow. FHWA/RD-88/181. FHWA, U.S. Department of Transportation, 1988.

39. Vennapusa, P., D. J. White, and D. K. Miller. Geo-Infrastructure Damage Assessment, Repair and Mitigation Strategies. *Tech Transfer Summaries,* 2013. 52.

40. Bonelli, S. *Erosion in Geomechanics Applied to Dams and Levees*. John Wiley & Sons, New York, 2013.

41. Briaud, J.-L., and L. Maddah. *Minimizing Roadway Embankment Damage from Flooding*. Transportation Research Board, Washington, D.C., 2016.

42. Rigby, E. H., and A. J. Barthelmess. Culvert Blockage Mechanisms and Their Impact on Flood Behaviour. In *Proceedings of the 34th World Congress of the International Association for Hydro- Environment Research and Engineering: 33rd Hydrology and Water Resources Symposium and 10th Conference on Hydraulics in Water Engineering* (E. M. Valentine, C. J. Apelt, J. Ball, H. Chanson, R. Cox, R. Ettema, G. Kuczera, M. Lambert, B. W. Melville, and J. E.Sargison, eds.), Engineers Australia, Barton, A.C.T., 2011. 380-387.

43. Rigby, E. H., M. J. Boyd, S. Roso, and P. Silveri. Causes and Effects of Culvert Blockage during Large Storms. In *Global Solutions for Urban Drainage: Proceedings of the Ninth International Conference on Urban Drainage* (E. W. Strecker, and W. C. Huber, eds.), American Society of Civil Engineers, 2002.

44. Barthelmess, A. J., and E. H. Rigby. Estimating Culvert and Bridge Blockages - a Simplified Procedure. In *Proceedings of the 34th World Congress of the International Association for Hydro- Environment Research and Engineering: 33rd Hydrology and Water Resources Symposium and 10th Conference on Hydraulics in Water Engineering* (E. M. Valentine, C. J. Apelt, J. Ball, H. Chanson, R. Cox, R. Ettema, G. Kuczera, M. Lambert, B. W. Melville, and J. E.Sargison, eds.), Engineers Australia, Barton, A.C.T., 2011. 39-47.

45. Barthelmess, A. J., and E. H. Rigby. Quantification of Debris Potential and the Evolution of a Regional Culvert Blockage Model. In: H2009: 32nd Hydrology and Water Resources Symposium, Newcastle : Adapting to Change (W. Melville, and J. E.Sargison, eds.), Engineers Australia, Barton, A.C.T., 2009. 218-229.

46. Tillery, A. C., M. J. Darr, S. H. Cannon, and J. A. Michael. Post-Wildfire *Preliminary Debris Flow Hazard Assessment for the Area Burned by the 2011 Las*

Conchas Fire in North-Central New Mexico. U.S. Geological Survey Open-File Report 2011-1308.

47. Dey, S., and R. V. Raikar. Characteristics of Horseshoe Vortex in Developing Scour Holes at Piers. *Journal of Hydraulic Engineering*, 2007. 133(4): 399–413. https://doi.org/10.1061/(ASCE)0733-9429(2007)133:4(399).

48. Lee, G. C., S. B. Mohan, C. Huang, and B. N. Fard. *A Study of US Bridge Failures (1980–2012)*. Technical Report MCEER 13-008. University at Buffalo, State University of New York, 2013.

49. Zarrati, A. R., M. R. Chamani, A. Shafaie, and M. Latifi. Scour Countermeasures for Cylindrical Piers Using Riprap and Combination of Collar and Riprap. *International Journal of Sediment Research*, 2010. 25(3): 313–322. https://doi.org/10.1016/S1001-6279(10)60048-0.

50. Coleman, S. E., and B. W. Melville. Case Study: New Zealand Bridge Scour Experiences. *Journal of Hydraulic Engineering*, 2001. 127(7): 535–546.

51. Zarrati, A. R., M. Nazariha, and M. B. Mashahir. Reduction of Local Scour in the Vicinity of Bridge Pier Groups Using Collars and Riprap. *Journal of Hydraulic Engineering*, 2006. 132(2): 154–162. https://doi.org/10.1061/(ASCE)0733-9429(2006)132:2(154).

52. Dai, F. C., C. F. Lee, and Y. Y. Ngai. Landslide Risk Assessment and Management: An Overview. *Engineering Geology*, 2002. 64(1): 65–87. https://doi.org/10.1016/S0013-7952(01)00093-X.

53. Lu, P., S. Bai, and N. Casagli. Spatial Relationships between Landslide Occurrences and Land Cover across the Arno River Basin (Italy). *Environmental Earth Sciences*, 2015. 74(7): 5541–5555. https://doi.org/10.1007/s12665-015-4569-2.

54. Busenberg, G. Wildfire Management in the United States: The Evolution of a Policy Failure. *Review of Policy Research*, 2004. 21(2): 145–156. https://doi.org/10.1111/j.1541-1338.2004.00066.x.

55. Calkin, D. E., M. P. Thompson, and M. A. Finney. Negative Consequences of Positive Feedbacks in US Wildfire Management. *Forest Ecosystems*, 2015. 2(1): 9. https://doi.org/10.1186/s40663-015-0033-8.

56. Butry, D. T. Fighting Fire with Fire: Estimating the Efficacy of Wildfire Mitigation Programs Using Propensity Scores. *Environmental Ecology Statistics*, 2009. 16:291-319.

57. Reinhardt, E. D., R. E. Keane, D. E. Calkin, and J. D. Cohen. Objectives and Considerations for Wildland Fuel Treatment in Forested Ecosystems of the Interior Western United States. *Forest Ecology and Management*, 2008. 256(12): 1997–2006. https://doi.org/10.1016/j.foreco.2008.09.016.

58. Robichaud, P. R., F. B. Pierson, R. E. Brown, and J. W. Wagenbrenner. Measuring Effectiveness of Three Postfire Hillslope Erosion Barrier Treatments, Western Montana, USA. *Hydrological Processes*, 2008. 22(2): 159–170. https://doi.org/10.1002/hyp.6558.

59. Robichaud, P. R., L. E. Ashmun, R. B. Foltz, C. G. Showers, J. S. Groenier, J. Kesler, C. DeLeo, and M. Moore. *Production and Aerial Application of Wood Shreds as a Post-Fire Hillslope Erosion Mitigation Treatment*. Gen. Tech. Rep. RMRS-GTR-307. U.S. Department of Agriculture, Forest Service, Rocky Mountain Research Station, 2013.

60. Tyler, R. N. *River Debris: Causes, Impacts, and Mitigation Techniques*. Alaska Center for Energy and Power, University of Alaska Fairbanks, 2011.

61. Santi, P., J. Higgins, S. H. Cannon, and J. DeGraff. *Evaluation of Post-Wildfire Debris Flow Mitigation Methods and Development of Decision-Support Tools: Final Report to the Joint Fire Science Program*. 2006.

62. Grimaldi, C., R. Gaudio, F. Calomino, and A. H. Cardoso. Control of Scour at Bridge Piers by a Downstream Bed Sill. *Journal of Hydraulic Engineering*, 2009. 135(1): 13–21. https://doi.org/10.1061/(ASCE)0733-9429(2009)135:1(13).

63. Chiew, Y.-M. Scour Protection at Bridge Piers. *Journal of Hydraulic Engineering*, 1992. 118(9): https://doi.org/10.1061/(ASCE)0733-9429(1992)118:9(1260).

64. Wang, C., F. Liang, and X. Yu. Experimental and Numerical Investigations on the Performance of 85(3): 1417–1435. https://doi.org/10.1007/s11069-016-2634-0.

65. Seville, E., and J. Metcalfe. *Developing a Hazard Risk Assessment Framework for the New Zealand State Highway Network*. Research Report 276. Land Transport New Zealand, 2005.

66. Wardhana, K., and F. C. Hadipriono. Analysis of Recent Bridge Failures in the United States. *Journal of Performance of Constructed Facilities*, 2003. 17(3): 144-150.

67. Thompson, P. L., M. L. Corry, F. J. Watts, D. L. Richards, J. S. Jones, and J. N. Bradley. *Hydraulic Design of Energy Dissipators for Culverts and Channels*. FHWA-EPD-86-110 HEC-14. FHWA, U.S. Department of Transportation, 1983.

68. Briaud, J-L., and L. Maddah. *Minimizing Roadway Embankment Damage from Flooding: A Synthesis of Highway Practice*. NCHRP Synthesis 496. Transportation Research Board, 2016. https://doi.org/10.17226/23604.

69. Chen, Y. H., and B. A. Anderson. *Development of a Methodology for Estimating Embankment Damage Due to Flood Overtopping*. FHWA/RD-86/126. FHWA, U.S. Department of Transportation, 1987.

70. Canfield, H. E., D. C. Goodrich, and I. S. Burns. Selection of Parameters Values to Model Post-Fire Runoff and Sediment Transport at the Watershed Scale in Southwestern Forests. In *Managing Watersheds for Human and Natural Impacts: Engineering, Ecological, and Economic Challenges*. *Proceedings of the 2005 Watershed Management Conference*, 2005. https://doi.org/10.1061/40763(178)48

71. Shakesby, R. A., J. A. Moody, D. A. Martin, and P. R. Robichaud. Synthesising Empirical Results to Improve Predictions of Post-Wildfire Runoff and Erosion Response. *International Journal of Wildland Fire*, 2016. 25(3): 257–261. https://doi.org/10.1071/WF16021.

72. Sidman, G., D. P. Guertin, D. C. Goodrich, C. L. Unkrich, and I. S. Burns. Risk Assessment of Post-Wildfire Hydrological Response in Semiarid Basins: The Effects of Varying Rainfall Representations in the KINEROS2/AGWA Model. *International Journal of Wildland Fire*, 2016. 25(3): 268-278. https://doi.org/10.1071/WF14071.

73. McLin, S. G., M. E. van Eeckhout, and A. Earles. *Mapping 100-Year Floodplain Boundaries Following the Cerro Grande Wildfire*. LA-UR-01-5218. Los Alamos National Laboratory, 2001.

74. McLin, S. G., E. P. Springer, and L. J. Lane. Predicting Floodplain Boundary Changes Following the Cerro Grande Wildfire. *Hydrological Processes*, 2001. 15(15): 2967–2980. https://doi.org/10.1002/hyp.385.

75. DeGaetano, A. T. Time-Dependent Changes in Extreme-Precipitation Return-Period Amounts in the Continental United States. *Journal of Applied Meteorology and Climatology*, 2009. 48(10) 2086–2099. https://doi.org/10.1175/2009JAMC2179.1.

76. Frei, C., R. Schöll, S. Fukutome, J. Schmidli, and P. L. Vidale. Future Change of Precipitation Extremes in Europe: Intercomparison of Scenarios from Regional Climate Models. *Journal of Geophysical Research: Atmospheres*, 2006. 111(D6): D06105. https://doi.org/10.1029/2005JD005965.

77. Huntingford, C., R. G. Jones, C. Prudhomme, R. Lamb, J. H. C. Gash, and D. A. Jones. Regional Climate-Model Predictions of Extreme Rainfall for a Changing Climate. *Quarterly Journal of the Royal Meteorological Society*, 2003. 129(590): 1607–1621. https://doi.org/10.1256/qj.02.97.

78. Kharin, V. V., F. W. Zwiers, X. Zhang, and G. C. Hegerl. Changes in Temperature and Precipitation Extremes in the IPCC Ensemble of Global Coupled Model Simulations. *Journal of Climate*, 2007. 20(8): 1419–1444. https://doi.org/10.1175/JCLI4066.1.

79. Meehl, G. A., F. Zwiers, J. Evans, T. Knutson, L. Mearns, and P. Whetton. Trends in Extreme Weather and Climate Events: Issues Related to Modeling Extremes in Projections of Future Climate Change. *Bulletin of the American Meteorological Society*, 2000. 81(3): 427–436. https://doi.org/10.1175/1520-0477(2000)081<0427:TIEWAC>2.3.CO;2.

80. Zwiers, F. W., and V. V. Kharin. Changes in the Extremes of the Climate Simulated by CCC GCM2 under CO2 Doubling. *Journal of Climate*, 1998. 11(9): 2200–2222. https://doi.org/10.1175/1520-0442(1998)011<2200:CITEOT>2.0.CO;2.

81. Homer, C., J. Dewitz, L. Yang, S. Jin, P. Danielson, G. Xian, J. Coulston, N. Herold, J. Wickham, and K. Megown. Completion of the 2011 National Land Cover Database for the Conterminous United States - Representing a Decade of Land Cover Change Information. *Photogrammetric Engineering and Remote Sensing*, 2015. 81: 346–354. https://doi.org/10.14358/PERS.81.5.345.

82. Soil Survey Staff, Natural Resources Conservation Service, United States Department of Agriculture. *Web Soil Survey*. https://websoilsurvey.sc.egov.usda.gov/. Accessed Jul. 23, 2018.

83. United States Geological Survey (USGS). *EarthExplorer*. https://earthexplorer.usgs.gov/. Accessed Jul. 23, 2018.

84. Los Alamos National Laboratory. NM 1 Feet Digital Elevation Model.

85. New Mexico Resource Geographic Information System (RGIS). *RGIS Data Portal*. https://rgis-data.unm.edu/rgisportal/. Accessed Jul. 23, 2018.

86. USDA Forest Service, Remote Sensing Applications Center. *BAER Imagery Support Data Download*. https://fsapps.nwcg.gov/afm/baer/download.php?year=2011. Accessed Jul. 23, 2018.

87. National Bridge Inventory (NBI), ArcGIS. https://www.arcgis.com/home/item.html?id=775f08232eb1424189a4e8091edf893e. Accessed Jul. 24, 2017.

88. Melville B. W. Pier and Abutment Scour: Integrated Approach. *Journal of Hydraulic Engineering*, 1997. 123(2): 125–136. https://doi.org/10.1061/(ASCE)0733-9429(1997)123:2(125).

89. Zarrati A. R., Nazariha M., and Mashahir M. B. Reduction of Local Scour in the Vicinity of Bridge Pier Groups Using Collars and Riprap. *Journal of Hydraulic Engineering*, 2006. 132(2): 154–162. https://doi.org/10.1061/(ASCE)0733-9429(2006)132:2(154).

90. Chiew, Y. M. Scour Protection at Bridge Piers. *Journal of Hydraulic Engineering*, 1992. 118(9): 1260–1269.

91. Sultana, M., G. W. Chai, T. C. Martin, and S. H. Chowdhury. A Review of the Structural Performance of Flooded Pavements. Presented at 26th ARRB Conference–Research driving efficiency, Sydney, New South Wales, 2014.

92. Huang, A.-B., J.-T. Lee, Y.-T. Ho, Y.-F. Chiu, and S.-Y. Cheng. Stability Monitoring of Rainfall-Induced Deep Landslides through Pore Pressure Profile

Measurements. *Soils and Foundations*, 2012. 52(4): 737–747. https://doi.org/10.1016/j.sandf.2012.07.013.

93. Herrera, E. K., A. Flannery, and M. Krimmer. Risk and Resilience Analysis for Highway Assets. *Transportation Research Record: Journal of the Transportation Research Board*, 2017. 2604: 1–8. https://doi.org/10.3141/2604-01.

94. Federal Highway Administration (FHWA). *Climate Change & Extreme Weather Vulnerability Assessment Framework*. FHWA-HEP-13-005. FHWA, U.S. Department of Transportation, 2012. https://www.fhwa.dot.gov/environment/sustainability/resilience/publications/vulnerability_assessment_framework/index.cfm. Accessed Jul. 17, 2018.

95. Papadopoulos, G. D., and F.-N. Pavlidou. A Comparative Review on Wildfire Simulators. *IEEE Systems Journal*, 2011. 5(2): 233–243. https://doi.org/10.1109/JSYST.2011.2125230.

96. *Transportation Systems Sector-Specific Plan - 2010*. Department of Homeland Security. https://www.dhs.gov/publication/nipp-ssp-transportation-systems-2010. Accessed Jun. 7, 2018.

97. *MnDOT Policies: Use of Prescribed Fire*. Minnesota Department of Transportation. http://www.dot.state.mn.us/policy/operations/op001.html. Accessed Jun. 9, 2018.

98. *Transportation Asset Management Guide: A Focus on Implementation*. American Association of State Highway and Transportation Officials (AASHTO), Washington, DC, 2013.

APPENDIX

Inundation Maps

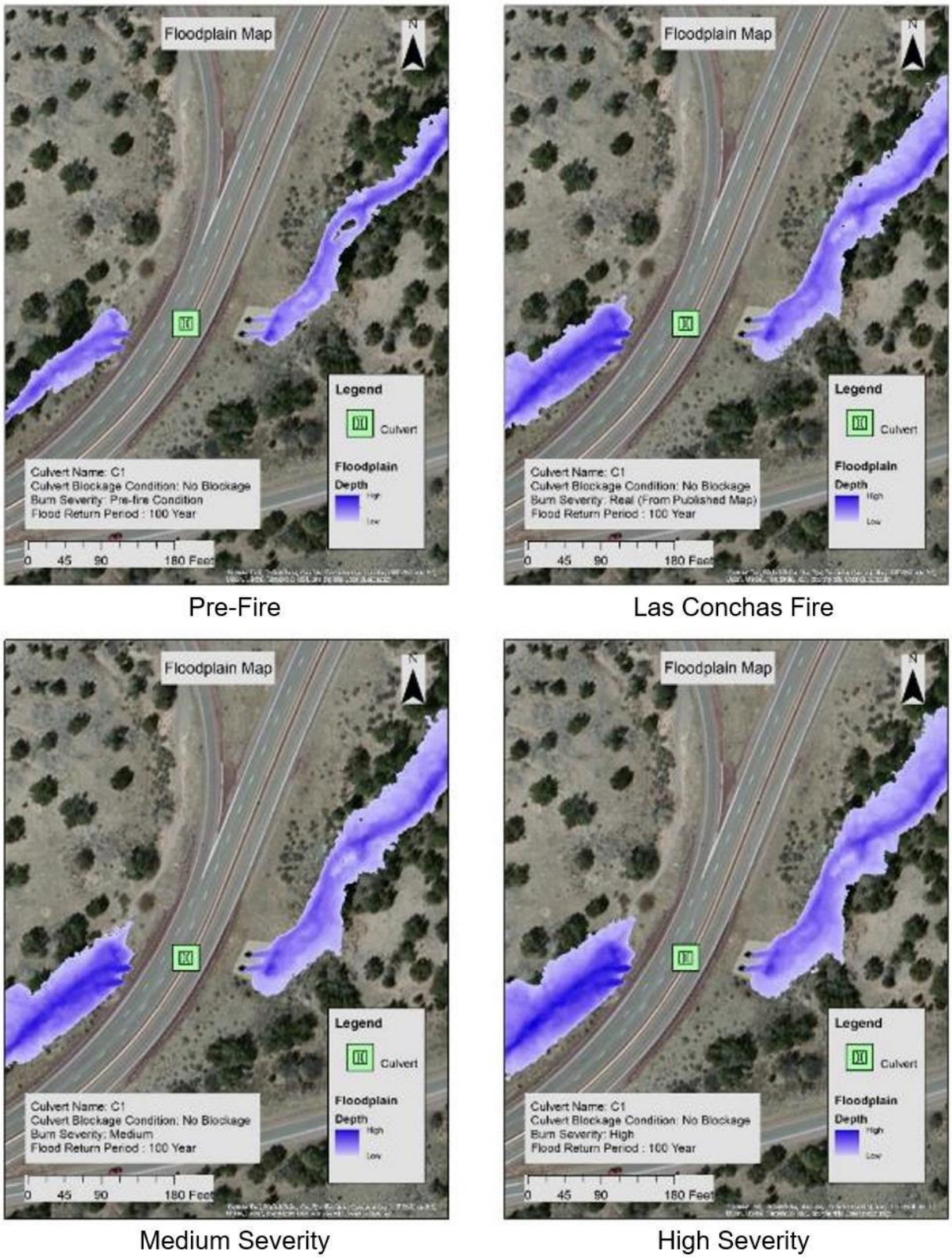

Figure 22. Floodplains at Culvert C1, No Blockage, Baseline Climate

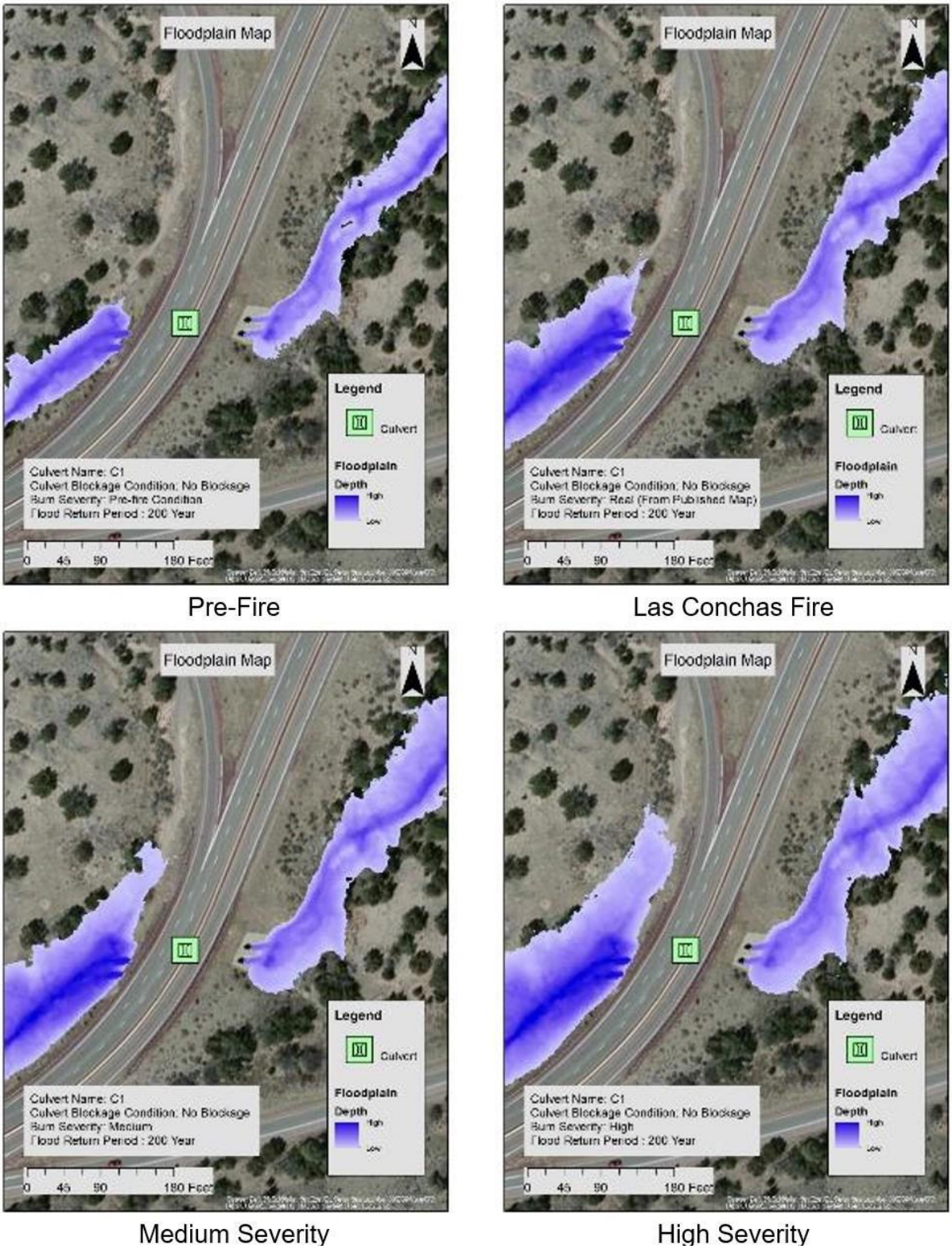

Figure 23. Floodplains at Culvert C1, No Blockage, Climate Change

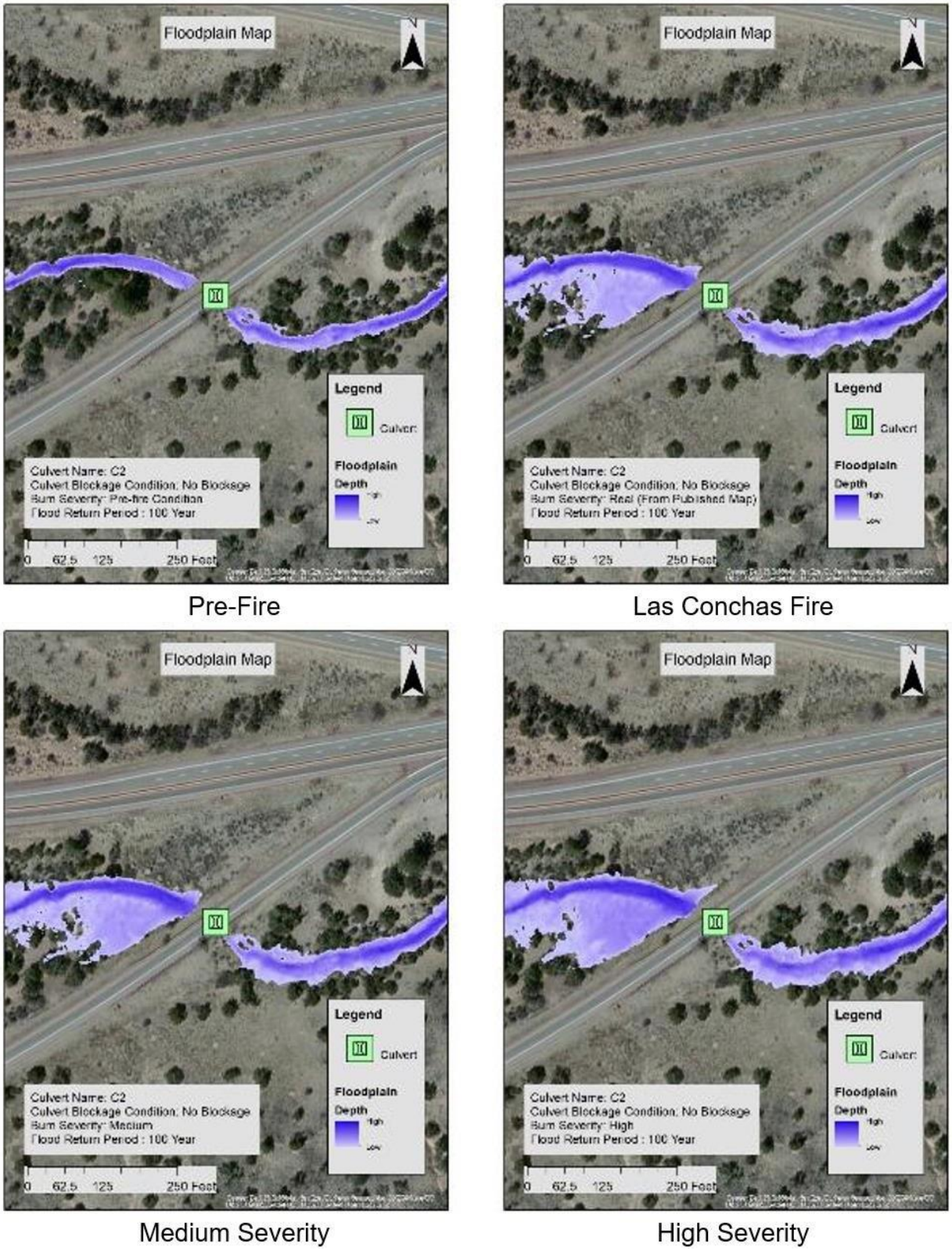

Figure 24. Floodplains at Culvert C2, No Blockage, Baseline Climate

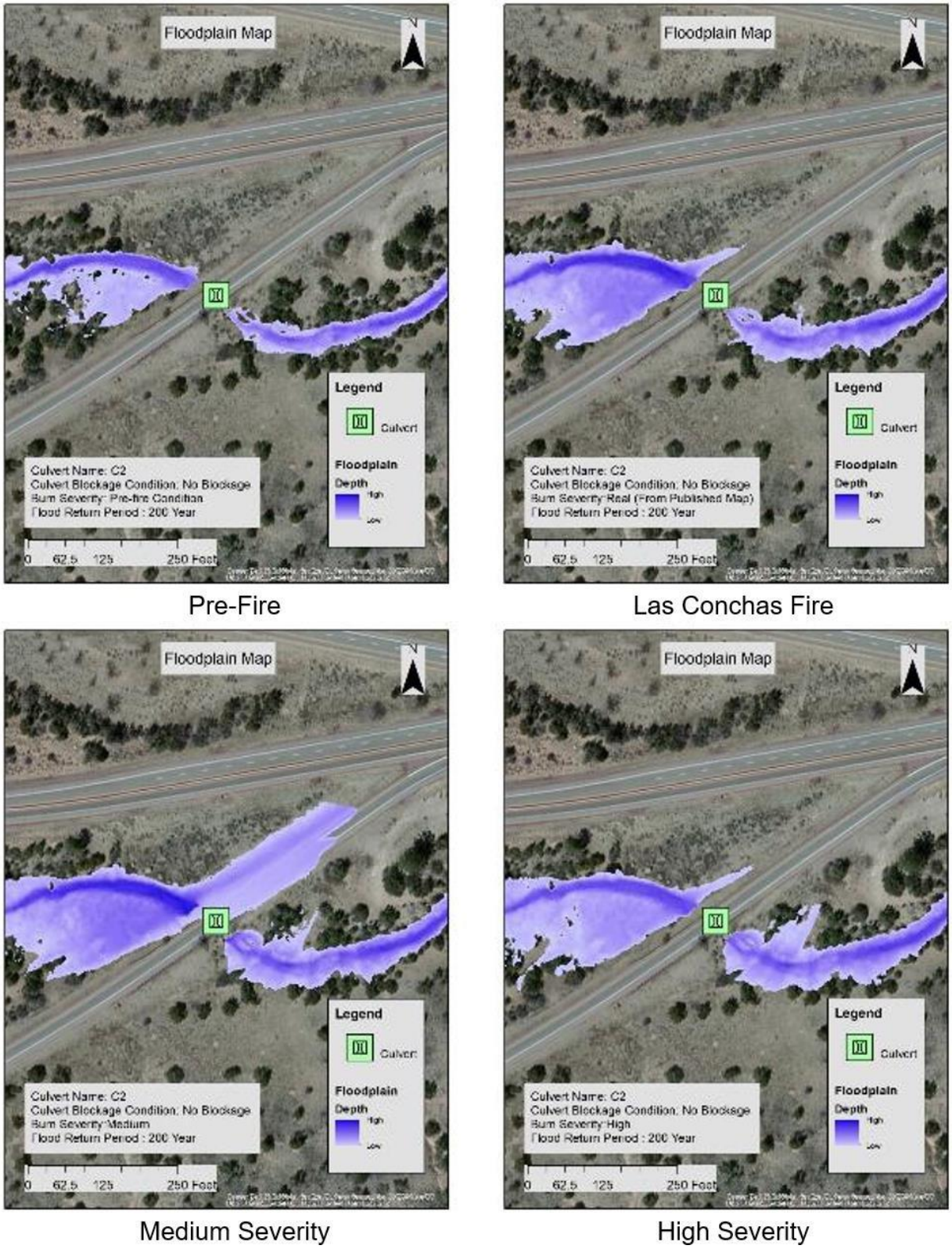

Figure 25. Floodplains at Culvert C2, No Blockage, Climate Change

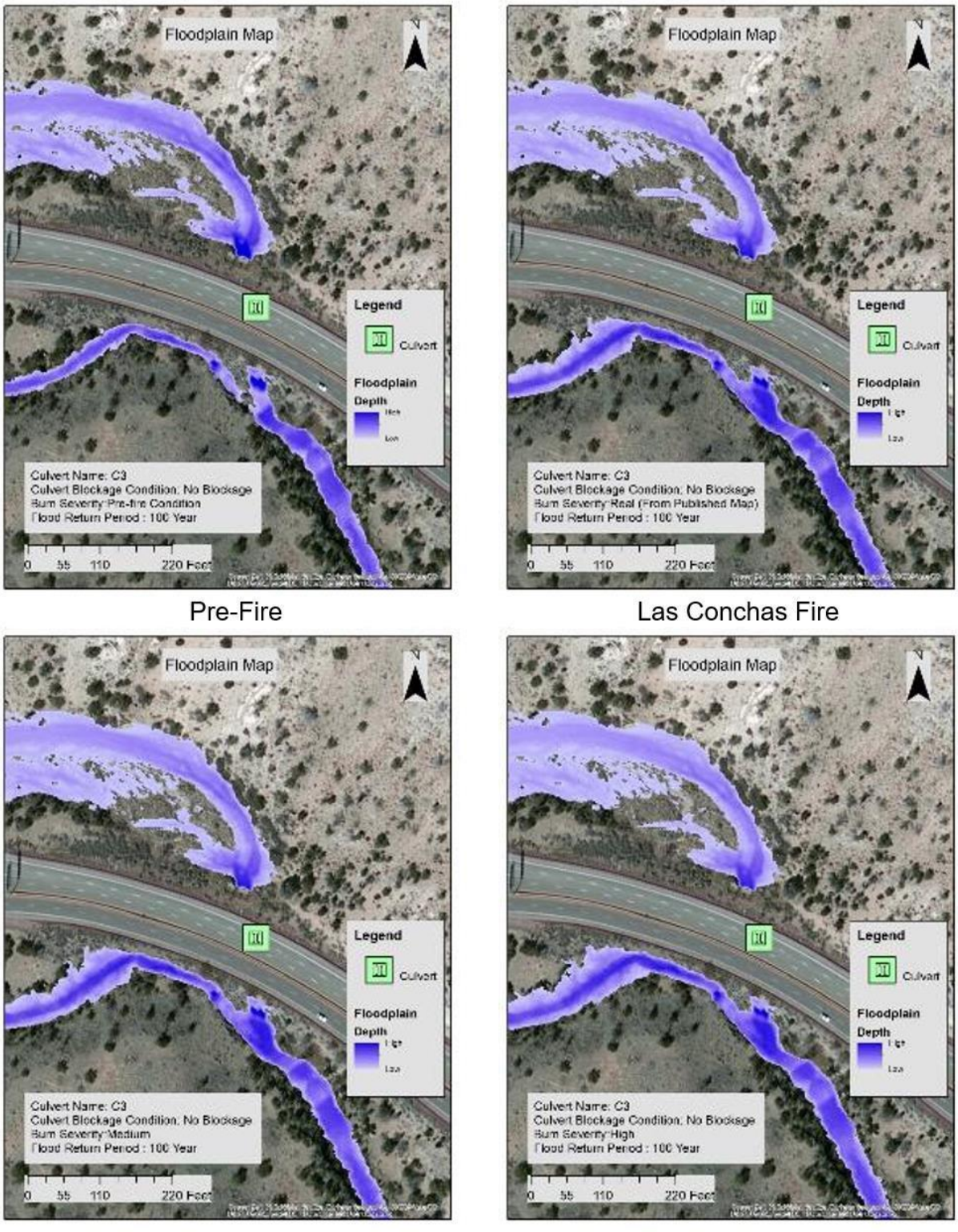

Figure 26. Floodplains at Culvert C3, No Blockage, Baseline Climate

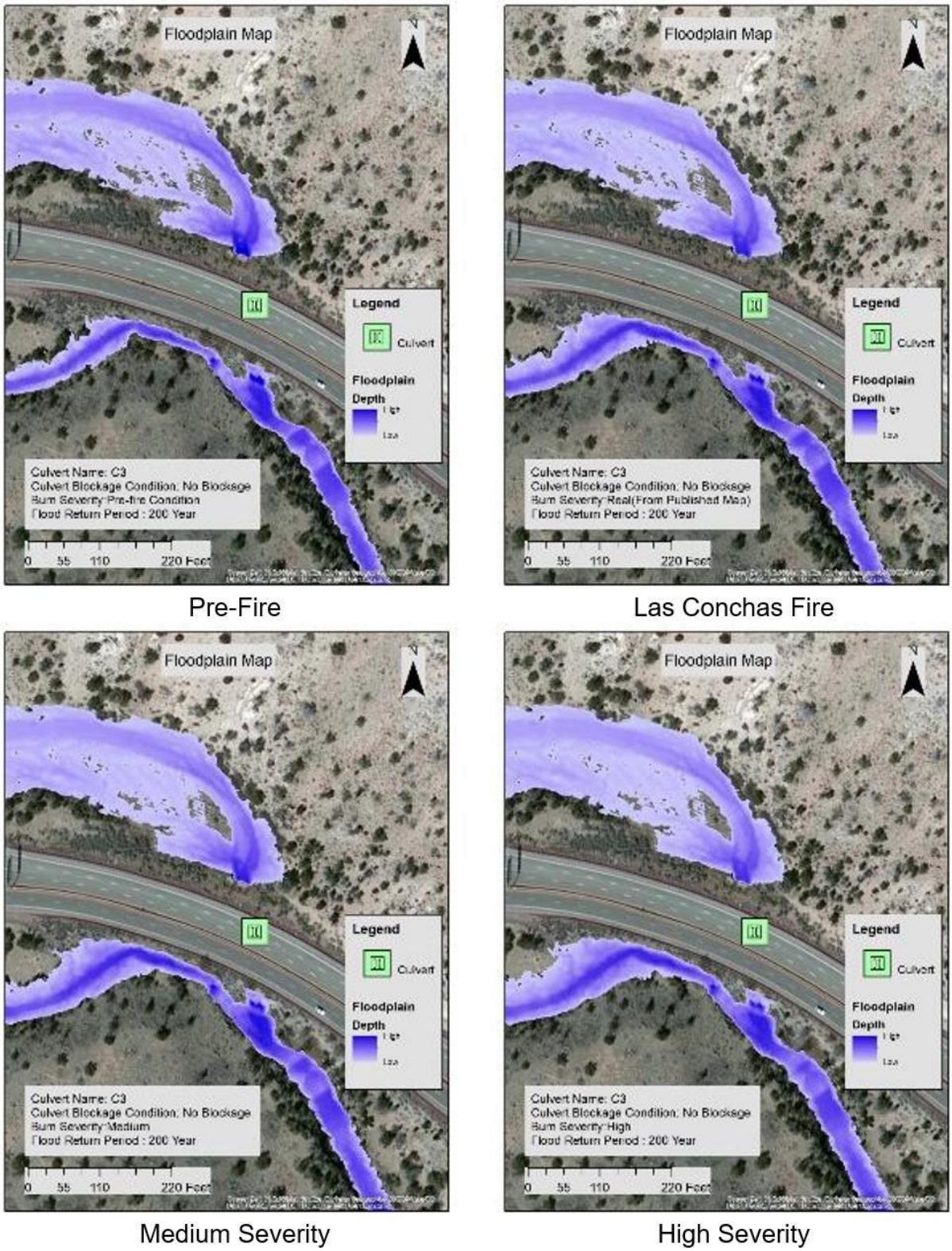

Figure 27. Floodplains at Culvert C3, No Blockage, Climate Change

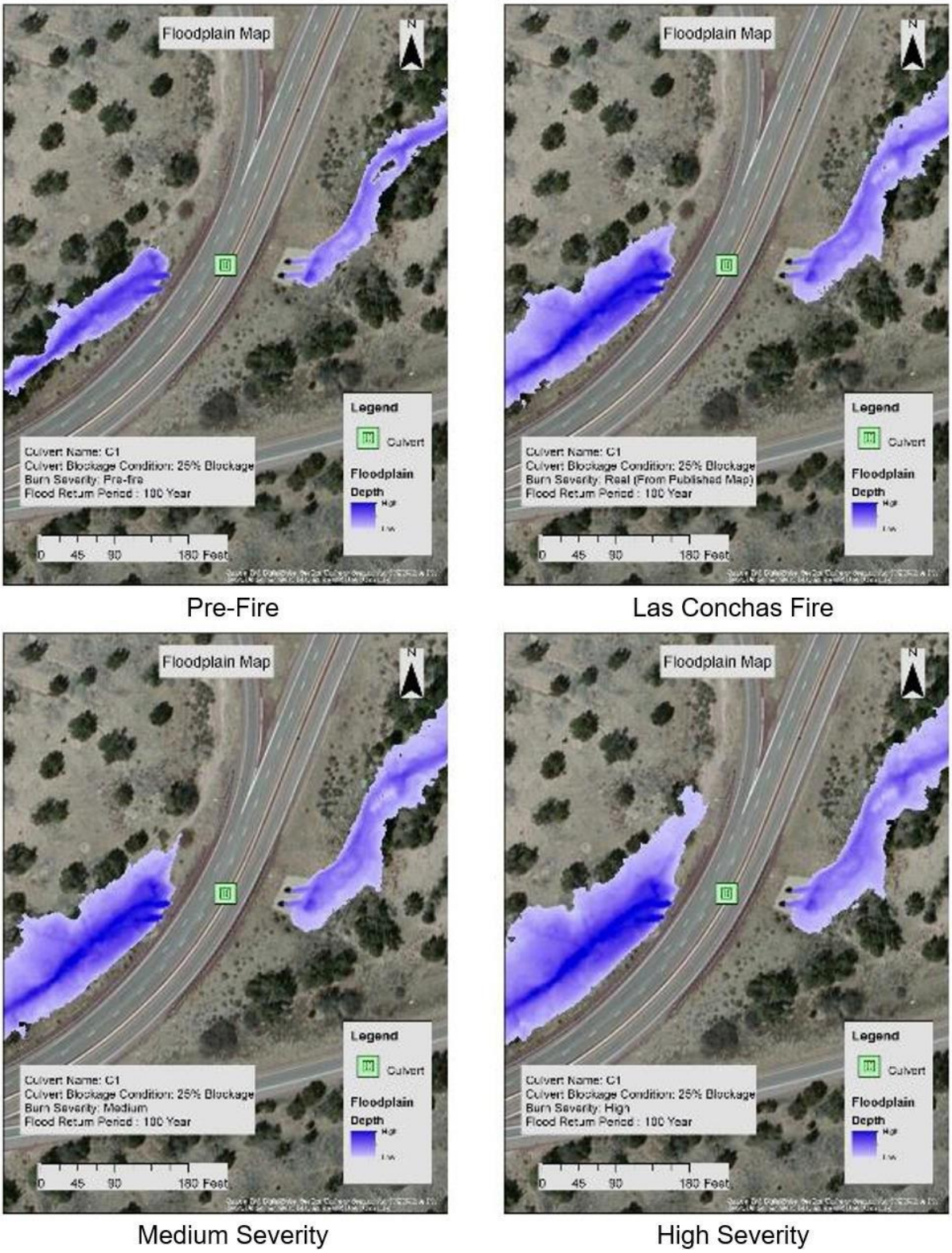

Figure 28. Floodplains at Culvert C1, 25% Blockage, Baseline Climate

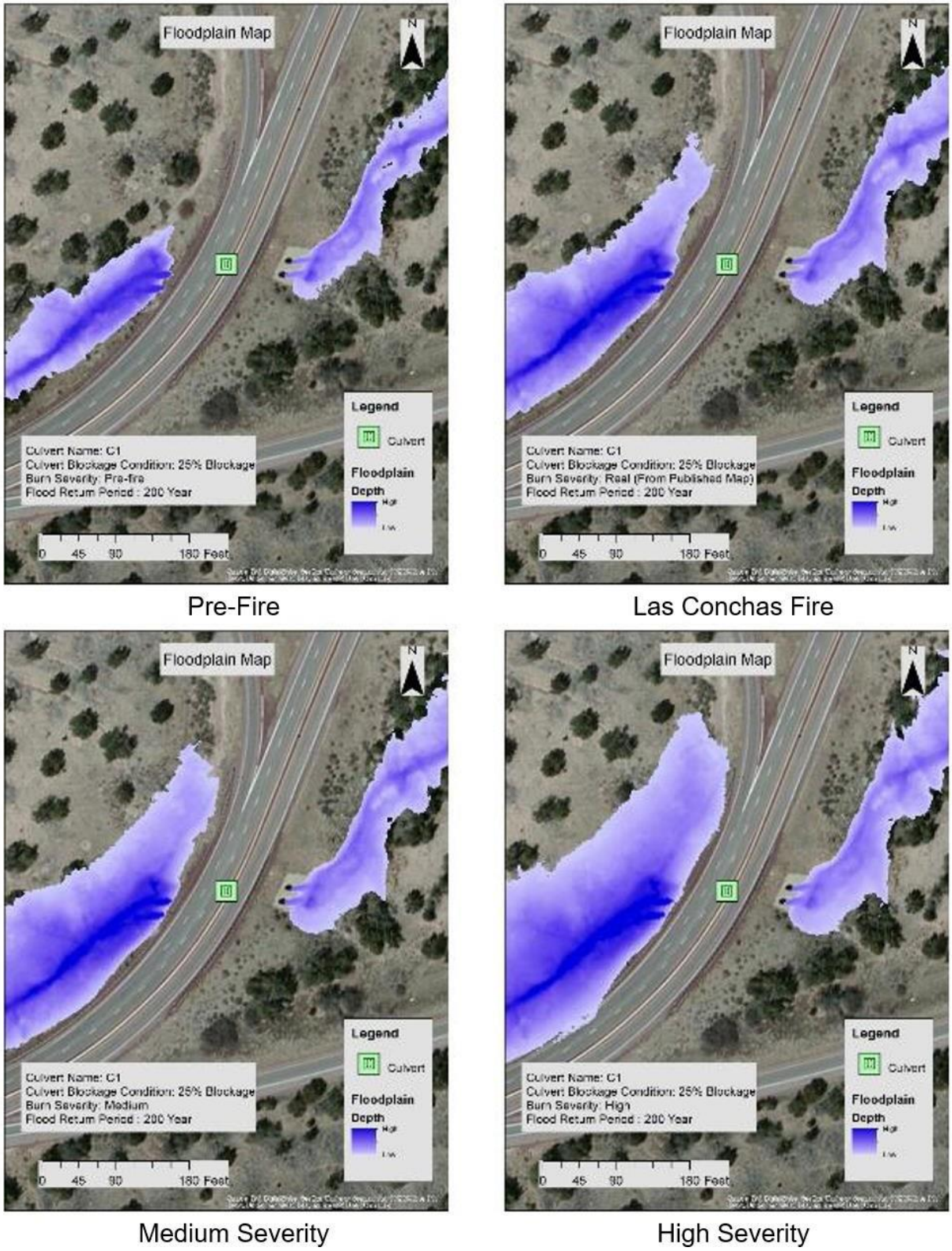

Figure 29. Floodplains at Culvert C1, 25% Blockage, Climate Change

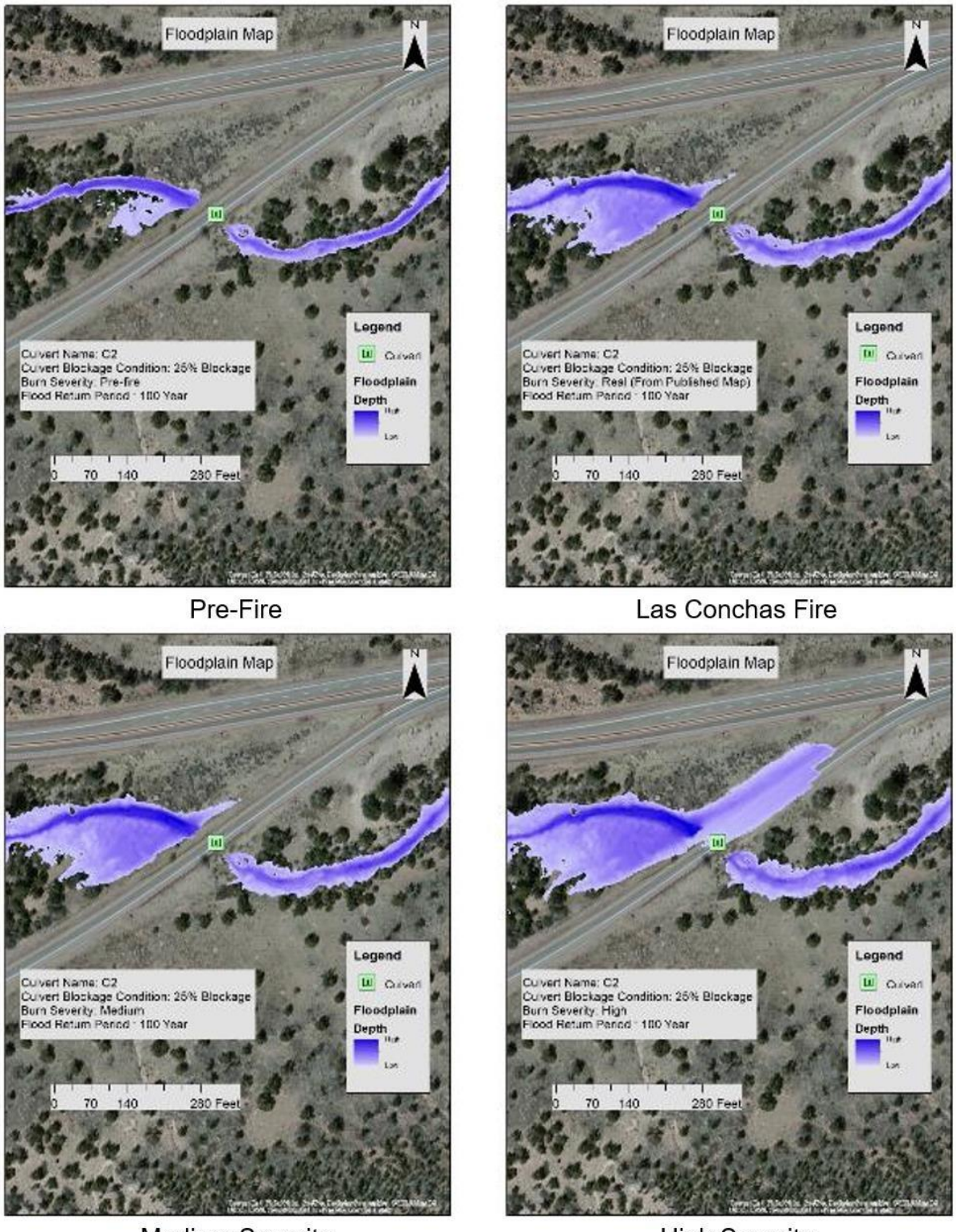

Figure 30. Floodplains at Culvert C2, 25% Blockage, Baseline Climate

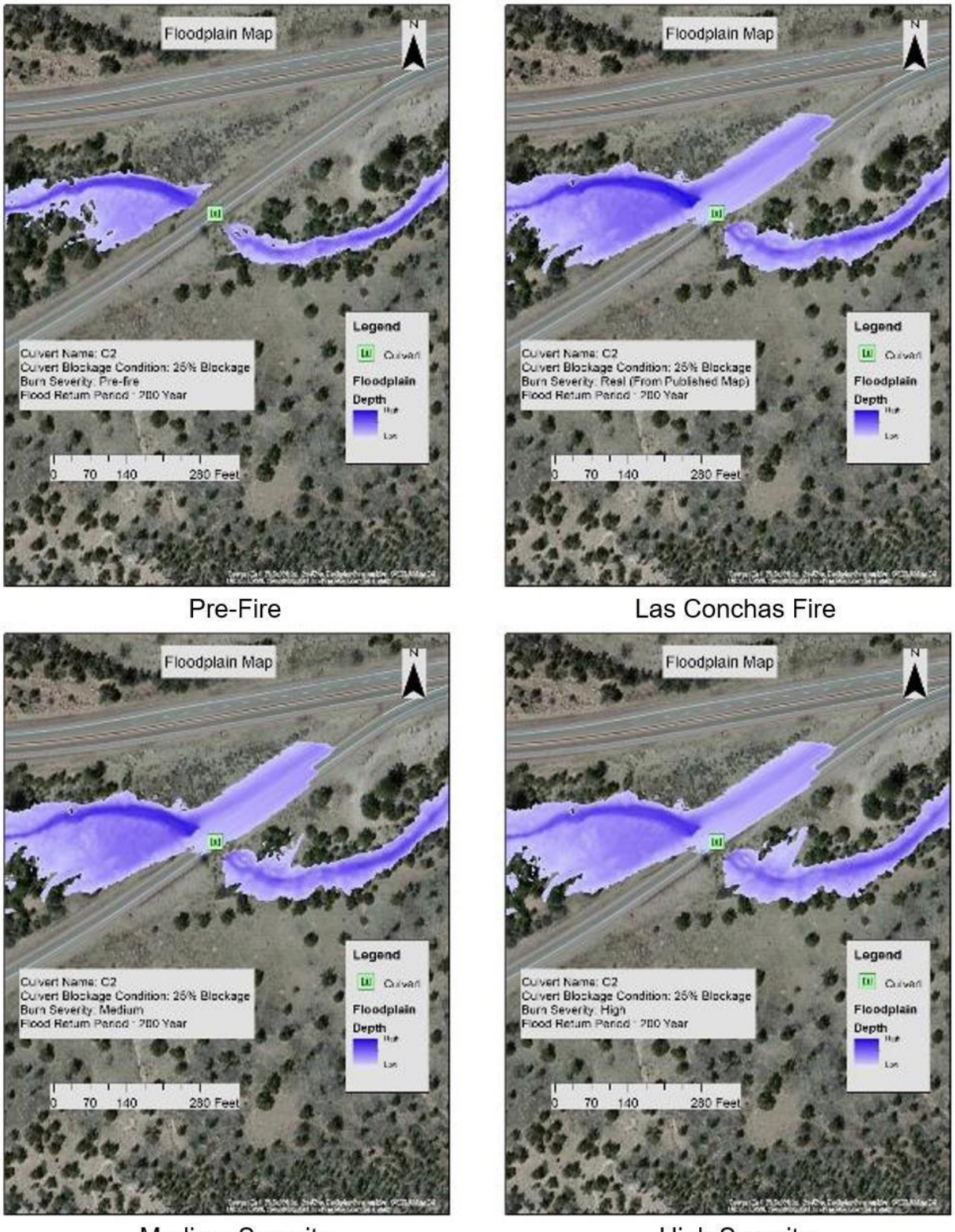

Figure 31. Floodplains at Culvert C2, 25% Blockage, Climate Change

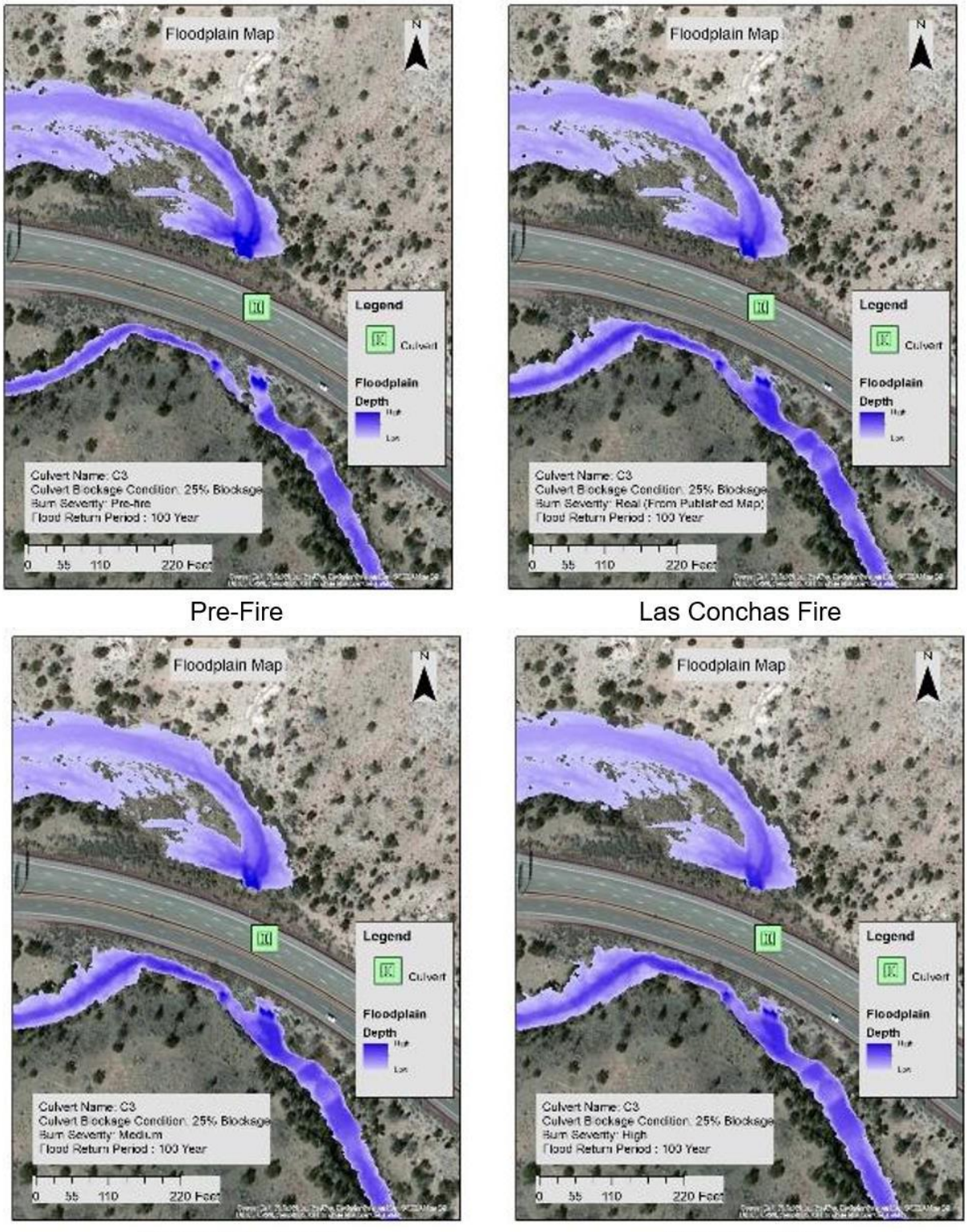

Figure 32. Floodplains at Culvert C3, 25% Blockage, Baseline Climate

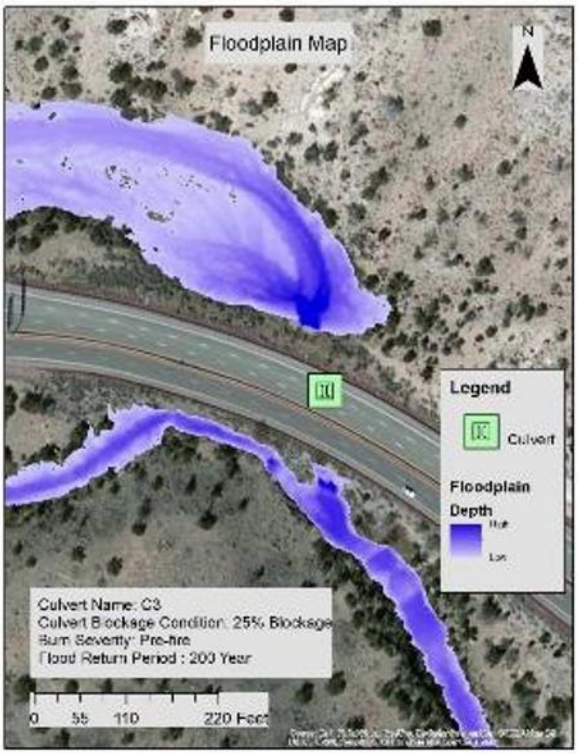

Pre-Fire

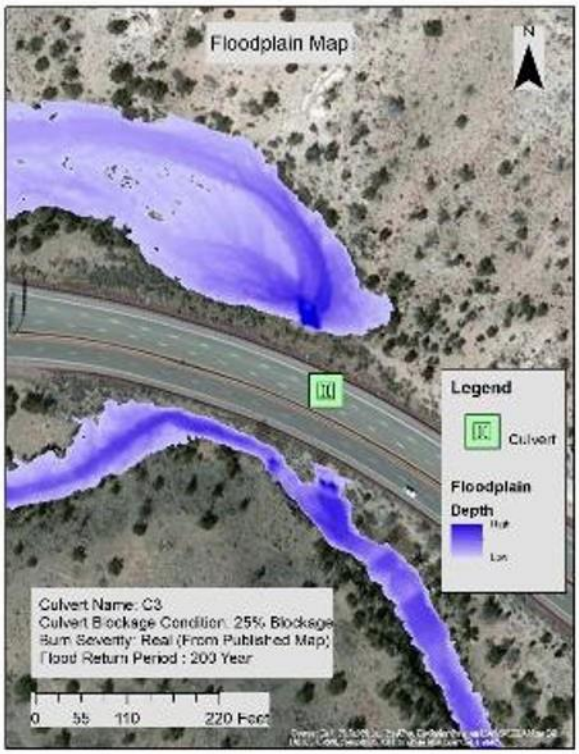

Las Conchas Fire

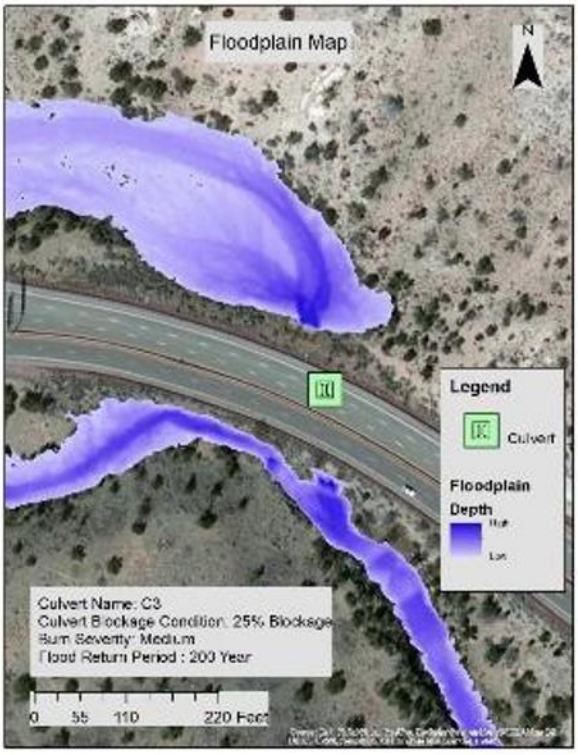

Medium Severity

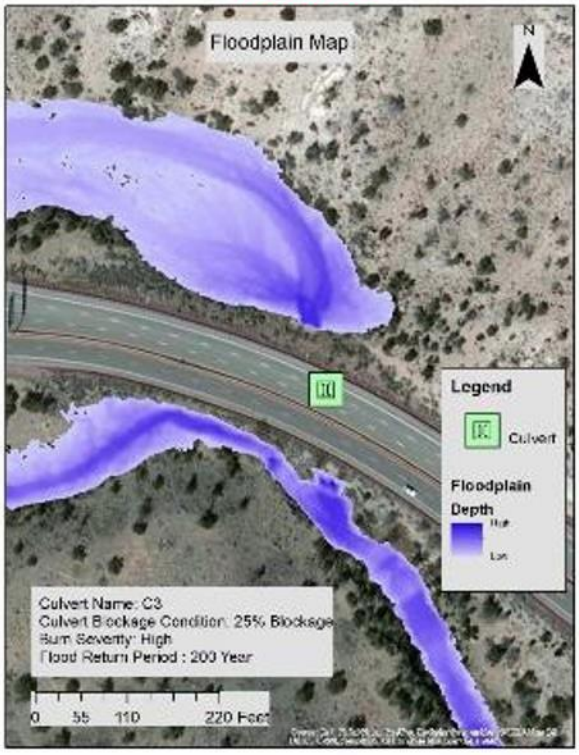

High Severity

Figure 33. Floodplains at Culvert C3, 25% Blockage, Climate Change

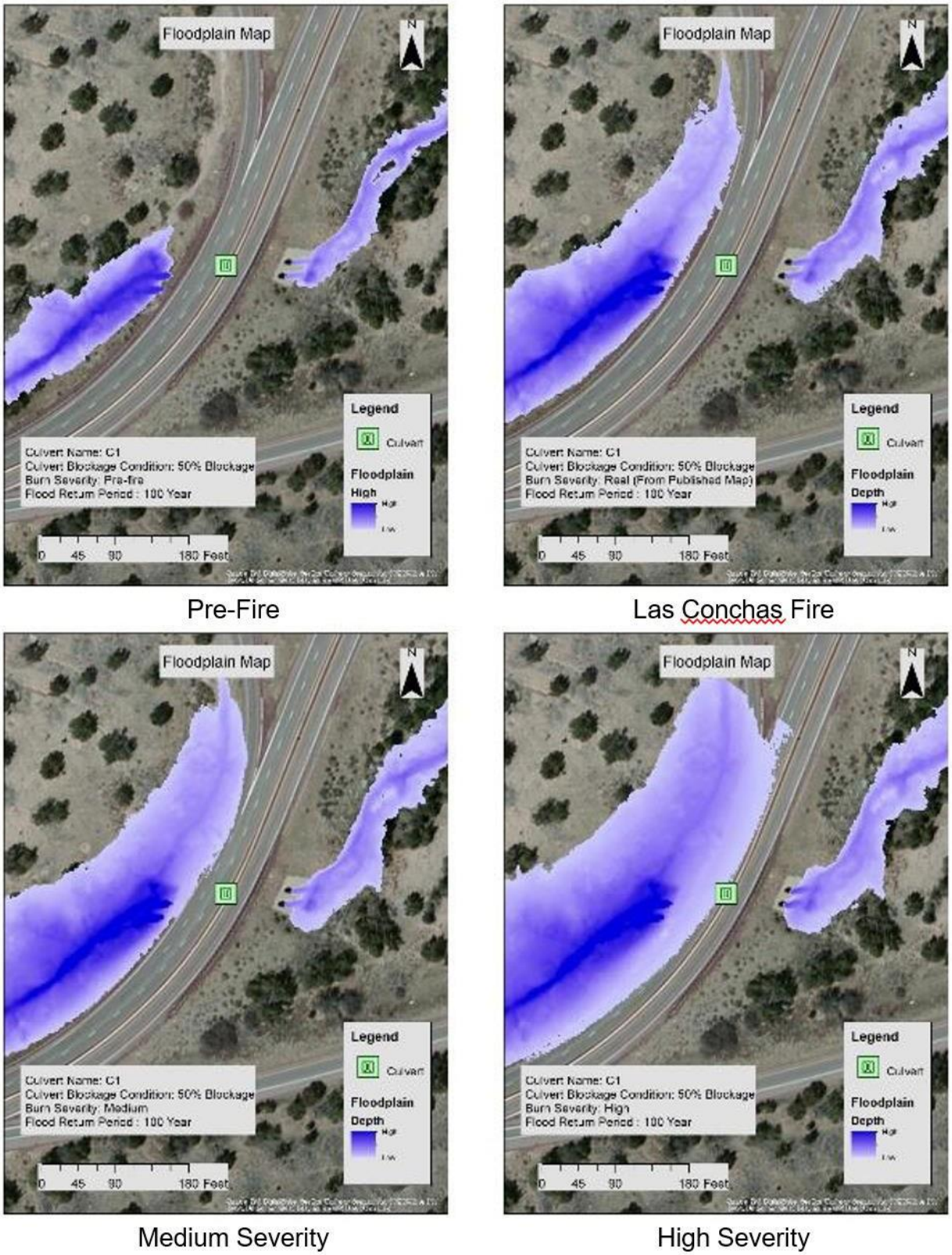

Figure 34. Floodplains at Culvert C1, 50% Blockage, Baseline Climate

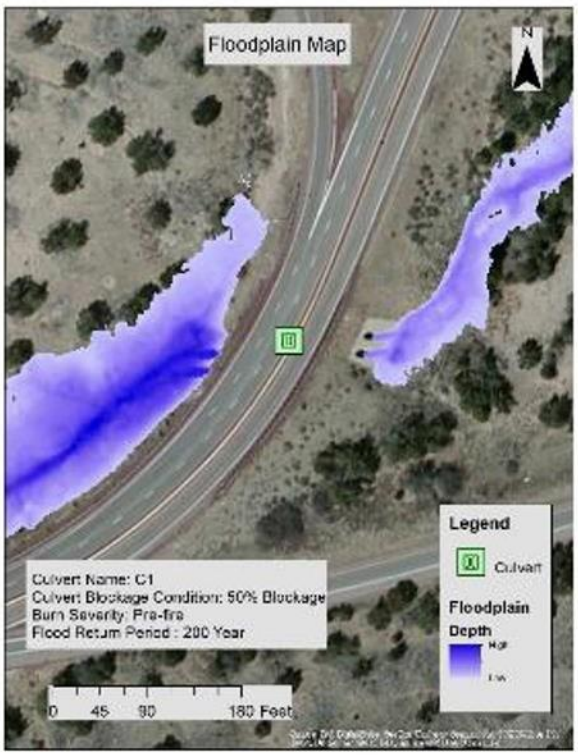

Pre-Fire

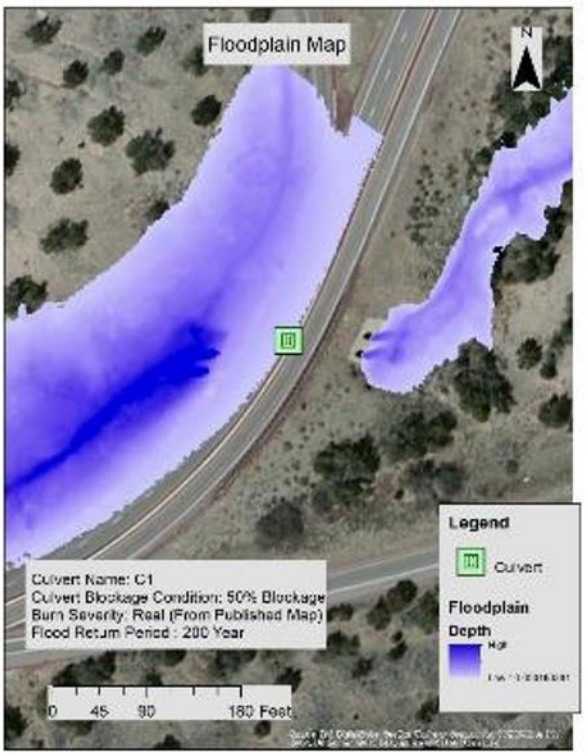

Las Conchas Fire

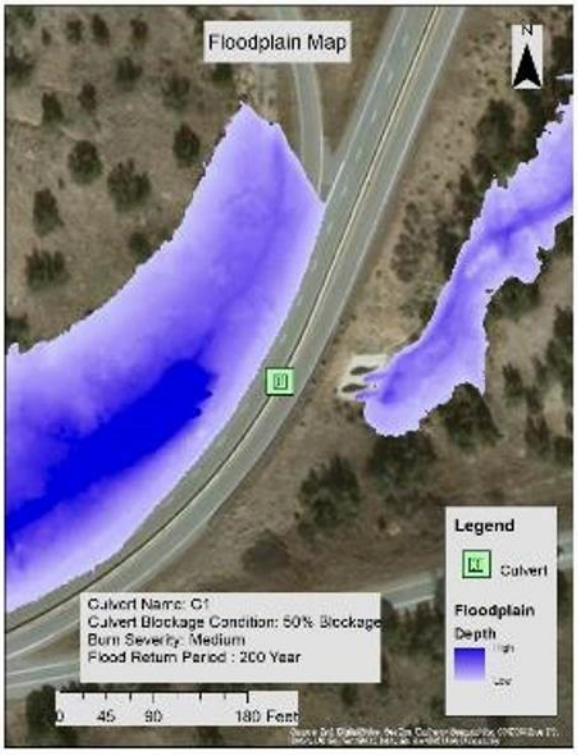

Medium Severity

High Severity

Figure 35. Floodplains at Culvert C1, 50% Blockage, Climate Change

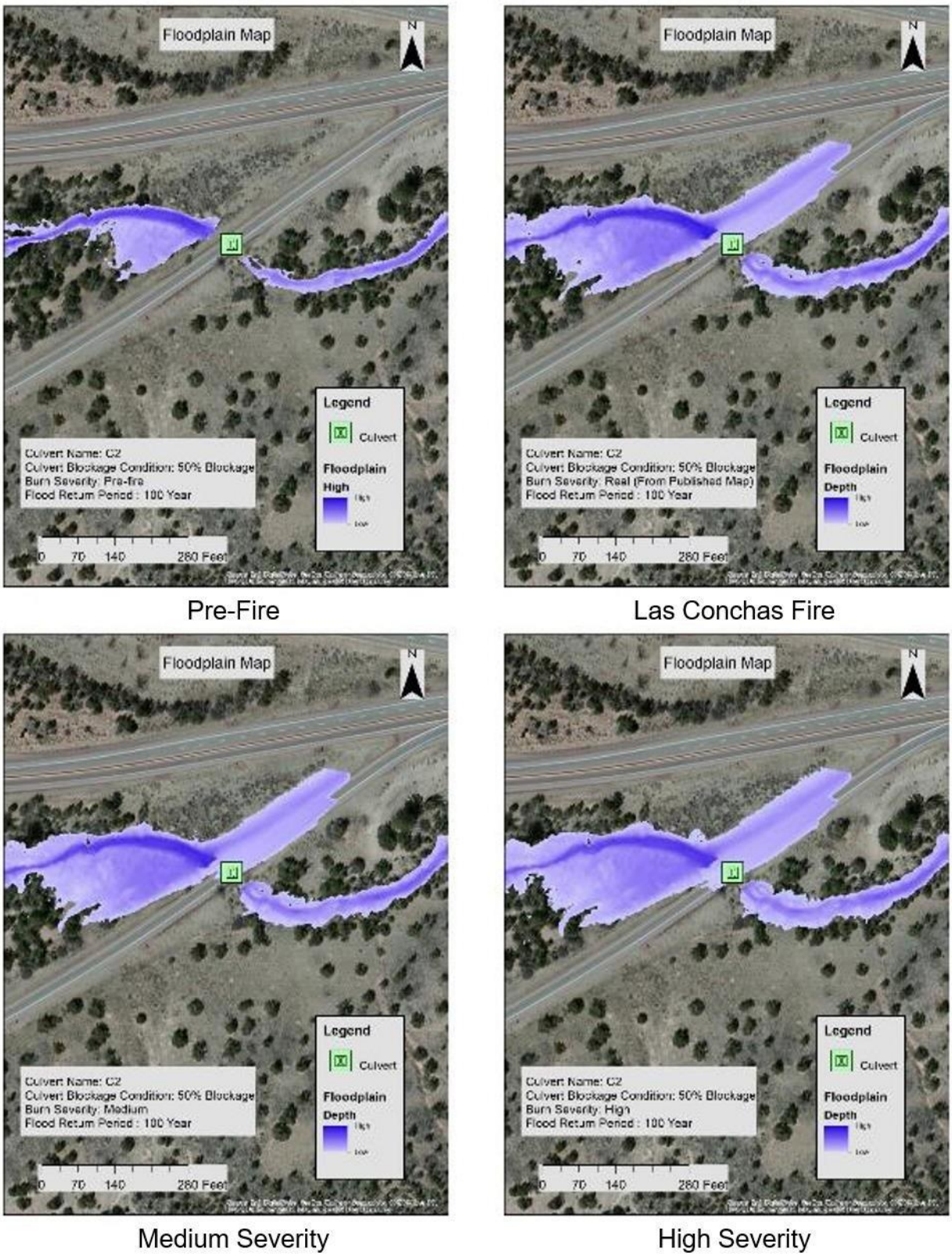

Figure 36. Floodplains at Culvert C2, 50% Blockage, Baseline Climate

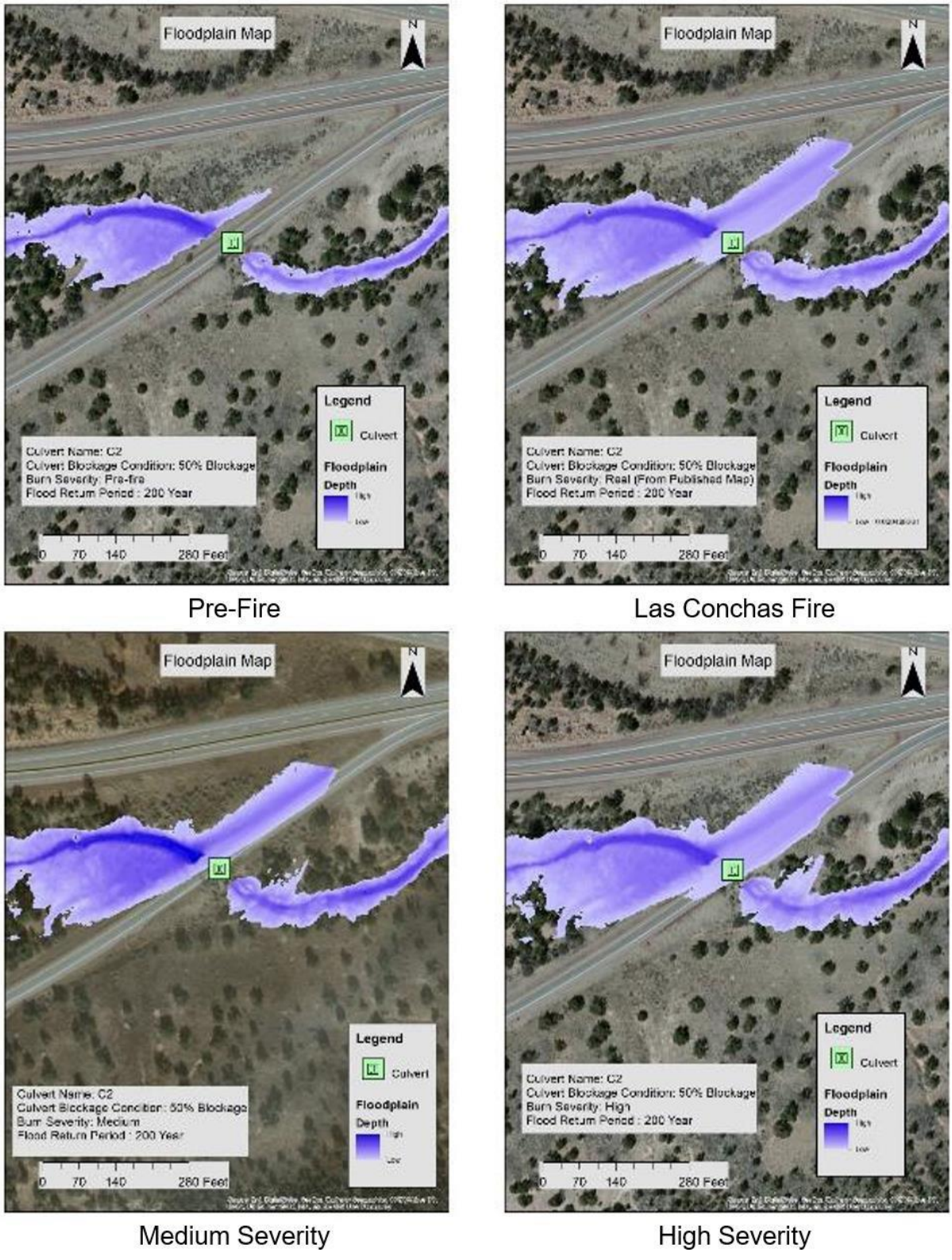

Figure 37. Floodplains at Culvert C2, 50% Blockage, Climate Change

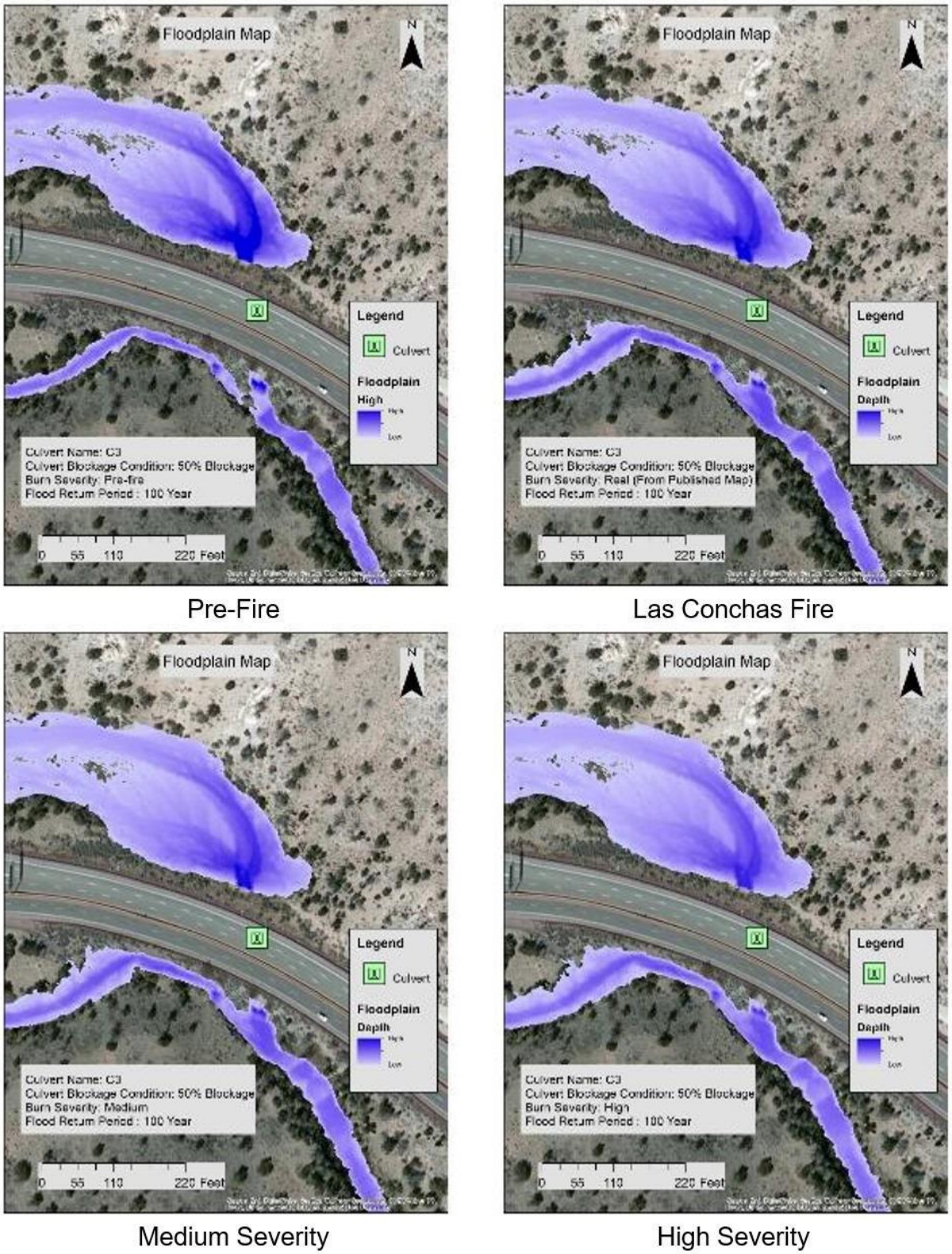

Figure 38. Floodplains at Culvert C3, 50% Blockage, Baseline Climate

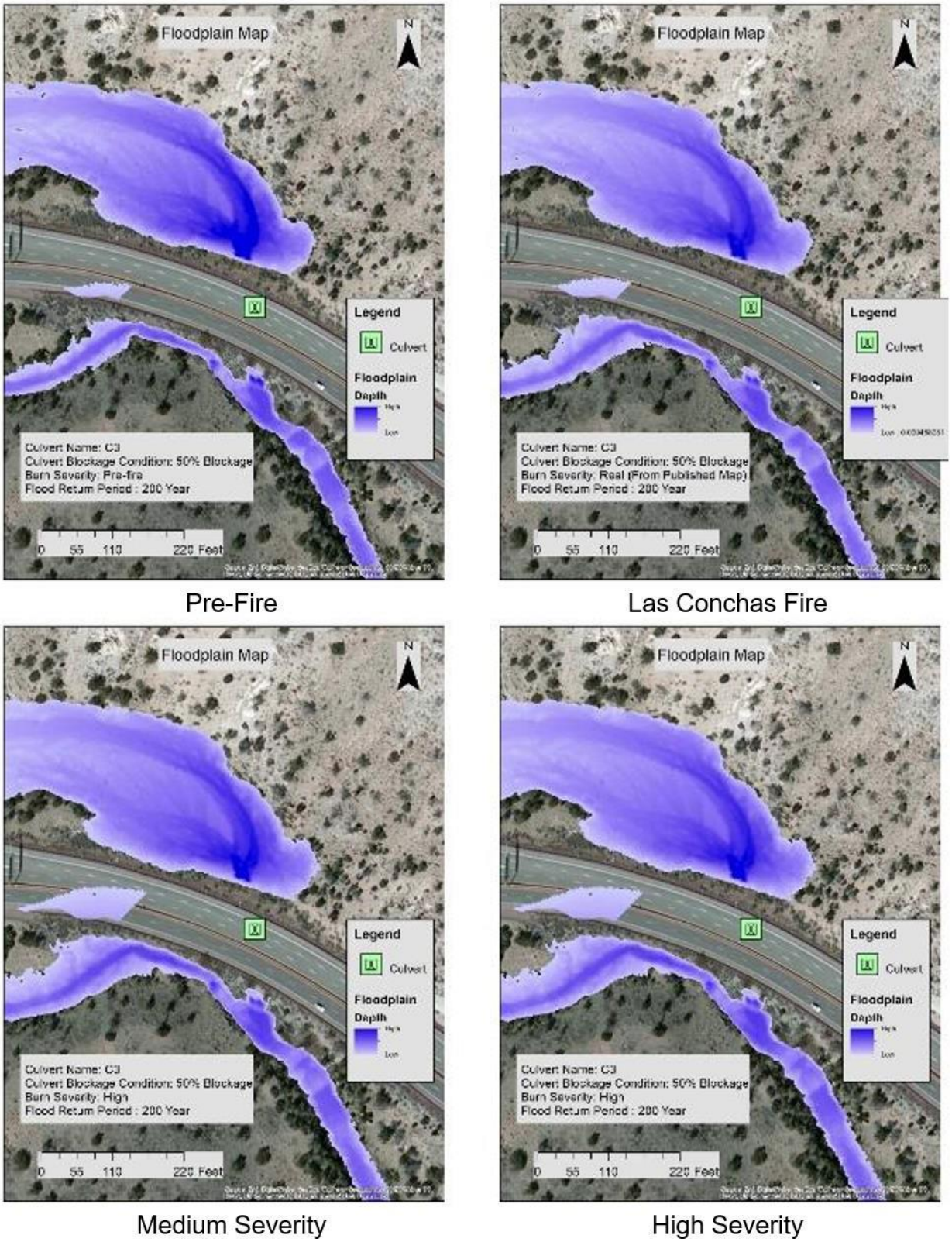

Figure 39. Floodplains at Culvert C3, 50% Blockage, Climate Change

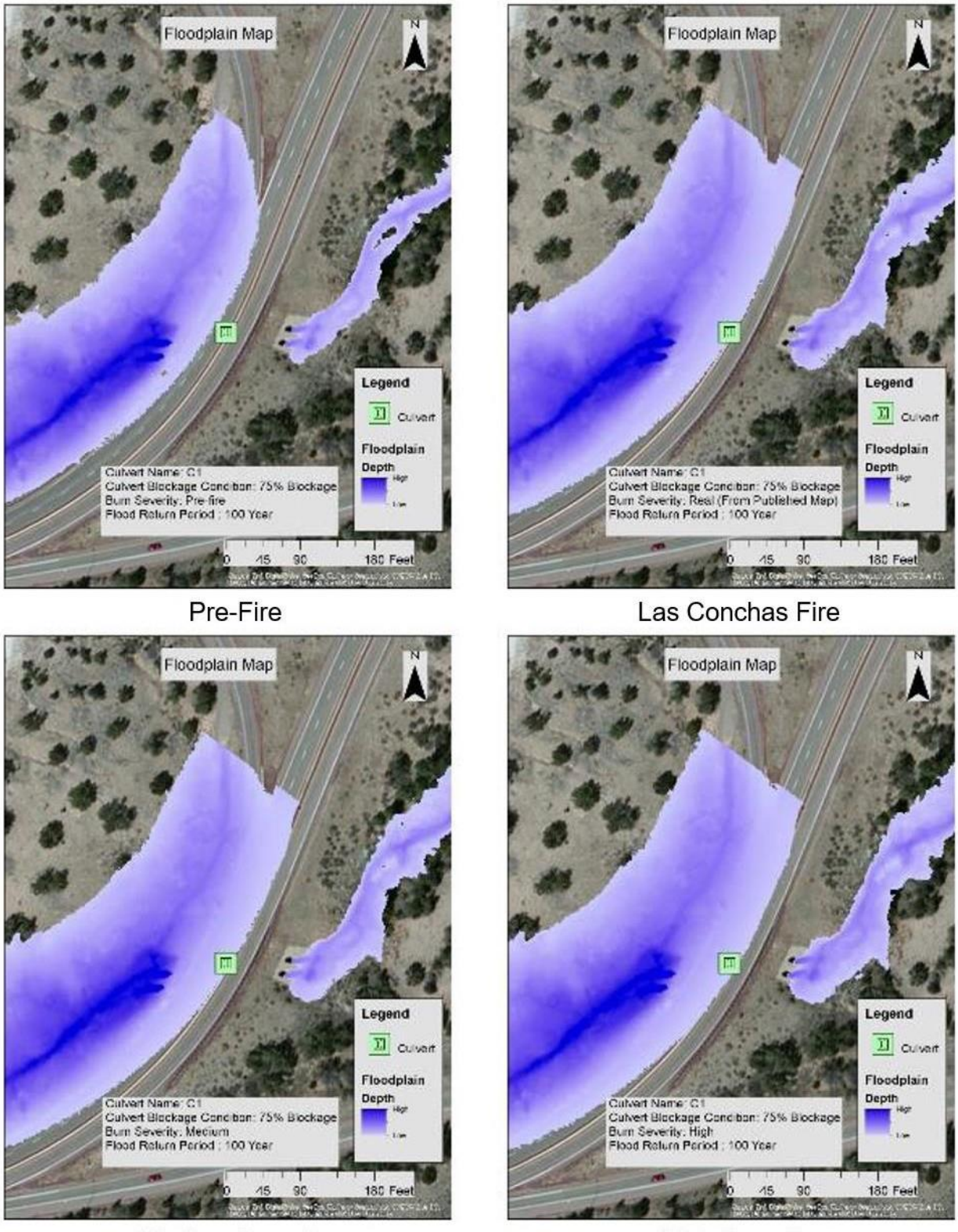

Figure 40. Floodplains at Culvert C1, 75% Blockage, Baseline Climate

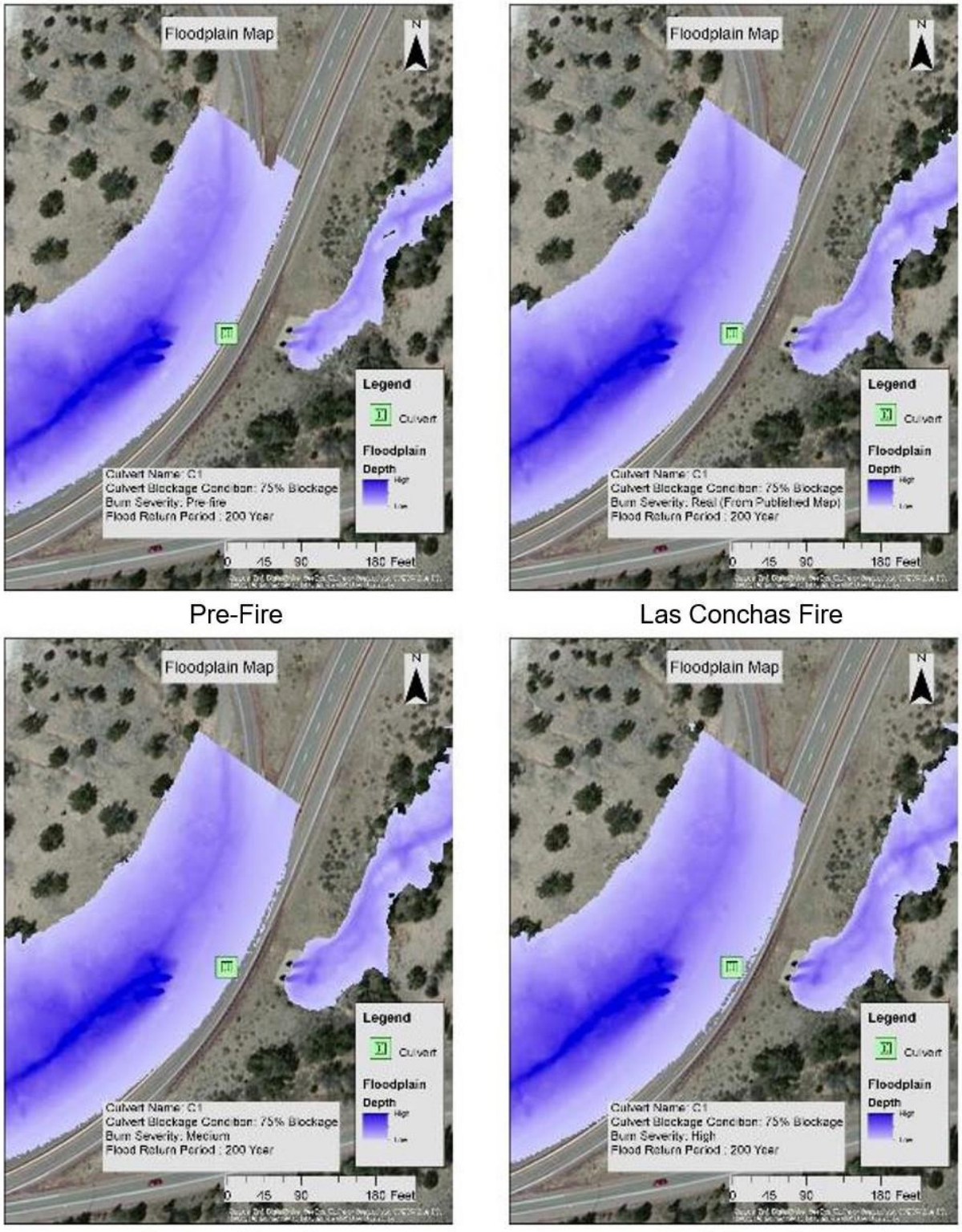

Figure 41. Floodplains at Culvert C1, 75% Blockage, Climate Change

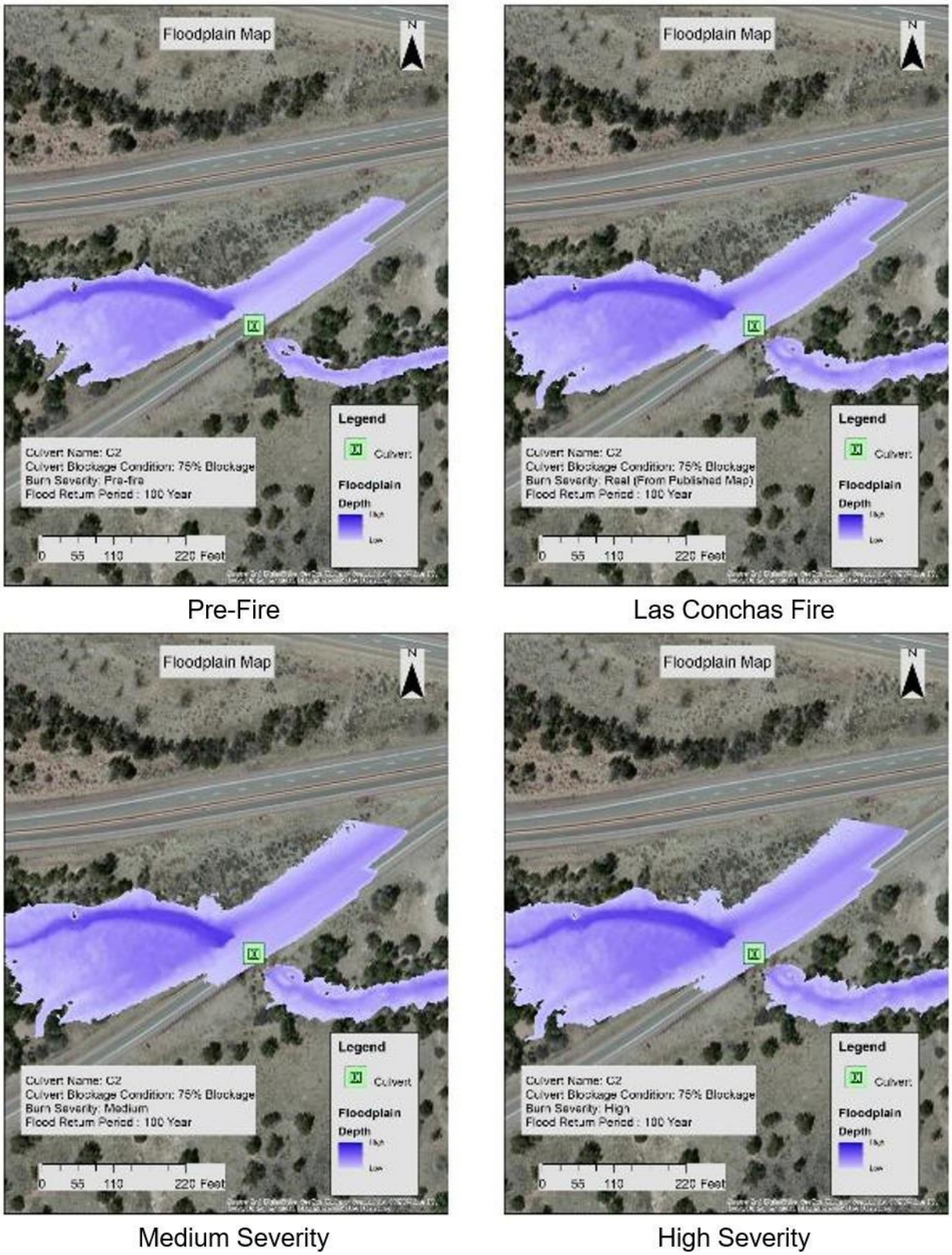

Figure 42. Floodplains at Culvert C2, 75% Blockage, Baseline Climate

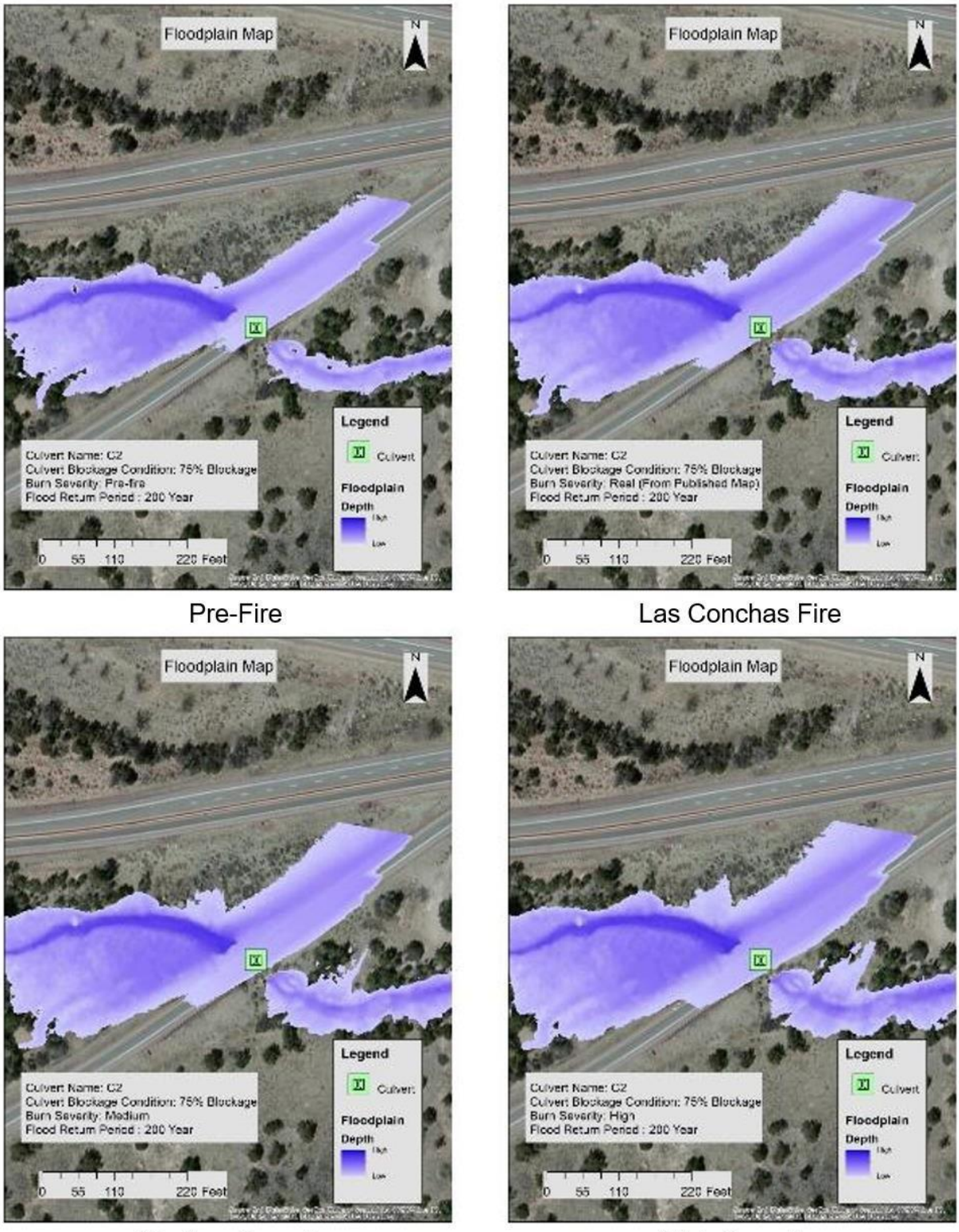

Figure 43. Floodplains at Culvert C2, 75% Blockage, Climate Change

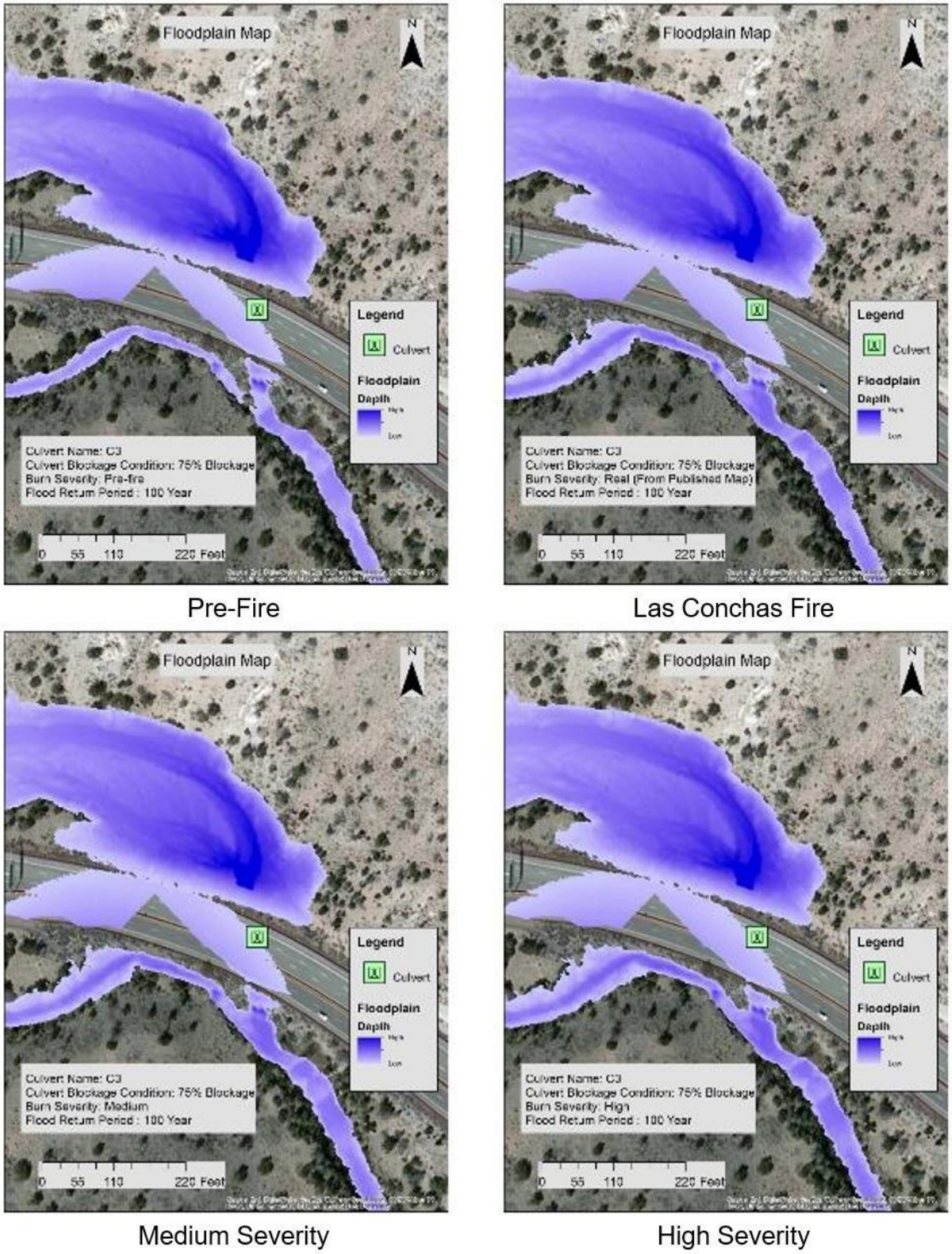

Figure 44. Floodplains at Culvert C3, 75% Blockage, Baseline Climate

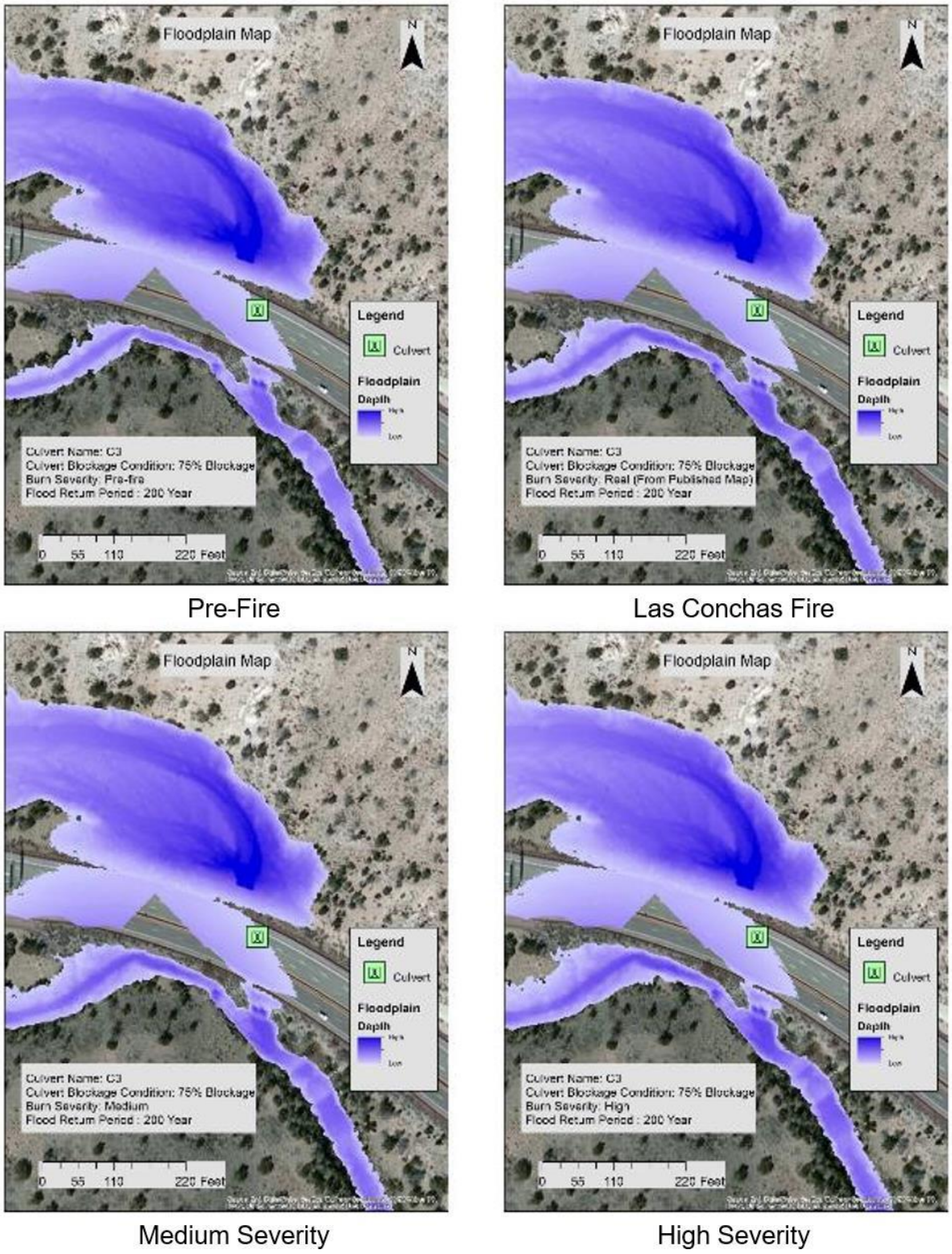

Figure 45. Floodplains at Culvert C3, 75% Blockage, Climate Change